



Observation of electroweak $W^\pm Z$ boson pair production in association with two jets in pp collisions at $\sqrt{s} = 13$ TeV with the ATLAS detector

The ATLAS Collaboration *

ARTICLE INFO

Article history:

Received 27 December 2018
 Received in revised form 16 April 2019
 Accepted 6 May 2019
 Available online 13 May 2019
 Editor: M. Doser

ABSTRACT

An observation of electroweak $W^\pm Z$ production in association with two jets in proton–proton collisions is presented. The data collected by the ATLAS detector at the Large Hadron Collider in 2015 and 2016 at a centre-of-mass energy of $\sqrt{s} = 13$ TeV are used, corresponding to an integrated luminosity of 36.1 fb^{-1} . Events containing three identified leptons, either electrons or muons, and two jets are selected. The electroweak production of $W^\pm Z$ bosons in association with two jets is measured with an observed significance of 5.3 standard deviations. A fiducial cross-section for electroweak production including interference effects and for a single leptonic decay mode is measured to be $\sigma_{WZjj-EW} = 0.57^{+0.14}_{-0.13} \text{ (stat.)}^{+0.07}_{-0.06} \text{ (syst.) fb}$. Total and differential fiducial cross-sections of the sum of $W^\pm Zjj$ electroweak and strong productions for several kinematic observables are also measured.

© 2019 The Author(s). Published by Elsevier B.V. This is an open access article under the CC BY license (<http://creativecommons.org/licenses/by/4.0/>). Funded by SCOAP³.

1. Introduction

The scattering of vector bosons (VBS), $VV \rightarrow VV$ with $V = W/Z/\gamma$, is a key process with which to probe the $SU(2)_L \times U(1)_Y$ gauge symmetry of the electroweak (EW) theory that determines the self-couplings of the vector bosons. New phenomena beyond the Standard Model (SM) can alter the couplings of vector bosons, generating additional contributions to quartic gauge couplings (QGC) compared with the SM predictions [1–3].

In proton–proton collisions, VBS is initiated by an interaction of two vector bosons radiated from the initial-state quarks, yielding a final state with two bosons and two jets, $VVjj$, in a purely electroweak process [4]. VBS diagrams are not independently gauge invariant and cannot be studied separately from other processes leading to the same $VVjj$ final state [5]. Two categories of processes give rise to $VVjj$ final states. The first category, which includes VBS contributions, involves exclusively weak interactions at Born level of order α_{EW}^6 including the boson decays, where α_{EW} is the electroweak coupling constant. It is referred to as electroweak production. The second category involves both the strong and electroweak interactions at Born level of order $\alpha_S^2 \alpha_{EW}^4$, where α_S is the strong interaction coupling constant. It is referred to as QCD production. According to the SM a small interference occurs between electroweak and QCD production.

Different searches for diboson electroweak production have been performed by the ATLAS and CMS collaborations at the LHC. So far, electroweak $VVjj$ production has only been observed in the same-sign $W^\pm W^\pm jj$ channel by CMS using data collected at a centre-of-mass energy of $\sqrt{s} = 13$ TeV [6]. Evidence of electroweak $VVjj$ production has also been obtained in the $W^\pm W^\pm jj$ [7,8] and $Z\gamma jj$ [9] channels by ATLAS and CMS, respectively, using smaller samples of data recorded at $\sqrt{s} = 8$ TeV. Limits on electroweak cross-sections for the production of two gauge boson have been reported for the $W^\pm Zjj$ [10,11], $ZZjj$ [12], $Z\gamma jj$ [13] and $W\gamma jj$ [14] channels by ATLAS and CMS.

This Letter reports on an observation and measurement of electroweak $W^\pm Zjj$ production, exploiting the fully leptonic final states where both the Z and W bosons decay into electrons or muons. The pp collision data were collected with the ATLAS detector in 2015 and 2016 at a centre-of-mass energy of $\sqrt{s} = 13$ TeV and correspond to an integrated luminosity of 36.1 fb^{-1} .

2. The ATLAS detector

The ATLAS detector [15] is a multipurpose detector with a cylindrical geometry¹ and nearly 4π coverage in solid angle. The collision point is surrounded by inner tracking detectors, collec-

¹ ATLAS uses a right-handed coordinate system with its origin at the nominal interaction point (IP) in the centre of the detector and the z -axis along the beam direction. The x -axis points from the IP to the centre of the LHC ring, and the y -axis points upward. Cylindrical coordinates (r, ϕ) are used in the transverse (x, y) plane,

* E-mail address: atlas.publications@cern.ch.

tively referred to as the inner detector (ID), located within a superconducting solenoid providing a 2 T axial magnetic field, followed by a calorimeter system and a muon spectrometer (MS).

The inner detector provides precise measurements of charged-particle tracks in the pseudorapidity range $|\eta| < 2.5$. It consists of three subdetectors arranged in a coaxial geometry around the beam axis: a silicon pixel detector, a silicon microstrip detector and a transition radiation tracker.

The electromagnetic calorimeter covers the region $|\eta| < 3.2$ and is based on high-granularity, lead/liquid-argon (LAr) sampling technology. The hadronic calorimeter uses a steel/scintillator-tile detector in the region $|\eta| < 1.7$ and a copper/LAr detector in the region $1.5 < |\eta| < 3.2$. The most forward region of the detector, $3.1 < |\eta| < 4.9$, is equipped with a forward calorimeter, measuring electromagnetic and hadronic energies in copper/LAr and tungsten/LAr modules.

The muon spectrometer comprises separate trigger and high-precision tracking chambers to measure the deflection of muons in a magnetic field generated by three large superconducting toroidal magnets arranged with an eightfold azimuthal coil symmetry around the calorimeters. The high-precision chambers cover the range $|\eta| < 2.7$ with three layers of monitored drift tubes, complemented by cathode strip chambers in the forward region, where the particle flux is highest. The muon trigger system covers the range $|\eta| < 2.4$ with resistive-plate chambers in the barrel and thin-gap chambers in the endcap regions.

A two-level trigger system is used to select events in real time [16]. It consists of a hardware-based first-level trigger and a software-based high-level trigger. The latter employs algorithms similar to those used offline to identify electrons, muons, photons and jets.

3. Phase space for cross-section measurements

The $W^\pm Zjj$ electroweak cross-section is measured in a fiducial phase space that is defined by the kinematics of the final-state leptons, electrons or muons, associated with the W^\pm and Z boson decays, and of two jets. Leptons produced in the decay of a hadron, a τ -lepton, or their descendants are not considered in the definition of the fiducial phase space. At particle level, the kinematics of the charged lepton after quantum electrodynamics (QED) final-state radiation (FSR) are ‘dressed’ by including contributions from photons with an angular distance $\Delta R \equiv \sqrt{(\Delta\eta)^2 + (\Delta\phi)^2} < 0.1$ from the lepton. Dressed charged leptons, and final-state neutrinos that do not originate from hadron or τ -lepton decays, are matched to the W^\pm and Z boson decay products using a Monte Carlo (MC) generator-independent algorithmic approach, called the ‘resonant shape’ algorithm. This algorithm is based on the value of an estimator expressing the product of the nominal line shapes of the W and Z resonances as detailed in Ref. [10].

The fiducial phase space of the measurement matches the one used in Refs. [10,17] and is defined at particle level by the following requirements: the charged leptons from the Z boson decay are required to have transverse momentum $p_T > 15$ GeV, the charged lepton from the W^\pm decay is required to have transverse momentum $p_T^\ell > 20$ GeV, the charged leptons from the W^\pm and Z bosons are required to have $|\eta| < 2.5$ and the invariant mass of the two leptons from the Z boson decay must be within 10 GeV of the nominal Z boson mass, taken from the world average value, m_Z^{PDG} [18]. The W boson transverse mass, defined as

$$m_T^W = \sqrt{2 \cdot p_T^\nu \cdot p_T^\ell \cdot [1 - \cos \Delta\phi(\ell, \nu)]},$$

ϕ being the azimuthal angle around the beam direction. The pseudorapidity is defined in terms of the polar angle θ as $\eta = -\ln[\tan(\theta/2)]$.

gle between the lepton and the neutrino in the transverse plane and p_T^ν is the transverse momentum of the neutrino, is required to be $m_T^W > 30$ GeV. The angular distance between the charged lepton from the W^\pm decay and each of the charged leptons from the Z decay is required to be $\Delta R > 0.3$, and the angular distance between the two leptons from the Z decay is required to be $\Delta R > 0.2$. Requiring that the transverse momentum of the leading lepton be above 27 GeV reduces the acceptance of the fiducial phase space by only 0.02% and is therefore not added to the definition of the fiducial phase space, although it is present in the selection at the detector level presented in Section 5.

In addition to these requirements that define an inclusive phase space, at least two jets with $p_T > 40$ GeV and $|\eta_j| < 4.5$ are required. These particle-level jets are reconstructed from stable particles with a lifetime of $\tau > 30$ ps in the simulation after parton showering, hadronisation, and decay of particles with $\tau < 30$ ps. Muons, electrons, neutrinos and photons associated with W and Z decays are excluded. The particle-level jets are reconstructed using the anti- k_t [10] algorithm with a radius parameter $R = 0.4$. The angular distance between all selected leptons and jets is required to be $\Delta R(j, \ell) > 0.3$. If the $\Delta R(j, \ell)$ requirement is not satisfied, the jet is discarded. The invariant mass, m_{jj} , of the two highest- p_T jets in opposite hemispheres, $\eta_{j1} \cdot \eta_{j2} < 0$, is required to be $m_{jj} > 500$ GeV to enhance the sensitivity to VBS processes. These two jets are referred to as tagging jets. Finally, processes with a b -quark in the initial state, such as tZj production, are not considered as signal. The production of tZj results from a t -channel exchange of a W boson between a b - and a u -quark giving a final state with a t -quark, a Z boson and a light-quark jet, but does not include diagrams with gauge boson couplings.

4. Signal and background simulation

Monte Carlo simulation is used to model signal and background processes. All generated MC events were passed through the ATLAS detector simulation [20], based on GEANT 4 [21], and processed using the same reconstruction software as used for the data. The event samples include the simulation of additional proton–proton interactions (pile-up) generated with PYTHIA 8.186 [22] using the MSTW2008LO [23] parton distribution functions (PDF) and the A2 [24] set of tuned parameters.

Scale factors are applied to simulated events to correct for the differences between data and MC simulation in the trigger, reconstruction, identification, isolation and impact parameter efficiencies of electrons and muons [25,26]. Furthermore, the electron energy and muon momentum in simulated events are smeared to account for differences in resolution between data and MC simulation [26, 27].

The SHERPA 2.2.2 MC event generator [28–35] was used to model $W^\pm Zjj$ events. It includes the modelling of hard scattering, parton showering, hadronisation and the underlying event. A MC event sample, referred to as $WZjj$ –EW, includes processes of order six (zero) in α_{EW} (α_S). In this sample, which includes VBS diagrams, two additional jets originating from electroweak vertices from matrix-element partons are included in the final state. Diagrams with a b -quark in either the initial or final state, i.e. b -quarks in the matrix-element calculation, are not considered. This sample provides a LO prediction for the $WZjj$ –EW signal process. A second MC event sample, referred to as $WZjj$ –QCD, includes processes of order four in α_{EW} in the matrix-element of $W^\pm Z$ production with up to one jet calculated at next-to-leading order (NLO) and with a second or third jet calculated at leading order (LO). This $WZjj$ –QCD sample includes matrix-element b -quarks. Both SHERPA samples were generated using the

NNPDF3.0 [36] PDF set. Interferences between the two processes were estimated at LO using the MADGRAPH5_aMC@NLO 2.3 [37] MC event generator with the NNPDF3.0 PDF set, including only contributions to the squared matrix-element of order one in α_s . They are found to be positive and approximately 10% of the $WZjj$ –EW cross-section in the fiducial phase space and are treated as an uncertainty in the measurement, as discussed in Section 8. For the estimation of modelling uncertainties, alternative MC samples of $WZjj$ –QCD and $WZjj$ –EW processes were generated with MADGRAPH5_aMC@NLO 2.3 at LO in QCD, including up to two partons in the matrix-element for $WZjj$ –QCD, and using the NNPDF3.0 PDF set. MC samples of inclusive $W^\pm Z$ production generated at NLO in QCD with the POWHEG-Box v2 [38–41] generator, interfaced to PYTHIA 8.210 or HERWIG++ 2.7.1 [42] for simulation of parton showering and hadronisation are also used for tests of the modelling of $WZjj$ –QCD events.

The $q\bar{q} \rightarrow ZZ^{(*)}$ processes were generated with SHERPA 2.2.2 and the NNPDF3.0 PDF set. Similarly to $W^\pm Z$ simulation, the $ZZjj$ –QCD and $ZZjj$ –EW processes are generated separately with the same matrix-element accuracy as for the $W^\pm Z$ SHERPA MC samples. The SHERPA 2.1.1 MC event generator was used to model the $gg \rightarrow ZZ^{(*)}$ and VVV processes at LO using the CT10 [43] PDF set. The $t\bar{t}V$ processes were generated at NLO with the MADGRAPH5_aMC@NLO 2.3 MC generator using the NNPDF3.0 PDF set interfaced to the PYTHIA 8.186 parton shower model. The associated production of a single top quark and a Z boson was simulated at LO with MADGRAPH5_aMC@NLO 2.3 using the NNPDF3.0 PDF set and interfaced to PYTHIA 8.186 for parton shower.

5. Event selection

Candidate events were selected using single-leptons triggers [16] that required at least one electron or muon. The transverse momentum threshold of the leptons in 2015 was 24 GeV for electrons and 20 GeV for muons satisfying a loose isolation requirement based only on ID track information. Due to the higher instantaneous luminosity in 2016 the trigger threshold was increased to 26 GeV for both the electrons and muons and tighter isolation requirements were applied. Possible inefficiencies for leptons with large transverse momenta were reduced by including additional electron and muon triggers that did not include any isolation requirements with transverse momentum thresholds of $p_T = 60$ GeV and 50 GeV, respectively. Finally, a single-electron trigger requiring $p_T > 120$ GeV or $p_T > 140$ GeV in 2015 and 2016, respectively, with less restrictive electron identification criteria was used to increase the selection efficiency for high- p_T electrons. The combined efficiency of these triggers is close to 100% for $W^\pm Zjj$ events. Only data recorded with stable beam conditions and with all relevant detector subsystems operational are considered.

Events are required to have a primary vertex reconstructed from at least two charged-particle tracks and compatible with the pp interaction region. If several such vertices are present in the event, the one with the highest sum of the p_T^2 of the associated tracks is selected as the production vertex of the $W^\pm Z$. All final states with three charged leptons (electrons or muons) and neutrinos from $W^\pm Z$ leptonic decays are considered.

Muon candidates are identified by tracks reconstructed in the muon spectrometer and matched to tracks reconstructed in the inner detector. Muons are required to satisfy a ‘medium’ identification selection that is based on requirements on the number of hits in the ID and the MS [26]. The efficiency of this selection averaged over p_T and η is $> 98\%$. The muon momentum is calculated by combining the MS measurement, corrected for the energy deposited in the calorimeters, with the ID measurement. The trans-

verse momentum of the muon must satisfy $p_T > 15$ GeV and its pseudorapidity must satisfy $|\eta| < 2.5$.

Electron candidates are reconstructed from energy clusters in the electromagnetic calorimeter matched to ID tracks. Electrons are identified using a likelihood function constructed from information from the shape of the electromagnetic showers in the calorimeter, track properties and track-to-cluster matching quantities [25]. Electrons must satisfy a ‘medium’ likelihood requirement, which provides an overall identification efficiency of 90%. The electron momentum is computed from the cluster energy and the direction of the track. The transverse momentum of the electron must satisfy $p_T > 15$ GeV and the pseudorapidity of the cluster must be in the ranges $|\eta| < 1.37$ or $1.52 < |\eta| < 2.47$.

Electron and muon candidates are required to originate from the primary vertex. The significance of the track’s transverse impact parameter relative to the beam line must satisfy $|d_0/\sigma_{d_0}| < 3$ (5) for muons (electrons), and the longitudinal impact parameter, z_0 (the difference between the value of z of the point on the track at which d_0 is defined and the longitudinal position of the primary vertex), is required to satisfy $|z_0 \cdot \sin(\theta)| < 0.5$ mm.

Electrons and muons are required to be isolated from other particles, according to calorimeter-cluster and ID-track information. The isolation requirement for electrons varies with p_T and is tuned for an efficiency of at least 90% for $p_T > 25$ GeV and at least 99% for $p_T > 60$ GeV [25]. Fixed thresholds values are used for the muon isolation variables, providing an efficiency above 90% for $p_T > 15$ GeV and at least 99% for $p_T > 60$ GeV [26].

Jets are reconstructed from clusters of energy depositions in the calorimeter [44] using the anti- k_t algorithm [19] with a radius parameter $R = 0.4$. Events with jets arising from detector noise or other non-collision sources are discarded [45]. All jets must have $p_T > 25$ GeV and be reconstructed in the pseudorapidity range $|\eta| < 4.5$. A multivariate combination of track-based variables is used to suppress jets originating from pile-up in the ID acceptance [46]. The energy of jets is calibrated using a jet energy correction derived from simulation and *in situ* methods using data [47]. Jets in the ID acceptance with $p_T > 25$ GeV containing a b -hadron are identified using a multivariate algorithm [48, 49] that uses impact parameter and reconstructed secondary vertex information of the tracks contained in the jets. Jets initiated by b -quarks are selected by setting the algorithm’s output threshold such that a 70% b -jet selection efficiency is achieved in simulated $t\bar{t}$ events.

The transverse momentum of the neutrino is estimated from the missing transverse momentum in the event, E_T^{miss} , calculated as the negative vector sum of the transverse momentum of all identified hard (high p_T) physics objects (electrons, muons and jets), as well as an additional soft term. A track-based measurement of the soft term [50,51], which accounts for low- p_T tracks not assigned to a hard object, is used.

Events are required to contain exactly three lepton candidates satisfying the selection criteria described above. To ensure that the trigger efficiency is well determined, at least one of the candidate leptons is required to have $p_T > 25$ GeV or $p_T > 27$ GeV for the 2015 or 2016 data, respectively, and to be geometrically matched to a lepton that was selected by the trigger.

To suppress background processes with at least four prompt leptons, events with a fourth lepton candidate satisfying looser selection criteria are rejected. For this looser selection, the p_T requirement for the leptons is lowered to $p_T > 5$ GeV and ‘loose’ identification requirements are used for both the electrons and muons. A less stringent requirement is applied for electron isolation based only on ID track information and electrons with cluster in the range $1.37 \leq |\eta| \leq 1.52$ are also considered.

Table 1

Expected and observed numbers of events in the $W^\pm Zjj$ signal region and in the three control regions, before the fit. The expected number of $WZjj$ –EW events from SHERPA and the estimated number of background events from the other processes are shown. The sum of the backgrounds containing misidentified leptons is labelled ‘Misid. leptons’. The contribution arising from interferences between $WZjj$ –QCD and $WZjj$ –EW processes is not included in the table. The total uncertainties are quoted.

	SR	$WZjj$ –QCD CR	b –CR	ZZ–CR
Data	161	213	141	52
Total predicted	200 ± 41	290 ± 61	160 ± 14	45.2 ± 7.5
$WZjj$ –EW (signal)	24.9 ± 1.4	8.45 ± 0.37	1.36 ± 0.10	0.21 ± 0.12
$WZjj$ –QCD	144 ± 41	231 ± 60	24.4 ± 1.7	1.43 ± 0.22
Misid. leptons	9.8 ± 3.9	17.7 ± 7.1	30 ± 12	0.47 ± 0.21
$ZZjj$ –QCD	8.1 ± 2.2	15.0 ± 3.9	1.96 ± 0.49	35 ± 11
tZj	6.5 ± 1.2	6.6 ± 1.1	36.2 ± 5.7	0.18 ± 0.04
$t\bar{t} + V$	4.21 ± 0.76	9.11 ± 1.40	65.4 ± 10.3	2.8 ± 0.61
$ZZjj$ –EW	1.80 ± 0.45	0.53 ± 0.14	0.12 ± 0.09	4.1 ± 1.4
VVV	0.59 ± 0.15	0.93 ± 0.23	0.13 ± 0.03	1.05 ± 0.30

Candidate events are required to have at least one pair of leptons of the same flavour and of opposite charge, with an invariant mass that is consistent with the nominal Z boson mass [52] to within 10 GeV. This pair is considered to be the Z boson candidate. If more than one pair can be formed, the pair whose invariant mass is closest to the nominal Z boson mass is taken as the Z boson candidate.

The remaining third lepton is assigned to the W boson decay. The transverse mass of the W candidate, computed using E_T^{miss} and the p_T of the associated lepton, is required to be greater than 30 GeV.

Backgrounds originating from misidentified leptons are suppressed by requiring the lepton associated with the W boson to satisfy more stringent selection criteria. Thus, the transverse momentum of these leptons is required to be $p_T > 20$ GeV. Furthermore, leptons associated with the W boson decay are required to satisfy the ‘tight’ identification requirements, which have an efficiency between 90% and 98% for muons and an efficiency of 85% for electrons. Finally, muons must also satisfy a tighter isolation requirement, tuned for an efficiency of at least 90% (99%) for $p_T > 25$ (60) GeV.

To select $W^\pm Zjj$ candidates, events are further required to be associated with at least two ‘tagging’ jets. The leading tagging jet is selected as the highest- p_T jet in the event with $p_T > 40$ GeV. The second tagging jet is selected as the one with the highest p_T among the remaining jets that have a pseudorapidity of opposite sign to the first tagging jet and a $p_T > 40$ GeV. These two jets are required to verify $m_{jj} > 150$ GeV, in order to minimise the contamination from triboson processes.

The final signal region (SR) for VBS processes is defined by requiring that the invariant mass of the two tagging jets, m_{jj} , be above 500 GeV and that no b -tagged jet be present in the event.

6. Background estimation

The background sources are classified into two groups: events where at least one of the candidate leptons is not a prompt lepton (reducible background) and events where all candidates are prompt leptons or are produced in the decay of a τ -lepton (irreducible background). Candidates that are not prompt leptons are also called ‘misidentified’ or ‘fake’ leptons.

The dominant source of background originates from the QCD-induced production of $W^\pm Z$ dibosons in association with two jets, $WZjj$ –QCD. The shapes of distributions of kinematic observables of this irreducible background are modelled by the SHERPA MC simulation. The normalisation of this background is, however, constrained by data in a dedicated control region. This region, referred

to as $WZjj$ –QCD CR, is defined by selecting a sub-sample of $W^\pm Zjj$ candidate events with $m_{jj} < 500$ GeV and no reconstructed b -jets.

The other main sources of irreducible background arise from ZZ and $t\bar{t} + V$ (where $V = Z$ or W). These irreducible backgrounds are also modelled using MC simulations. Data in two additional dedicated control regions, referred to as ZZ –CR and b –CR, respectively, are used to constrain the normalisations of the $ZZjj$ –QCD and $t\bar{t} + V$ backgrounds. The control region ZZ –CR, enriched in ZZ events, is defined by applying the $W^\pm Zjj$ event selection defined in Section 5, with the exception that instead of vetoing a fourth lepton it is required that events have at least a fourth lepton candidate with looser identification requirements. This region is dominated by $ZZjj$ –QCD events with a small contribution of $ZZjj$ –EW events. The control region b –CR, enriched in $t\bar{t} + V$ events, is defined by selecting $W^\pm Zjj$ candidate events having at least one reconstructed b -jet. Remaining sources of irreducible background are $ZZjj$ –EW VVV and tZj events. Their contributions in the control and signal regions are estimated from MC simulations.

The reducible backgrounds originate from $Z + j$, $Z\gamma$, $t\bar{t}$, Wt and WW production processes. The reducible backgrounds are estimated using a data-driven method based on the inversion of a global matrix containing the efficiencies and the misidentification probabilities for prompt and fake leptons [10,53]. The method exploits the classification of the lepton as loose or tight candidates and the probability that a fake lepton is misidentified as a loose or tight lepton candidate. Tight leptons candidates are signal lepton candidates as defined in Section 5. Loose lepton candidates are leptons that do not meet the isolation and identification criteria of signal lepton candidates but satisfy only looser criteria. The misidentification probabilities for fake leptons are determined from data, using dedicated control samples enriched in non-prompt leptons from heavy-flavour jets and in misidentified leptons from photon conversions or charged hadrons in light-flavour jets. The lepton misidentification probabilities are applied to samples of $W^\pm Zjj$ candidate events in data where at least one and up to three of the lepton candidates are loose. Then, using a matrix inversion, the number of events with at least one misidentified lepton, which represents the amount of reducible background in the selected $W^\pm Zjj$ sample, is obtained.

The number of observed events together with the expected background contributions are summarised in Table 1 for the signal region and the three control regions. All sources of uncertainties, as described in Section 8, are included. The expected signal purity in the $W^\pm Zjj$ signal region is about 13%, and 72% of the events arise from $WZjj$ –QCD production.

7. Signal extraction procedure

Given the small contribution to the signal region of $WZjj$ –EW processes, a multivariate discriminant is used to separate the signal from the backgrounds. A boosted decision tree (BDT), as implemented in the TMVA package [54], is used to exploit the kinematic differences between the $WZjj$ –EW signal and the $WZjj$ –QCD and other backgrounds. The BDT is trained and optimised on simulated events to separate $WZjj$ –EW events from all background processes.

A total of 15 variables are combined into one discriminant, the BDT score output value in the range $[-1, 1]$. The variables can be classified into three categories: jet-kinematic variables, vector-bosons-kinematics variables, and variables related to both jets and leptons kinematics. The variables related to the kinematic properties of the two tagging jets are the invariant mass of the two jets, m_{jj} , the transverse momenta of the jets, the difference in pseudorapidity and azimuthal angle between the two jets, $\Delta\eta_{jj}$ and $\Delta\phi_{jj}$, the rapidity of the leading jet and the jet multiplicity. Variables related to the kinematic properties of the vector bosons are the transverse momenta of the W and Z bosons, the pseudorapidity of the W boson, the absolute difference between the rapidities of the Z boson and the lepton from the decay of the W boson, $|y_Z - y_{\ell,W}|$, and the transverse mass of the $W^\pm Z$ system m_T^{WZ} . The pseudorapidity of the W boson is reconstructed using an estimate of the longitudinal momentum of the neutrino obtained using the W mass constraint as detailed in Ref. [55]. The m_T^{WZ} observable is reconstructed following Ref. [10]. Variables that relate the kinematic properties of jets and leptons are the distance in the pseudorapidity–azimuth plane between the Z boson and the leading jet, $\Delta R(j_1, Z)$, the event balance $N_{p_T}^{\text{hard}}$, defined as the transverse component of the vector sum of the WZ bosons and tagging jets momenta, normalised to their scalar p_T sum, and, finally the centrality of the WZ system relative to the tagging jets, defined as $\zeta_{\text{lep}} = \min(\Delta\eta_-, \Delta\eta_+)$, with $\Delta\eta_- = \min(\eta_{\ell_1}^W, \eta_{\ell_2}^Z, \eta_{\ell_1}^Z) - \min(\eta_{j_1}, \eta_{j_2})$ and $\Delta\eta_+ = \max(\eta_{j_1}, \eta_{j_2}) - \max(\eta_{\ell_1}^W, \eta_{\ell_2}^Z, \eta_{\ell_1}^Z)$. A larger set of discriminating observables was studied but only variables improving signal-to-background were retained. The good modelling by MC simulations of the distribution shapes and the correlations of all input variables to the BDT is verified in the $WZjj$ –QCD CR, as exemplified by the good description of the BDT score distribution of data in the $WZjj$ –QCD CR shown in Fig. 1.

The distribution of the BDT score in the $W^\pm Zjj$ signal region is used to extract the significance of the $WZjj$ –EW signal and to measure its fiducial cross-section via a maximum-likelihood fit. An extended likelihood is built from the product of four likelihoods corresponding to the BDT score distribution in the $W^\pm Zjj$ SR, the m_{jj} distribution in the $WZjj$ –QCD CR, the multiplicity of reconstructed b -quarks in the b -CR and the m_{jj} distribution in the ZZ -CR. The inclusion of the three control regions in the fit allows the yields of the $WZjj$ –QCD, $t\bar{t} + V$ and $ZZjj$ –QCD backgrounds to be constrained by data. The shapes of these backgrounds are taken from MC predictions and can vary within the uncertainties affecting the measurement as described in Section 8. The normalisations of these backgrounds are introduced in the likelihood as parameters, labelled $\mu_{WZjj\text{--}QCD}$, $\mu_{t\bar{t}+V}$ and $\mu_{ZZjj\text{--}QCD}$ for $WZjj$ –QCD, $t\bar{t} + V$ and $ZZjj$ –QCD backgrounds, respectively. They are treated as unconstrained nuisance parameters that are determined mainly by the data in the respective control region. The normalisation and shape of the other irreducible backgrounds are taken from MC simulations and are allowed to vary within their respective uncertainties. The distribution of the reducible background is estimated from data using the matrix method pre-

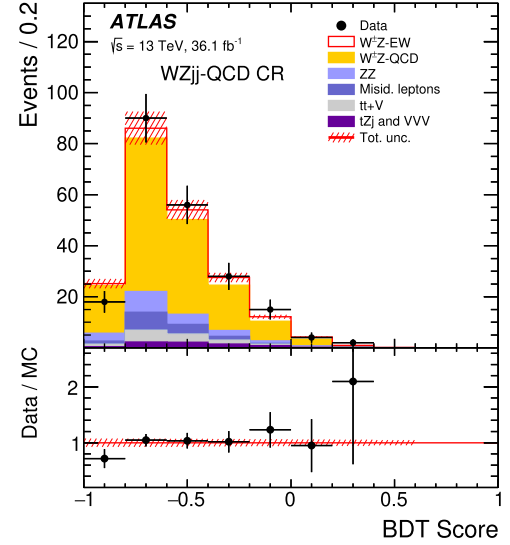


Fig. 1. Post-fit distribution of the BDT score distribution in the $WZjj$ –QCD control region. Signal and backgrounds are normalised to the expected number of events after the fit. The uncertainty band around the MC expectation includes all systematic uncertainties as obtained from the fit.

sented in Section 6 and is allowed to vary within its uncertainty.

The determination of the fiducial cross-section is carried out using the signal strength parameter $\mu_{WZjj\text{--}EW}$:

$$\mu_{WZjj\text{--}EW} = \frac{N_{\text{data}}^{\text{signal}}}{N_{\text{MC}}^{\text{signal}}} = \frac{\sigma_{WZjj\text{--}EW}^{\text{fid.}}}{\sigma_{WZjj\text{--}EW}^{\text{fid.,MC}}},$$

where $N_{\text{data}}^{\text{signal}}$ is the signal yield extracted from data by the fit and $N_{\text{MC}}^{\text{signal}}$ is the number of signal events predicted by the SHERPA MC simulation. The measured cross-section $\sigma_{WZjj\text{--}EW}^{\text{fid.}}$ is derived from the signal strength $\mu_{WZjj\text{--}EW}$ by multiplying it by the SHERPA MC cross-section prediction $\sigma_{WZjj\text{--}EW}^{\text{fid.,MC}}$ in the fiducial region. The $WZjj$ –QCD contribution that is considered as background in the fit procedure does not contain interference between the $WZjj$ –QCD and $WZjj$ –EW processes. The measured cross-section $\sigma_{WZjj\text{--}EW}^{\text{fid.}}$ therefore formally corresponds to the cross-section of the electroweak production including interference effects.

8. Systematic uncertainties

Systematic uncertainties in the signal and control regions affecting the shape and normalisation of the BDT score, m_{jj} and $N_{b\text{--}jets}$ distributions for the individual backgrounds, as well as the acceptance of the signal and the shape of its template are considered. If the variation of a systematic uncertainty as a function of the BDT score is consistent with being due to statistical fluctuations, this systematic uncertainty is neglected.

Systematic uncertainties due to the theoretical modelling in the event generator used to evaluate the $WZjj$ –QCD and $WZjj$ –EW templates are considered. Uncertainties due to higher order QCD corrections are evaluated by varying the renormalisation and factorisation scales independently by factors of two and one-half, removing combinations where the variations differ by a factor of four. These uncertainties are of -20% to $+30\%$ on the $WZjj$ –QCD background normalisation and up to $\pm 5\%$ on the $WZjj$ –EW signal shape. The uncertainties due to the PDF and the α_S value used in the PDF determination are evaluated using the PDF4LHC

prescription [56]. They are of the order of 1% to 2% in shape of the predicted cross-section. A global modelling uncertainty in the $WZjj$ -QCD background template that includes effects of the parton shower model is estimated by comparing predictions of the BDT score distribution in the signal region from the SHERPA and MADGRAPH MC event generators. The difference between the predicted shapes of the BDT score distribution from the two generators is considered as an uncertainty. The resulting uncertainty ranges from 5% to 20% at medium and high values of the BDT score, respectively. Alternatively, using two MC samples with different parton shower models, POWHEG+PYTHIA8 and POWHEG+HERWIG, it was verified that for $WZjj$ -QCD events the variations of the BDT score shape due to different parton shower models are within the global modelling uncertainty defined above. A global modelling uncertainty in the $WZjj$ -EW signal template is also estimated by comparing predictions of the BDT score distribution in the signal region from the SHERPA and MADGRAPH MC event generators. This modelling uncertainty affects the shape of the BDT score distribution by at most 14% at large values of the BDT score. The Sherpa $WZjj$ -EW sample used in this analysis was recently found to implement a colour flow computation in VBS-like processes that increases central parton emissions from the parton shower [57]. It was verified that possible effects on kinematic distributions and especially on the BDT score distribution are covered by the modelling uncertainty used. The interference between electroweak- and QCD-induced processes is not included in the probability distribution functions of the fit but is considered as an uncertainty affecting only the shape of the $WZjj$ -EW MC template. The effect is determined using the MADGRAPH MC generator, resulting for the signal region in shape-only uncertainties ranging from 10% to 5% at low and high values of the BDT score, respectively. The effect of interference on the shape of the $WZjj$ -EW MC template in the $W^\pm Zjj$ -QCD CR is negligible and is therefore not included.

Systematic uncertainties affecting the reconstruction and energy calibration of jets, electrons and muons are propagated through the analysis. The dominant sources of uncertainties are the jet energy scale calibration, including the modelling of pile-up. The uncertainties in the jet energy scale are obtained from $\sqrt{s} = 13$ TeV simulations and *in situ* measurements [47]. The uncertainty in the jet energy resolution [58] and in the suppression of jets originating from pile-up are also considered [46]. The uncertainties in the b -tagging efficiency and the mistag rate are also taken into account. The effect of jet uncertainties on the expected number of events ranges from 10% to 3% at low and high values of the BDT score, respectively, with a similar effect for $WZjj$ -QCD and $WZjj$ -EW events.

The uncertainty in the E_T^{miss} measurement is estimated by propagating the uncertainties in the transverse momenta of hard physics objects and by applying momentum scale and resolution uncertainties to the track-based soft term [50,51].

The uncertainties due to lepton reconstruction, identification, isolation requirements and trigger efficiencies are estimated using tag-and-probe methods in $Z \rightarrow \ell\ell$ events [25,26]. Uncertainties in the lepton momentum scale and resolution are also assessed using $Z \rightarrow \ell\ell$ events [26,27]. These uncertainties impact the expected number of events by 1.4% and 0.4% for electrons and muons, respectively, and are independent of the BDT score. Their effect is similar for $WZjj$ -QCD and $WZjj$ -EW events.

A 40% yield uncertainty is assigned to the reducible background estimate. This takes into account the limited number of events in the control regions as well as the differences in background composition between the control regions used to determine the lepton misidentification rate and the control regions used to estimate the yield in the signal region. The uncertainty due to irreducible

Table 2

Summary of the relative uncertainties in the measured fiducial cross-section $\sigma_{WZjj-EW}^{\text{fid}}$. The uncertainties are reported as percentages.

Source	Uncertainty [%]
$WZjj$ -EW theory modelling	4.8
$WZjj$ -QCD theory modelling	5.2
$WZjj$ -EW and $WZjj$ -QCD interference	1.9
Jets	6.6
Pile-up	2.2
Electrons	1.4
Muons	0.4
b -tagging	0.1
MC statistics	1.9
Misid. lepton background	0.9
Other backgrounds	0.8
Luminosity	2.1
Total Systematics	10.9

background sources other than $WZjj$ -QCD is evaluated by propagating the uncertainty in their MC cross-sections. These are 20% for VVV [59], 15% for tZj [10] and $t\bar{t} + V$ [60], and 25% for $ZZjj$ -QCD to account for the potentially large impact of scale variations.

The uncertainty in the combined 2015+2016 integrated luminosity is 2.1%. It is derived, following a methodology similar to that detailed in Ref. [61], and using the LUCID-2 detector for the baseline luminosity measurements [62], from a calibration of the luminosity scale using x - y beam-separation scans.

The effect of the systematic uncertainties on the final results after the maximum-likelihood fit is shown in Table 2 where the breakdown of the contributions to the uncertainties in the measured fiducial cross-section $\sigma_{WZjj-EW}^{\text{fid}}$ is presented. The individual sources of systematic uncertainty are combined into theory modelling and experimental categories. As shown in the table, the systematic uncertainties in the jet reconstruction and calibration play a dominant role, followed by the uncertainties in the modelling of the $WZjj$ -EW signal and of the $WZjj$ -QCD background. Systematic uncertainties in the missing transverse momentum computation arise directly from the momentum and energy calibration of jets, electrons and muons and are included in the respective lines of Table 2. Systematic uncertainties in the modelling of the reducible and irreducible backgrounds other than $WZjj$ -QCD are also detailed.

9. Cross-section measurements

The signal strength $\mu_{WZjj-EW}$ and its uncertainty are determined with a profile-likelihood-ratio test statistic [63]. Systematic uncertainties in the input templates are treated as nuisance parameters with an assumed Gaussian distribution. The distributions of m_{jj} in the ZZ -CR control region, of $N_{b\text{-jets}}$ in the b -CR, of m_{jj} in the $WZjj$ -QCD control region and of the BDT score in the signal region, with background normalisations, signal normalisation and nuisance parameters adjusted by the profile-likelihood fit are shown in Fig. 2. The corresponding post-fit yields are detailed in Table 3. The table presents the integral of the BDT score distribution in the SR, but the uncertainty on the measured signal cross section is dominated by events at high BDT score. The signal strength is measured to be

$$\begin{aligned} \mu_{WZjj-EW} &= 1.77_{-0.40}^{+0.44} \text{ (stat.) }_{-0.12}^{+0.15} \text{ (exp. syst.)} \\ &\quad_{-0.12}^{+0.15} \text{ (mod. syst.) }_{-0.13}^{+0.15} \text{ (theory) }_{-0.02}^{+0.04} \text{ (lumi.)} \\ &= 1.77_{-0.45}^{+0.51}, \end{aligned}$$

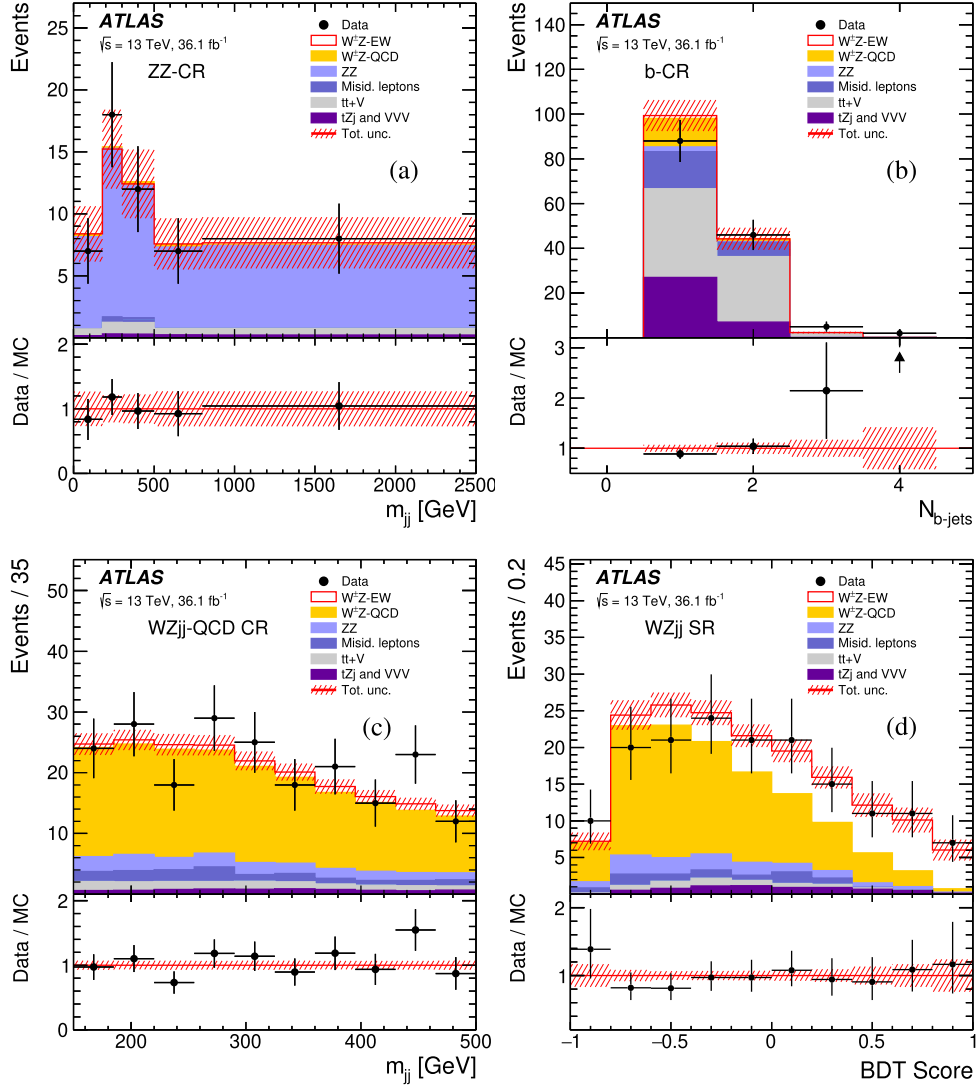


Fig. 2. Post-fit distributions of (a) m_{jj} in the ZZ-CR control region, (b) $N_{b\text{-jets}}$ in the b -CR, (c) m_{jj} in the $WZjj\text{-QCD}$ control region and (d) the BDT score distribution in the signal region. Signal and backgrounds are normalised to the expected number of events after the fit. The uncertainty band around the MC expectation includes all systematic uncertainties as obtained from the fit.

Table 3

Observed and expected numbers of events in the $W^\pm Zjj$ signal region and in the three control regions, after the fit. The expected number of $WZjj\text{-EW}$ events from SHERPA and the estimated number of background events from the other processes are shown. The sum of the backgrounds containing misidentified leptons is labelled 'Misid. leptons'. The total correlated post-fit uncertainties are quoted.

	SR	$WZjj\text{-QCD}$ CR	b -CR	ZZ-CR
Data	161	213	141	52
Total predicted	167 ± 11	204 ± 12	146 ± 11	51.3 ± 7.0
$WZjj\text{-EW}$ (signal)	44 ± 11	8.52 ± 0.41	1.38 ± 0.10	0.211 ± 0.004
$WZjj\text{-QCD}$	91 ± 10	144 ± 14	13.9 ± 3.8	0.94 ± 0.14
Misid. leptons	7.8 ± 3.2	14.0 ± 5.7	23.5 ± 9.6	0.41 ± 0.18
$ZZjj\text{-QCD}$	11.1 ± 2.8	18.3 ± 1.1	2.35 ± 0.06	40.8 ± 7.2
tZj	6.2 ± 1.1	6.3 ± 1.1	34.0 ± 5.3	0.17 ± 0.04
$t\bar{t} + V$	4.7 ± 1.0	11.14 ± 0.37	71 ± 15	3.47 ± 0.54
$ZZjj\text{-EW}$	1.80 ± 0.45	0.44 ± 0.10	0.10 ± 0.03	4.2 ± 1.2
VVV	0.59 ± 0.15	0.93 ± 0.23	0.13 ± 0.03	1.06 ± 0.30

where the uncertainties correspond to statistical, experimental systematic, theory modelling and interference systematic, theory $\sigma_{WZjj\text{-EW}}^{\text{fid.,MC}}$ normalisation and luminosity uncertainties, respectively. The background-only hypothesis is excluded with a significance of

5.3 standard deviations, compared with 3.2 standard deviations expected. The normalisation parameters of the $WZjj\text{-QCD}$, $t\bar{t} + V$ and ZZ backgrounds constrained by data in the control and signal regions are measured to be $\mu_{WZjj\text{-QCD}} = 0.56 \pm 0.16$, $\mu_{t\bar{t}+V} =$

1.07 ± 0.28 and $\mu_{ZZjj\text{-QCD}} = 1.34 \pm 0.44$. The observed $WZjj\text{-EW}$ production integrated fiducial cross-section derived from this signal strength for a single leptonic decay mode is

$$\begin{aligned} \sigma_{WZjj\text{-EW}}^{\text{fid.}} &= 0.57^{+0.14}_{-0.13} \text{ (stat.) }^{+0.05}_{-0.04} \text{ (exp. syst.)} \\ &\quad +0.05^{+0.01}_{-0.04} \text{ (mod. syst.) }^{+0.01}_{-0.01} \text{ (lumi.) fb} \\ &= 0.57^{+0.16}_{-0.14} \text{ fb.} \end{aligned}$$

It corresponds to the cross-section of electroweak $W^\pm Zjj$ production, including interference effects between $WZjj\text{-QCD}$ and $WZjj\text{-EW}$ processes, in the fiducial phase space defined in Section 3 using dressed-level leptons.

The SM LO prediction from SHERPA for electroweak production without interference effects is

$$\sigma_{WZjj\text{-EW}}^{\text{fid., SHERPA}} = 0.321 \pm 0.002 \text{ (stat.) } \pm 0.005 \text{ (PDF)}^{+0.027}_{-0.023} \text{ (scale) fb,}$$

where the effects of uncertainties in the PDF and the α_s value used in the PDF determination, as well as the uncertainties due to the renormalisation and factorisation scales, are evaluated using the same procedure as the one described in Section 8.

A larger cross-section of $\sigma_{WZjj\text{-EW}}^{\text{fid., MadGraph}} = 0.366 \pm 0.004 \text{ (stat.) fb}$ is predicted by MADGRAPH. These predictions are at LO only and include neither the effects of interference, estimated at LO to be 10%, nor the effects of NLO electroweak corrections as calculated recently in Ref. [64].

From the number of observed events in the SR, the integrated cross-section of $W^\pm Zjj$ production in the VBS fiducial phase space defined in Section 3, including $WZjj\text{-EW}$ and $WZjj\text{-QCD}$ contributions and their interference, is measured. For a given channel $W^\pm Z \rightarrow \ell'^{\pm} \nu \ell'^+ \ell'^-$, where ℓ and ℓ' indicates each type of lepton (e or μ), the integrated fiducial cross section that includes the leptonic branching fractions of the W and Z bosons is calculated as

$$\sigma_{W^\pm Zjj}^{\text{fid.}} = \frac{N_{\text{data}} - N_{\text{bkg}}}{\mathcal{L} \cdot C_{WZjj}} \times \left(1 - \frac{N_\tau}{N_{\text{all}}} \right),$$

where N_{data} and N_{bkg} are the number of observed events and the estimated number of background events in the SR, respectively, and \mathcal{L} is the integrated luminosity. The factor C_{WZjj} , obtained from simulation, is the ratio of the number of selected signal events at detector level to the number of events at particle level in the fiducial phase space. This factor corrects for detector efficiencies and for QED final-state radiation effects. The contribution from τ -lepton decays, amounting to 4.7%, is removed from the cross-section definition by introducing the term in parentheses. This term is computed using simulation, where N_τ is the number of selected events at detector level in which at least one of the bosons decays into a τ -lepton and N_{all} is the number of selected WZ events with decays into any lepton. The C_{WZjj} factor calculated with SHERPA for the sum of the four measured decay channels is 0.52 with a negligible statistical uncertainty. This factor is the same for $WZjj\text{-QCD}$ and $WZjj\text{-EW}$ events, as predicted by SHERPA. The theory modelling uncertainty in this factor is 8%, as estimated from the difference between the SHERPA and MADGRAPH predictions. The uncertainties on this factor due to higher order QCD scale corrections or PDF are negligible.

The measured $W^\pm Zjj$ cross-section in the fiducial phase space for a single leptonic decay mode is

$$\begin{aligned} \sigma_{W^\pm Zjj}^{\text{fid.}} &= 1.68 \pm 0.16 \text{ (stat.) } \pm 0.12 \text{ (exp. syst.)} \\ &\quad \pm 0.13 \text{ (mod. syst.) } \pm 0.044 \text{ (lumi.) fb,} \\ &= 1.68 \pm 0.25 \text{ fb,} \end{aligned}$$

where the uncertainties correspond to statistical, experimental systematic, theory modelling systematic, and luminosity uncertainties, respectively. The corresponding prediction from SHERPA for strong and electroweak production without interference effects is

$$\sigma_{W^\pm Zjj}^{\text{fid., SHERPA}} = 2.15 \pm 0.01 \text{ (stat.) } \pm 0.05 \text{ (PDF)}^{+0.65}_{-0.44} \text{ (scale) fb.}$$

Events in the SR are also used to measure the $W^\pm Zjj$ differential production cross-section in the VBS fiducial phase space. The differential detector-level distributions are corrected for detector resolution using an iterative Bayesian unfolding method [65], as implemented in the RooUnfold toolkit [66]. Three iterations were used for the unfolding of each variable. The width of the bins in each distribution is chosen according to the experimental resolution and to the statistical significance of the expected number of events in that bin. The fraction of signal MC events reconstructed in the same bin as generated is always greater than 40% and around 70% on average.

For each distribution, simulated $W^\pm Zjj$ events are used to obtain a response matrix that accounts for bin-to-bin migration effects between the reconstruction-level and particle-level distributions. The SHERPA MC samples for $WZjj\text{-EW}$ and $WZjj\text{-QCD}$ production are added together to model $W^\pm Zjj$ production. To more closely model the data and to minimise unfolding uncertainties, their predicted cross-sections are rescaled by the respective signal strengths of 1.77 and 0.56 for the $WZjj\text{-EW}$ and $WZjj\text{-QCD}$ contributions, respectively, as measured in data by the maximum-likelihood fit.

Uncertainties in the unfolding due to imperfect modelling of the data by the MC simulation are evaluated using a data-driven method [67], where the MC differential distribution is corrected to match the data distribution and the resulting weighted MC distribution at reconstruction level is unfolded with the response matrix used in the data unfolding. The new unfolded distribution is compared with the weighted MC distribution at generator level and the difference is taken as the systematic uncertainty. The uncertainties obtained range from 0.1% to 25% depending on the resolution of the unfolded observables and on the quality of its description by SHERPA.

Measurements are performed as a function of three variables sensitive to anomalies in the quartic gauge coupling in $W^\pm Zjj$ events [10], namely the scalar sum of the transverse momenta of the three charged leptons associated with the W and Z bosons $\sum p_T^\ell$, the difference in azimuthal angle $\Delta\phi(W, Z)$ between the W and Z bosons' directions, and the transverse mass of the $W^\pm Z$ system m_\perp^{WZ} , defined following Ref. [10]. These are presented in Fig. 3.

Measurements are also performed as a function of variables related to the kinematics of jets. The exclusive multiplicity of jets, N_{jets} , is shown in Fig. 4. The absolute difference in rapidity between the two tagging jets Δy_{jj} , the invariant mass of the tagging jets m_{jj} , the exclusive multiplicity $N_{\text{jets}}^{\text{gap}}$ of jets with $p_T > 25$ GeV in the gap in η between the two tagging jets, and the azimuthal angle between the two tagging jets $\Delta\phi_{jj}$ are shown in Fig. 5.

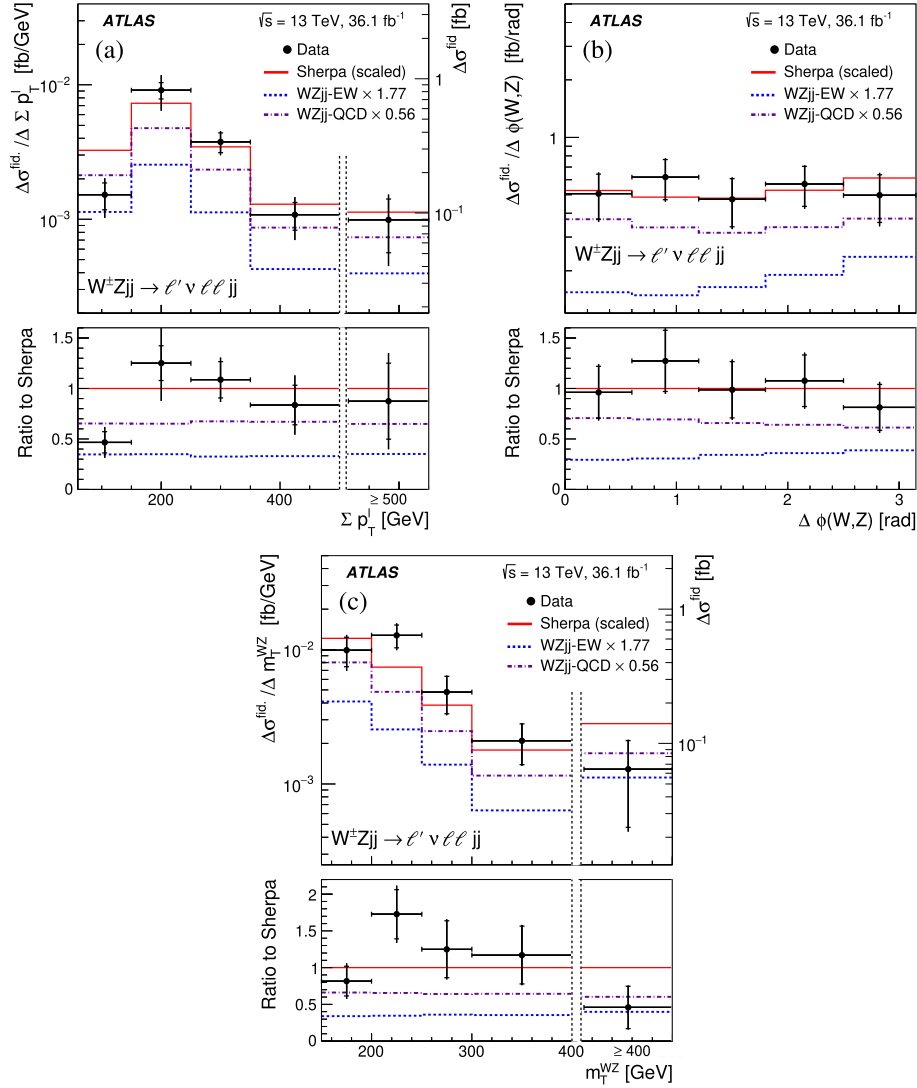


Fig. 3. The measured $W^\pm Zjj$ differential cross-section in the VBS fiducial phase space as a function of (a) $\sum p_T^\ell$, (b) $\Delta\phi(W, Z)$ and (c) m_{WZ}^{WZ} . The inner and outer error bars on the data points represent the statistical and total uncertainties, respectively. The measurements are compared with the sum of the rescaled $WZjj$ -QCD and $WZjj$ -EW predictions from SHERPA (solid line). The $WZjj$ -EW and $WZjj$ -QCD contributions are also represented by dashed and dashed-dotted lines, respectively. In (a) and (c), the right y-axis refers to the last cross-section point, separated from the others by a vertical dashed line, as this last bin is integrated up to the maximum value reached in the phase space. The lower panels show the ratios of the data to the predictions from SHERPA. The uncertainty on the SHERPA prediction is dominated by the QCD scale uncertainty on the $WZjj$ -QCD predicted cross-section, whose envelope is of $^{+30\%}_{-20\%}$ and it is not represented on the figure.

Total uncertainties in the measurements are dominated by statistical uncertainties. The differential measurements are compared with the prediction from SHERPA, after having rescaled the separate $WZjj$ -QCD and $WZjj$ -EW components by the global $\mu_{WZjj-QCD}$ and $\mu_{WZjj-EW}$ parameters, respectively, obtained from the profile-likelihood fit to data. Interference effects between the $WZjj$ -QCD and $WZjj$ -EW processes are incorporated via the $\mu_{WZjj-EW}$ parameter as a change of the global normalisation of the SHERPA electroweak prediction.

10. Conclusion

An observation of electroweak production of a diboson $W^\pm Z$ system in association with two jets and measurements of its production cross-section in $\sqrt{s} = 13$ TeV pp collisions at the LHC are presented. The data were collected with the ATLAS detector and correspond to an integrated luminosity of 36.1 fb^{-1} . The measurements use leptonic decays of the gauge bosons into electrons or muons and are performed in a fiducial phase space approximating

the detector acceptance that increases the sensitivity to $W^\pm Zjj$ electroweak production modes.

The electroweak production of $W^\pm Z$ bosons in association with two jets is measured with observed and expected significances of 5.3 and 3.2 standard deviations, respectively. The measured fiducial cross-section for electroweak production including interference effects is

$$\sigma_{WZjj-EW} = 0.57^{+0.14}_{-0.13} (\text{stat.})^{+0.05}_{-0.04} (\text{exp. syst.}) \\ +^{+0.05}_{-0.04} (\text{mod. syst.})^{+0.01}_{-0.01} (\text{lumi.}) \text{ fb.}$$

It is found to be larger than the LO SM prediction of $0.32 \pm 0.03 \text{ fb}$ as calculated with the SHERPA MC event generator that includes neither interference effects, estimated at LO to be 10%, nor NLO electroweak corrections. Differential cross-sections of $W^\pm Zjj$ production, including both the strong and electroweak processes, are also measured in the same fiducial phase space as a function of several kinematic observables.

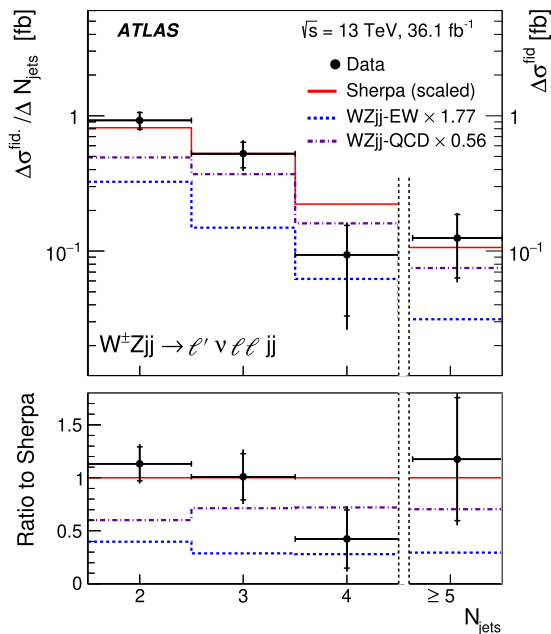


Fig. 4. The measured $W^\pm Zjj$ differential cross-section in the VBS fiducial phase space as a function of the exclusive jet multiplicity of jets with $p_T > 40$ GeV. The inner and outer error bars on the data points represent the statistical and total uncertainties, respectively. The measurements are compared with the sum of the scaled $WZjj$ -QCD and $WZjj$ -EW predictions from SHERPA (solid line). The $WZjj$ -EW and $WZjj$ -QCD contributions are also represented by dashed and dashed-dotted lines, respectively. The right y-axis refers to the last cross-section point, separated from the others by a vertical dashed line, as this last bin is integrated up to the maximum value reached in the phase space. The lower panel shows the ratio of the data to the prediction from SHERPA. The uncertainty on the SHERPA prediction is dominated by the QCD scale uncertainty on the $WZjj$ -QCD predicted cross-section, whose envelope is of $^{+30\%}_{-20\%}$ and it is not represented on the figure.

Acknowledgements

We thank CERN for the very successful operation of the LHC, as well as the support staff from our institutions without whom ATLAS could not be operated efficiently.

We acknowledge the support of ANPCyT, Argentina; YerPhI, Armenia; ARC, Australia; BMWFW and FWF, Austria; ANAS, Azerbaijan; SSTC, Belarus; CNPq and FAPESP, Brazil; NSERC, NRC and CFI, Canada; CERN; CONICYT, Chile; CAS, MOST and NSFC, China; COLCIENCIAS, Colombia; MSMT CR, MPO CR and VSC CR, Czech Republic; DNRf and DNSRC, Denmark; IN2P3-CNRS, CEA-DRF/IRFU, France; SRNSFG, Georgia; BMBF, HGF, and MPG, Germany; GSRT, Greece; RGC, Hong Kong SAR, China; ISF and Benozzi Center, Israel; INFN, Italy; MEXT and JSPS, Japan; CNRS, Morocco; NWO, Netherlands; RCN, Norway; MNiSW and NCN, Poland; FCT, Portugal; MNE/IFA, Romania; MES of Russia and NRC KI, Russian Federation; JINR; MESTD, Serbia; MSSR, Slovakia; ARRS and MIZŠ, Slovenia; DST/NRF, South Africa; MINECO, Spain; SRC and Wallenberg Foundation, Sweden; SERI, SNSF and Cantons of Bern and Geneva, Switzerland; MOST, Taiwan; TAEK, Turkey; STFC, United Kingdom; DOE and NSF, United States of America. In addition, individual groups and members have received support from BCKDF, Canarie, CRC and Compute Canada, Canada; COST, ERC, ERDF, Horizon 2020, and Marie Skłodowska-Curie Actions, European Union; Investissements d'Avenir Labex and Idex, ANR, France; DFG and AvH Foundation, Germany; Herakleitos, Thales and Aristeia programmes co-financed by EU-ESF and the Greek NSRF, Greece; BSF-NSF and GIF, Israel; CERCA Programme Generalitat de Catalunya, Spain; The Royal Society and Leverhulme Trust, United Kingdom.

The crucial computing support from all WLCG partners is acknowledged gratefully, in particular from CERN, the ATLAS Tier-1 facilities at TRIUMF (Canada), NDGF (Denmark, Norway, Sweden), CC-IN2P3 (France), KIT/GridKA (Germany), INFN-CNAF (Italy), NL-T1 (Netherlands), PIC (Spain), ASGC (Taiwan), RAL (UK) and BNL (USA), the Tier-2 facilities worldwide and large non-WLCG resource providers. Major contributors of computing resources are listed in Ref. [68].

References

- [1] O.J.P. Eboli, M.C. Gonzalez-Garcia, S.M. Lietti, Bosonic quartic couplings at CERN LHC, *Phys. Rev. D* 69 (2004) 095005, arXiv:hep-ph/0310141 [hep-ph].
- [2] O. Eboli, M. Gonzalez-Garcia, J. Mizukoshi, $pp \rightarrow jj e^\pm \mu^\pm \nu \nu$ and $jj e^\pm \mu^\pm \nu \nu$ at $O(\alpha_{em}^6)$ and $O(\alpha_{em}^4 \alpha_s^2)$ for the study of the quartic electroweak gauge boson vertex at CERN LHC, *Phys. Rev. D* 74 (2006) 073005, arXiv:hep-ph/0606118 [hep-ph].
- [3] C. Degrande, et al., Effective field theory: a modern approach to anomalous couplings, *Ann. Phys.* 335 (2013) 21, arXiv:1205.4231 [hep-ph].
- [4] R.N. Cahn, S.D. Ellis, R. Kleiss, W.J. Stirling, Transverse-momentum signatures for heavy Higgs bosons, *Phys. Rev. D* 35 (1987) 1626.
- [5] E. Accomando, A. Ballestrero, A. Belhouari, E. Maina, Isolating vector boson scattering at the CERN LHC: gauge cancellations and the equivalent vector boson approximation versus complete calculations, *Phys. Rev. D* 74 (2006) 073010, arXiv:hep-ph/0608019 [hep-ph].
- [6] CMS Collaboration, Observation of electroweak production of same-sign W boson pairs in the two jet and two same-sign lepton final state in proton-proton collisions at $\sqrt{s} = 13$ TeV, *Phys. Rev. Lett.* 120 (2018) 081801, arXiv:1709.05822 [hep-ex].
- [7] ATLAS Collaboration, Evidence for electroweak production of $W^\pm W^\pm jj$ in pp collisions at $\sqrt{s} = 8$ TeV with the ATLAS detector, *Phys. Rev. Lett.* 113 (2014) 141803, arXiv:1405.6241 [hep-ex].
- [8] ATLAS Collaboration, Measurement of $W^\pm W^\pm$ vector-boson scattering and limits on anomalous quartic gauge couplings with the ATLAS detector, *Phys. Rev. D* 96 (2017) 012007, arXiv:1611.02428 [hep-ex].
- [9] CMS Collaboration, Measurement of the cross section for electroweak production of $Z\gamma$ in association with two jets and constraints on anomalous quartic gauge couplings in proton-proton collisions at $\sqrt{s} = 8$ TeV, *Phys. Lett. B* 770 (2017) 380, arXiv:1702.03025 [hep-ex].
- [10] ATLAS Collaboration, Measurements of $W^\pm Z$ production cross sections in pp collisions at $\sqrt{s} = 8$ TeV with the ATLAS detector and limits on anomalous gauge boson self-couplings, *Phys. Rev. D* 93 (2016) 092004, arXiv:1603.02151 [hep-ex].
- [11] CMS Collaboration, Measurement of electroweak WZ boson production and search for new physics in $WZ +$ two jets events in pp collisions at $\sqrt{s} = 13$ TeV, arXiv:1901.04060 [hep-ex], 2019.
- [12] CMS Collaboration, Measurement of vector boson scattering and constraints on anomalous quartic couplings from events with four leptons and two jets in proton-proton collisions at $\sqrt{s} = 13$ TeV, *Phys. Lett. B* 774 (2017) 682, arXiv:1708.02812 [hep-ex].
- [13] ATLAS Collaboration, Studies of $Z\gamma$ production in association with a high-mass dijet system in pp collisions at $\sqrt{s} = 8$ TeV with the ATLAS detector, *J. High Energy Phys.* 07 (2017) 107, arXiv:1705.01966 [hep-ex].
- [14] CMS Collaboration, Measurement of electroweak-induced production of $W\gamma$ with two jets in pp collisions at $\sqrt{s} = 8$ TeV and constraints on anomalous quartic gauge couplings, *J. High Energy Phys.* 06 (2017) 106, arXiv:1612.09256 [hep-ex].
- [15] ATLAS Collaboration, The ATLAS experiment at the CERN large hadron collider, *J. Instrum.* 3 (2008) S08003.
- [16] ATLAS Collaboration, Performance of the ATLAS trigger system in 2015, *Eur. Phys. J. C* 77 (2017) 317, arXiv:1611.09661 [hep-ex].
- [17] ATLAS Collaboration, Measurement of the $W^\pm Z$ boson pair-production cross section in pp collisions at $\sqrt{s} = 13$ TeV with the ATLAS detector, *Phys. Lett. B* 762 (2016) 1, arXiv:1606.04017 [hep-ex].
- [18] M. Tanabashi, et al., Review of Particle Physics, *Phys. Rev. D* 98 (2018) 030001.
- [19] M. Cacciari, G.P. Salam, G. Soyez, The anti- k_t jet clustering algorithm, *J. High Energy Phys.* 04 (2008) 063, arXiv:0802.1189 [hep-ph].
- [20] ATLAS Collaboration, The ATLAS simulation infrastructure, *Eur. Phys. J. C* 70 (2010) 823, arXiv:1005.4568 [physics.ins-det].
- [21] S. Agostinelli, et al., GEANT4: a simulation toolkit, *Nucl. Instrum. Methods A* 506 (2003) 250.
- [22] T. Sjöstrand, S. Mrenna, P.Z. Skands, A brief introduction to PYTHIA 8.1, *Comput. Phys. Commun.* 178 (2008) 852, arXiv:0710.3820 [hep-ph].
- [23] A.D. Martin, W.J. Stirling, R.S. Thorne, G. Watt, Parton distributions for the LHC, *Eur. Phys. J. C* 63 (2009) 189, arXiv:0901.0002 [hep-ph].
- [24] ATLAS Collaboration, Summary of ATLAS Pythia 8 Tunes, ATL-PHYS-PUB-2012-003. CERN, 2012, <http://cds.cern.ch/record/1474107>.

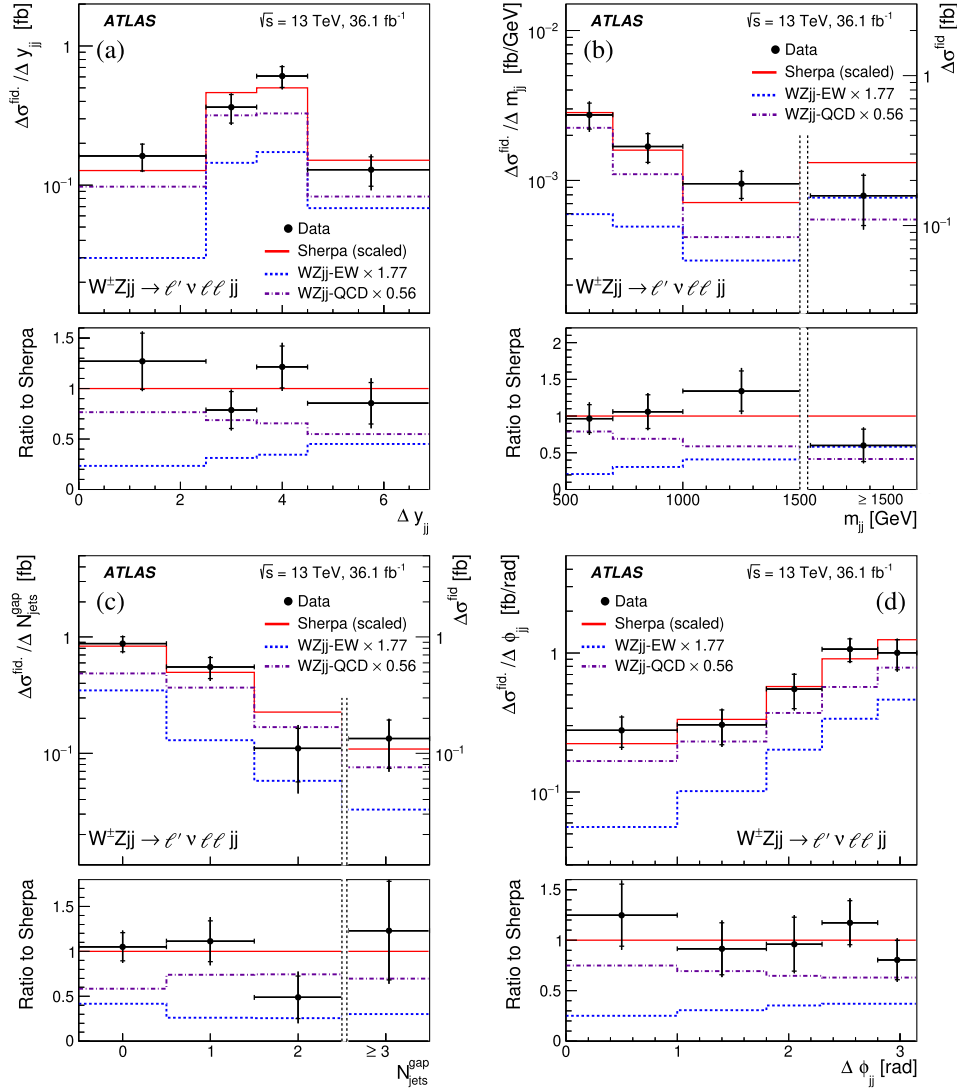


Fig. 5. The measured $W^\pm Zjj$ differential cross-section in the VBS fiducial phase space as a function of (a) the absolute difference in rapidity between the two tagging jets Δy_{jj} , (b) the invariant mass of the tagging jets m_{jj} , (c) N_{jets}^{gap} the exclusive jet multiplicity of jets with $p_T > 25$ GeV in the gap between the two tagging jets, and (d) the azimuthal angle between the two tagging jets $\Delta\phi_{jj}$. The inner and outer error bars on the data points represent the statistical and total uncertainties, respectively. The measurements are compared with the sum of the rescaled $WZjj$ -QCD and $WZjj$ -EW predictions from SHERPA (solid line). The $WZjj$ -EW and $WZjj$ -QCD contributions are also represented by dashed and dashed-dotted lines, respectively. In (b) and (c), the right y-axis refers to the last cross-section point, separated from the others by a vertical dashed line, as this last bin is integrated up to the maximum value reached in the phase space. The lower panels show the ratios of the data to the predictions from SHERPA. The uncertainty on the SHERPA prediction is dominated by the QCD scale uncertainty on the $WZjj$ -QCD predicted cross-section, whose envelope is of $_{-30}^{+30}\%$ and it is not represented on the figure.

- [25] ATLAS Collaboration, Electron Efficiency Measurements With the ATLAS Detector Using the 2015 LHC Proton-Proton Collision Data, Tech. rep. ATLAS-CONF-2016-024, CERN, 2016, <http://cds.cern.ch/record/2157687>.
- [26] ATLAS Collaboration, Muon reconstruction performance of the ATLAS detector in proton-proton collision data at $\sqrt{s} = 13$ TeV, Eur. Phys. J. C 76 (2016) 292, arXiv:1603.05598 [hep-ex].
- [27] ATLAS Collaboration, Electron and photon energy calibration with the ATLAS detector using 2015-2016 LHC proton-proton collision data, arXiv:1812.03848 [hep-ex], 2018.
- [28] T. Gleisberg, et al., Event generation with SHERPA 1.1, J. High Energy Phys. 02 (2009) 007, arXiv:0811.4622 [hep-ph].
- [29] T. Gleisberg, S. Höche, Comix, a new matrix element generator, J. High Energy Phys. 12 (2008) 039, arXiv:0808.3674 [hep-ph].
- [30] S. Schumann, F. Krauss, A parton shower algorithm based on Catani-Seymour dipole factorisation, J. High Energy Phys. 03 (2008) 038, arXiv:0709.1027 [hep-ph].
- [31] S. Catani, F. Krauss, R. Kuhn, B.R. Webber, QCD matrix elements + parton showers, J. High Energy Phys. 11 (2001) 063, arXiv:hep-ph/0109231 [hep-ph].
- [32] S. Höche, F. Krauss, S. Schumann, F. Siegert, QCD matrix elements and truncated showers, J. High Energy Phys. 05 (2009) 053, arXiv:0903.1219 [hep-ph].
- [33] S. Höche, F. Krauss, M. Schonherr, F. Siegert, QCD matrix elements + parton showers: the NLO case, J. High Energy Phys. 04 (2013) 027, arXiv:1207.5030 [hep-ph].
- [34] J.-C. Winter, F. Krauss, G. Soff, A modified cluster-hadronisation model, Eur. Phys. J. C 36 (2004) 381, arXiv:hep-ph/0311085 [hep-ph].
- [35] M. Schönherr, F. Krauss, Soft photon radiation in particle decays in SHERPA, J. High Energy Phys. 12 (2008) 018, arXiv:0810.5071 [hep-ph].
- [36] R.D. Ball, et al., Parton distributions for the LHC run II, J. High Energy Phys. 04 (2015) 040, arXiv:1410.8849 [hep-ph].
- [37] J. Alwall, et al., The automated computation of tree-level and next-to-leading order differential cross sections, and their matching to parton shower simulations, J. High Energy Phys. 07 (2014) 079, arXiv:1405.0301 [hep-ph].
- [38] P. Nason, A new method for combining NLO QCD with shower Monte Carlo algorithms, J. High Energy Phys. 11 (2004) 040, arXiv:hep-ph/0409146 [hep-ph].
- [39] S. Frixione, P. Nason, C. Oleari, Matching NLO QCD computations with parton shower simulations: the POWHEG method, J. High Energy Phys. 11 (2007) 070, arXiv:0709.2092 [hep-ph].
- [40] S. Alioli, P. Nason, C. Oleari, E. Re, A general framework for implementing NLO calculations in shower Monte Carlo programs: the POWHEG BOX, J. High Energy Phys. 06 (2010) 043, arXiv:1002.2581 [hep-ph].

- [41] T. Melia, P. Nason, R. Röntsch, G. Zanderighi, W^+W^- , WZ and ZZ production in the POWHEG BOX, *J. High Energy Phys.* 11 (2011) 078, arXiv:1107.5051 [hep-ph].
- [42] M. Bähr, et al., Herwig++ physics and manual, *Eur. Phys. J. C* 58 (2008) 639, arXiv:0803.0883 [hep-ph].
- [43] H.-L. Lai, et al., New parton distributions for collider physics, *Phys. Rev. D* 82 (2010) 074024, arXiv:1007.2241 [hep-ph].
- [44] ATLAS Collaboration, Topological cell clustering in the ATLAS calorimeters and its performance in LHC Run 1, *Eur. Phys. J. C* 77 (2017) 490, arXiv:1603.02934 [hep-ex].
- [45] ATLAS Collaboration, Selection of jets produced in 13 TeV proton-proton collisions with the ATLAS detector, ATLAS-CONF-2015-029, <http://cdsweb.cern.ch/record/2037702>, 2015.
- [46] ATLAS Collaboration, Performance of pile-up mitigation techniques for jets in pp collisions at $\sqrt{s} = 8$ TeV using the ATLAS detector, *Eur. Phys. J. C* 76 (2016) 581, arXiv:1510.03823 [hep-ex].
- [47] ATLAS Collaboration, Jet energy scale measurements and their systematic uncertainties in proton-proton collisions at $\sqrt{s} = 13$ TeV with the ATLAS detector, *Phys. Rev. D* 96 (2017) 072002, arXiv:1703.09665 [hep-ex].
- [48] ATLAS Collaboration, Performance of b -jet identification in the ATLAS experiment, *J. Instrum.* 11 (2016) P04008, arXiv:1512.01094 [hep-ex].
- [49] ATLAS Collaboration, Optimisation of the ATLAS b -Tagging Performance for the 2016 LHC Run, Tech. rep. ATL-PHYS-PUB-2016-012, CERN, 2016, <http://cdsweb.cern.ch/record/2160731>.
- [50] ATLAS Collaboration, Performance of missing transverse momentum reconstruction with the ATLAS detector using proton-proton collisions at $\sqrt{s} = 13$ TeV, *Eur. Phys. J. C* 78 (2018) 903, arXiv:1802.08168 [hep-ex].
- [51] ATLAS Collaboration, E_T^{miss} Performance in the ATLAS Detector Using 2015–2016 LHC $p-p$ Collisions, Tech. rep. ATLAS-CONF-2018-023, CERN, 2018, <http://cds.cern.ch/record/2625233>.
- [52] K.A. Olive, et al., *Rev. Part. Phys., Chin. Phys. C* 38 (2014) 090001.
- [53] ATLAS Collaboration, Search for supersymmetry at $\sqrt{s} = 8$ TeV in final states with jets and two same-sign leptons or three leptons with the ATLAS detector, *J. High Energy Phys.* 06 (2014) 035, arXiv:1404.2500 [hep-ex].
- [54] A. Hoecker, et al., TMVA: toolkit for multivariate data analysis, *PoS ACAT* (2007) 040, arXiv:physics/0703039.
- [55] ATLAS Collaboration, Measurement of WZ production in proton-proton collisions at $\sqrt{s} = 7$ TeV with the ATLAS detector, *Eur. Phys. J. C* 72 (2012) 2173, arXiv:1208.1390 [hep-ex].
- [56] J. Butterworth, et al., PDF4LHC recommendations for LHC Run II, *J. Phys. G* 43 (2016) 023001, arXiv:1510.03865 [hep-ph].
- [57] ATLAS Collaboration, Modelling of the Vector Boson Scattering Process $pp \rightarrow W^\pm W^\pm jj$ in Monte Carlo Generators in ATLAS, Tech. rep. ATL-PHYS-PUB-2019-004, CERN, 2019, <http://cds.cern.ch/record/2655303>.
- [58] ATLAS Collaboration, Jet energy resolution in proton-proton collisions at $\sqrt{s} = 7$ TeV recorded in 2010 with the ATLAS detector, *Eur. Phys. J. C* 73 (2013) 2306, arXiv:1210.6210 [hep-ex].
- [59] ATLAS Collaboration, Multi-boson simulation for 13 TeV ATLAS analyses, ATL-PHYS-PUB-2016-002, 2016, <http://cds.cern.ch/record/2119986>.
- [60] Modelling of the $t\bar{t}H$ and $t\bar{t}V$ ($V = W, Z$) Processes for $\sqrt{s} = 13$ TeV ATLAS Analyses, tech. rep. ATL-PHYS-PUB-2016-005, CERN, 2016, <https://cds.cern.ch/record/2120826>.
- [61] ATLAS Collaboration, Luminosity determination in pp collisions at $\sqrt{s} = 8$ TeV using the ATLAS detector at the LHC, *Eur. Phys. J. C* 76 (2016) 653, arXiv:1608.03953 [hep-ex].
- [62] G. Avoni, et al., The new LUCID-2 detector for luminosity measurement and monitoring in ATLAS, *J. Instrum.* 13 (2018) P07017.
- [63] G. Cowan, K. Cranmer, E. Gross, O. Vitells, Asymptotic formulae for likelihood-based tests of new physics, *Eur. Phys. J. C* 71 (2011) 1554, arXiv:1007.1727 [physics.data-an].
- [64] A. Denner, S. Dittmaier, P. Maierhöfer, M. Pellen, C. Schwan, QCD and electroweak corrections to WZ scattering at the LHC, arXiv:1904.00882 [hep-ph], 2019.
- [65] G. D'Agostini, A multidimensional unfolding method based on Bayes' theorem, *Nucl. Instrum. Methods A* 362 (1995) 487.
- [66] T. Adye, Unfolding Algorithms and Tests Using RooUnfold, Proceedings of the PHYSTAT 2011 Workshop, CERN, Geneva, Switzerland, 2011, p. 313, arXiv:1105.1160 [physics.data-an].
- [67] B. Malaescu, An Iterative, Dynamically Stabilized (IDS) Method of Data Unfolding, Proceedings of the PHYSTAT 2011 Workshop, CERN, Geneva, Switzerland, 2011, p. 271, arXiv:1106.3107 [physics.data-an].
- [68] ATLAS Collaboration, ATLAS computing acknowledgements, ATL-GEN-PUB-2016-002, <https://cds.cern.ch/record/2202407>.

The ATLAS Collaboration

M. Aaboud^{35d}, G. Aad¹⁰⁰, B. Abbott¹²⁷, O. Abidinov^{13,*}, B. Abeloos¹³¹, D.K. Abhayasinghe⁹², S.H. Abidi¹⁶⁶, O.S. AbouZeid⁴⁰, N.L. Abraham¹⁵⁵, H. Abramowicz¹⁶⁰, H. Abreu¹⁵⁹, Y. Abulaiti⁶, B.S. Acharya^{65a,65b,n}, S. Adachi¹⁶², L. Adam⁹⁸, C. Adam Bourdarios¹³¹, L. Adamczyk^{82a}, J. Adelman¹²⁰, M. Adersberger¹¹³, A. Adiguzel^{12c}, T. Adye¹⁴³, A.A. Affolder¹⁴⁵, Y. Afik¹⁵⁹, C. Agheorghiesei^{27c}, J.A. Aguilar-Saavedra^{139f,139a}, F. Ahmadov^{78,ac}, G. Aielli^{72a,72b}, S. Akatsuka⁸⁴, T.P.A. Åkesson⁹⁵, E. Akilli⁵³, A.V. Akimov¹⁰⁹, G.L. Alberghi^{23b,23a}, J. Albert¹⁷⁵, P. Albicocco⁵⁰, M.J. Alconada Verzini⁸⁷, S. Alderweireldt¹¹⁸, M. Aleksa³⁶, I.N. Aleksandrov⁷⁸, C. Alexa^{27b}, T. Alexopoulos¹⁰, M. Alhroob¹²⁷, B. Ali¹⁴¹, G. Alimonti^{67a}, J. Alison³⁷, S.P. Alkire¹⁴⁷, C. Allaire¹³¹, B.M.M. Allbrooke¹⁵⁵, B.W. Allen¹³⁰, P.P. Allport²¹, A. Aloisio^{68a,68b}, A. Alonso⁴⁰, F. Alonso⁸⁷, C. Alpigiani¹⁴⁷, A.A. Alshehri⁵⁶, M.I. Alstady¹⁰⁰, B. Alvarez Gonzalez³⁶, D. Álvarez Piqueras¹⁷³, M.G. Alviggi^{68a,68b}, B.T. Amadio¹⁸, Y. Amaral Coutinho^{79b}, A. Ambler¹⁰², L. Ambroz¹³⁴, C. Amelung²⁶, D. Amidei¹⁰⁴, S.P. Amor Dos Santos^{139a,139c}, S. Amoroso⁴⁵, C.S. Amrouche⁵³, C. Anastopoulos¹⁴⁸, L.S. Ancu⁵³, N. Andari¹⁴⁴, T. Andeen¹¹, C.F. Anders^{60b}, J.K. Anders²⁰, K.J. Anderson³⁷, A. Andreazza^{67a,67b}, V. Andrei^{60a}, C.R. Anelli¹⁷⁵, S. Angelidakis³⁸, I. Angelozzi¹¹⁹, A. Angerami³⁹, A.V. Anisenkov^{121b,121a}, A. Annovi^{70a}, C. Antel^{60a}, M.T. Anthony¹⁴⁸, M. Antonelli⁵⁰, D.J.A. Antrim¹⁷⁰, F. Anulli^{71a}, M. Aoki⁸⁰, J.A. Aparisi Pozo¹⁷³, L. Aperio Bella³⁶, G. Arabidze¹⁰⁵, J.P. Araque^{139a}, V. Araujo Ferraz^{79b}, R. Araujo Pereira^{79b}, A.T.H. Arce⁴⁸, R.E. Ardell⁹², F.A. Arduh⁸⁷, J-F. Arguin¹⁰⁸, S. Argyropoulos⁷⁶, A.J. Armbruster³⁶, L.J. Armitage⁹¹, A. Armstrong¹⁷⁰, O. Arnaez¹⁶⁶, H. Arnold¹¹⁹, M. Arratia³², O. Arslan²⁴, A. Artamonov^{110,*}, G. Artoni¹³⁴, S. Artz⁹⁸, S. Asai¹⁶², N. Asbah⁵⁸, E.M. Asimakopoulou¹⁷¹, L. Asquith¹⁵⁵, K. Assamagan²⁹, R. Astalos^{28a}, R.J. Atkin^{33a}, M. Atkinson¹⁷², N.B. Atlay¹⁵⁰, K. Augsten¹⁴¹, G. Avolio³⁶, R. Avramidou^{59a}, M.K. Ayoub^{15a}, A.M. Azoulay^{167b}, G. Azuelos^{108,aq}, A.E. Baas^{60a}, M.J. Baca²¹, H. Bachacou¹⁴⁴, K. Bachas^{66a,66b}, M. Backes¹³⁴, P. Bagnaia^{71a,71b}, M. Bahmani⁸³, H. Bahrasemani¹⁵¹, A.J. Bailey¹⁷³, J.T. Baines¹⁴³, M. Bajic⁴⁰, C. Bakalis¹⁰, O.K. Baker¹⁸², P.J. Bakker¹¹⁹, D. Bakshi Gupta⁸, S. Balaji¹⁵⁶, E.M. Baldin^{121b,121a}, P. Balek¹⁷⁹, F. Balli¹⁴⁴, W.K. Balunas¹³⁶, J. Balz⁹⁸, E. Banas⁸³, A. Bandyopadhyay²⁴, Sw. Banerjee^{180,i}, A.A.E. Bannoura¹⁸¹, L. Barak¹⁶⁰, W.M. Barbe³⁸, E.L. Barberio¹⁰³, D. Barberis^{54b,54a},

M. Barbero ¹⁰⁰, T. Barillari ¹¹⁴, M-S. Barisits ³⁶, J. Barkeloo ¹³⁰, T. Barklow ¹⁵², R. Barnea ¹⁵⁹, S.L. Barnes ^{59c}, B.M. Barnett ¹⁴³, R.M. Barnett ¹⁸, Z. Barnovska-Blenessy ^{59a}, A. Baroncelli ^{73a}, G. Barone ²⁹, A.J. Barr ¹³⁴, L. Barranco Navarro ¹⁷³, F. Barreiro ⁹⁷, J. Barreiro Guimarães da Costa ^{15a}, R. Bartoldus ¹⁵², A.E. Barton ⁸⁸, P. Bartos ^{28a}, A. Basaliev ¹³⁷, A. Bassalat ^{131.ak}, R.L. Bates ⁵⁶, S.J. Batista ¹⁶⁶, S. Batlamous ^{35e}, J.R. Batley ³², M. Battaglia ¹⁴⁵, M. Baucé ^{71a,71b}, F. Bauer ¹⁴⁴, K.T. Bauer ¹⁷⁰, H.S. Bawa ^{31.l}, J.B. Beacham ¹²⁵, T. Beau ¹³⁵, P.H. Beauchemin ¹⁶⁹, P. Bechtel ²⁴, H.C. Beck ⁵², H.P. Beck ^{20.p}, K. Becker ⁵¹, M. Becker ⁹⁸, C. Becot ⁴⁵, A. Beddall ^{12d}, A.J. Beddall ^{12a}, V.A. Bednyakov ⁷⁸, M. Bedognetti ¹¹⁹, C.P. Bee ¹⁵⁴, T.A. Beermann ⁷⁵, M. Begalli ^{79b}, M. Biegel ²⁹, A. Behera ¹⁵⁴, J.K. Behr ⁴⁵, A.S. Bell ⁹³, G. Bella ¹⁶⁰, L. Bellagamba ^{23b}, A. Bellerive ³⁴, M. Bellomo ¹⁵⁹, P. Bellos ⁹, K. Belotskiy ¹¹¹, N.L. Belyaev ¹¹¹, O. Benary ^{160.*}, D. Bencheikroun ^{35a}, M. Bender ¹¹³, N. Benekos ¹⁰, Y. Benhammou ¹⁶⁰, E. Benhar Noccioli ¹⁸², J. Benitez ⁷⁶, D.P. Benjamin ⁴⁸, M. Benoit ⁵³, J.R. Bensinger ²⁶, S. Bentvelsen ¹¹⁹, L. Beresford ¹³⁴, M. Beretta ⁵⁰, D. Berge ⁴⁵, E. Bergeaas Kuutmann ¹⁷¹, N. Berger ⁵, B. Bergmann ¹⁴¹, L.J. Bergsten ²⁶, J. Beringer ¹⁸, S. Berlendis ⁷, N.R. Bernard ¹⁰¹, G. Bernardi ¹³⁵, C. Bernius ¹⁵², F.U. Bernlochner ²⁴, T. Berry ⁹², P. Berta ⁹⁸, C. Bertella ^{15a}, G. Bertoli ^{44a,44b}, I.A. Bertram ⁸⁸, G.J. Besjes ⁴⁰, O. Bessidskaia Bylund ¹⁸¹, M. Bessner ⁴⁵, N. Besson ¹⁴⁴, A. Bethani ⁹⁹, S. Bethke ¹¹⁴, A. Betti ²⁴, A.J. Bevan ⁹¹, J. Beyer ¹¹⁴, R. Bi ¹³⁸, R.M. Bianchi ¹³⁸, O. Biebel ¹¹³, D. Biedermann ¹⁹, R. Bielski ³⁶, K. Bierwagen ⁹⁸, N.V. Biesuz ^{70a,70b}, M. Biglietti ^{73a}, T.R.V. Billoud ¹⁰⁸, M. Bindi ⁵², A. Bingul ^{12d}, C. Bini ^{71a,71b}, S. Biondi ^{23b,23a}, M. Birman ¹⁷⁹, T. Bisanz ⁵², J.P. Biswal ¹⁶⁰, C. Bittrich ⁴⁷, D.M. Bjergaard ⁴⁸, J.E. Black ¹⁵², K.M. Black ²⁵, T. Blazek ^{28a}, I. Bloch ⁴⁵, C. Blocker ²⁶, A. Blue ⁵⁶, U. Blumenschein ⁹¹, S. Blunier ^{146a}, G.J. Bobbink ¹¹⁹, V.S. Bobrovnikov ^{121b,121a}, S.S. Bocchetta ⁹⁵, A. Bocci ⁴⁸, D. Boerner ¹⁸¹, D. Bogavac ¹¹³, A.G. Bogdanchikov ^{121b,121a}, C. Böhm ^{44a}, V. Boisvert ⁹², P. Bokan ¹⁷¹, T. Bold ^{82a}, A.S. Boldyrev ¹¹², A.E. Bolz ^{60b}, M. Bomben ¹³⁵, M. Bona ⁹¹, J.S. Bonilla ¹³⁰, M. Boonekamp ¹⁴⁴, A. Borisov ¹²², G. Borissov ⁸⁸, J. Bortfeldt ³⁶, D. Bortoletto ¹³⁴, V. Bortolotto ^{72a,72b}, D. Boscherini ^{23b}, M. Bosman ¹⁴, J.D. Bossio Sola ³⁰, K. Bouaouda ^{35a}, J. Boudreau ¹³⁸, E.V. Bouhova-Thacker ⁸⁸, D. Boumediene ³⁸, S.K. Boutle ⁵⁶, A. Boveia ¹²⁵, J. Boyd ³⁶, D. Boye ^{33b}, I.R. Boyko ⁷⁸, A.J. Bozson ⁹², J. Bracinik ²¹, N. Brahimi ¹⁰⁰, A. Brandt ⁸, G. Brandt ¹⁸¹, O. Brandt ^{60a}, F. Braren ⁴⁵, U. Bratzler ¹⁶³, B. Brau ¹⁰¹, J.E. Brau ¹³⁰, W.D. Breaden Madden ⁵⁶, K. Brendlinger ⁴⁵, L. Brenner ⁴⁵, R. Brenner ¹⁷¹, S. Bressler ¹⁷⁹, B. Brickwedde ⁹⁸, D.L. Briglin ²¹, D. Britton ⁵⁶, D. Britzger ¹¹⁴, I. Brock ²⁴, R. Brock ¹⁰⁵, G. Brooijmans ³⁹, T. Brooks ⁹², W.K. Brooks ^{146b}, E. Brost ¹²⁰, J.H. Broughton ²¹, P.A. Bruckman de Renstrom ⁸³, D. Bruncko ^{28b}, A. Bruni ^{23b}, G. Bruni ^{23b}, L.S. Bruni ¹¹⁹, S. Bruno ^{72a,72b}, B.H. Brunt ³², M. Bruschi ^{23b}, N. Brusino ¹³⁸, P. Bryant ³⁷, L. Bryngemark ⁴⁵, T. Buanes ¹⁷, Q. Buat ³⁶, P. Buchholz ¹⁵⁰, A.G. Buckley ⁵⁶, I.A. Budagov ⁷⁸, M.K. Bugge ¹³³, F. Bühner ⁵¹, O. Bulekov ¹¹¹, D. Bullock ⁸, T.J. Burch ¹²⁰, S. Burdin ⁸⁹, C.D. Burgard ¹¹⁹, A.M. Burger ⁵, B. Burghgrave ¹²⁰, K. Burka ⁸³, S. Burke ¹⁴³, I. Burmeister ⁴⁶, J.T.P. Burr ¹³⁴, V. Büscher ⁹⁸, E. Buschmann ⁵², P.J. Bussey ⁵⁶, J.M. Butler ²⁵, C.M. Buttar ⁵⁶, J.M. Butterworth ⁹³, P. Butti ³⁶, W. Buttinger ³⁶, A. Buzatu ¹⁵⁷, A.R. Buzykaev ^{121b,121a}, G. Cabras ^{23b,23a}, S. Cabrera Urbán ¹⁷³, D. Caforio ¹⁴¹, H. Cai ¹⁷², V.M.M. Cairo ², O. Cakir ^{4a}, N. Calace ⁵³, P. Calafiura ¹⁸, A. Calandri ¹⁰⁰, G. Calderini ¹³⁵, P. Calfayan ⁶⁴, G. Callea ^{41b,41a}, L.P. Caloba ^{79b}, S. Calvente Lopez ⁹⁷, D. Calvet ³⁸, S. Calvet ³⁸, T.P. Calvet ¹⁵⁴, M. Calvetti ^{70a,70b}, R. Camacho Toro ¹³⁵, S. Camarda ³⁶, D. Camarero Munoz ⁹⁷, P. Camarri ^{72a,72b}, D. Cameron ¹³³, R. Caminal Armadans ¹⁰¹, C. Camincher ³⁶, S. Campana ³⁶, M. Campanelli ⁹³, A. Camplani ⁴⁰, A. Campoverde ¹⁵⁰, V. Canale ^{68a,68b}, M. Cano Bret ^{59c}, J. Cantero ¹²⁸, T. Cao ¹⁶⁰, Y. Cao ¹⁷², M.D.M. Capeans Garrido ³⁶, I. Caprini ^{27b}, M. Caprini ^{27b}, M. Capua ^{41b,41a}, R.M. Carbone ³⁹, R. Cardarelli ^{72a}, F.C. Cardillo ¹⁴⁸, I. Carli ¹⁴², T. Carli ³⁶, G. Carlino ^{68a}, B.T. Carlson ¹³⁸, L. Carminati ^{67a,67b}, R.M.D. Carney ^{44a,44b}, S. Caron ¹¹⁸, E. Carquin ^{146b}, S. Carrá ^{67a,67b}, G.D. Carrillo-Montoya ³⁶, D. Casadei ^{33b}, M.P. Casado ^{14.f}, A.F. Casha ¹⁶⁶, D.W. Casper ¹⁷⁰, R. Castelijin ¹¹⁹, F.L. Castillo ¹⁷³, V. Castillo Gimenez ¹⁷³, N.F. Castro ^{139a,139e}, A. Catinaccio ³⁶, J.R. Catmore ¹³³, A. Cattai ³⁶, J. Caudron ²⁴, V. Cavaliere ²⁹, E. Cavallaro ¹⁴, D. Cavalli ^{67a}, M. Cavalli-Sforza ¹⁴, V. Cavasinni ^{70a,70b}, E. Celebi ^{12b}, F. Ceradini ^{73a,73b}, L. Cerda Alberich ¹⁷³, A.S. Cerqueira ^{79a}, A. Cerri ¹⁵⁵, L. Cerrito ^{72a,72b}, F. Cerutti ¹⁸, A. Cervelli ^{23b,23a}, S.A. Cetin ^{12b}, A. Chafaq ^{35a}, D. Chakraborty ¹²⁰, S.K. Chan ⁵⁸, W.S. Chan ¹¹⁹, Y.L. Chan ^{62a}, J.D. Chapman ³², B. Chargeishvili ^{158b}, D.G. Charlton ²¹, C.C. Chau ³⁴, C.A. Chavez Barajas ¹⁵⁵, S. Che ¹²⁵, A. Chegwidden ¹⁰⁵, S. Chekanov ⁶, S.V. Chekulaev ^{167a}, G.A. Chelkov ^{78.ap}, M.A. Chelstowska ³⁶, C. Chen ^{59a}, C.H. Chen ⁷⁷, H. Chen ²⁹, J. Chen ^{59a}, J. Chen ³⁹, S. Chen ¹³⁶, S.J. Chen ^{15c}, X. Chen ^{15b,ao}, Y. Chen ⁸¹, Y-H. Chen ⁴⁵, H.C. Cheng ¹⁰⁴, H.J. Cheng ^{15a,15d}, A. Cheplakov ⁷⁸, E. Cheremushkina ¹²², R. Cherkaoui El Moursli ^{35e}, E. Cheu ⁷, K. Cheung ⁶³, L. Chevalier ¹⁴⁴, V. Chiarella ⁵⁰, G. Chiarelli ^{70a},

G. Chiodini ^{66a}, A.S. Chisholm ^{36,21}, A. Chitan ^{27b}, I. Chiu ¹⁶², Y.H. Chiu ¹⁷⁵, M.V. Chizhov ⁷⁸, K. Choi ⁶⁴, A.R. Chomont ¹³¹, S. Chouridou ¹⁶¹, Y.S. Chow ¹¹⁹, V. Christodoulou ⁹³, M.C. Chu ^{62a}, J. Chudoba ¹⁴⁰, A.J. Chuinard ¹⁰², J.J. Chwastowski ⁸³, L. Chytka ¹²⁹, D. Cinca ⁴⁶, V. Cindro ⁹⁰, I.A. Cioară ²⁴, A. Ciochio ¹⁸, F. Ciroto ^{68a,68b}, Z.H. Citron ¹⁷⁹, M. Citterio ^{67a}, A. Clark ⁵³, M.R. Clark ³⁹, P.J. Clark ⁴⁹, C. Clement ^{44a,44b}, Y. Coadou ¹⁰⁰, M. Cobal ^{65a,65c}, A. Coccaro ^{54b}, J. Cochran ⁷⁷, H. Cohen ¹⁶⁰, A.E.C. Coimbra ¹⁷⁹, L. Colasurdo ¹¹⁸, B. Cole ³⁹, A.P. Colijn ¹¹⁹, J. Collot ⁵⁷, P. Conde Muiño ^{139a}, E. Coniavitis ⁵¹, S.H. Connell ^{33b}, I.A. Connelly ⁹⁹, S. Constantinescu ^{27b}, F. Conventi ^{68a,as}, A.M. Cooper-Sarkar ¹³⁴, F. Cormier ¹⁷⁴, K.J.R. Cormier ¹⁶⁶, L.D. Corpe ⁹³, M. Corradi ^{71a,71b}, E.E. Corrigan ⁹⁵, F. Corriveau ^{102,aa}, A. Cortes-Gonzalez ³⁶, M.J. Costa ¹⁷³, F. Costanza ⁵, D. Costanzo ¹⁴⁸, G. Cottin ³², G. Cowan ⁹², B.E. Cox ⁹⁹, J. Crane ⁹⁹, K. Cranmer ¹²³, S.J. Crawley ⁵⁶, R.A. Creager ¹³⁶, G. Cree ³⁴, S. Crépe-Renaudin ⁵⁷, F. Crescioli ¹³⁵, M. Cristinziani ²⁴, V. Croft ¹²³, G. Crosetti ^{41b,41a}, A. Cueto ⁹⁷, T. Cuhadar Donszelmann ¹⁴⁸, A.R. Cukierman ¹⁵², S. Czekierda ⁸³, P. Czodrowski ³⁶, M.J. Da Cunha Sargedas De Sousa ^{59b}, C. Da Via ⁹⁹, W. Dabrowski ^{82a}, T. Dado ^{28a,w}, S. Dahbi ^{35e}, T. Dai ¹⁰⁴, F. Dallaire ¹⁰⁸, C. Dallapiccola ¹⁰¹, M. Dam ⁴⁰, G. D'amen ^{23b,23a}, J. Damp ⁹⁸, J.R. Dandoy ¹³⁶, M.F. Daneri ³⁰, N.P. Dang ¹⁸⁰, N.D. Dann ⁹⁹, M. Danninger ¹⁷⁴, V. Dao ³⁶, G. Darbo ^{54b}, S. Darmora ⁸, O. Dartsis ⁵, A. Dattagupta ¹³⁰, T. Daubney ⁴⁵, S. D'Auria ^{67a,67b}, W. Davey ²⁴, C. David ⁴⁵, T. Davidek ¹⁴², D.R. Davis ⁴⁸, E. Dawe ¹⁰³, I. Dawson ¹⁴⁸, K. De ⁸, R. De Asmundis ^{68a}, A. De Benedetti ¹²⁷, M. De Beurs ¹¹⁹, S. De Castro ^{23b,23a}, S. De Cecco ^{71a,71b}, N. De Groot ¹¹⁸, P. de Jong ¹¹⁹, H. De la Torre ¹⁰⁵, F. De Lorenzi ⁷⁷, A. De Maria ^{70a,70b}, D. De Pedis ^{71a}, A. De Salvo ^{71a}, U. De Sanctis ^{72a,72b}, M. De Santis ^{72a,72b}, A. De Santo ¹⁵⁵, K. De Vasconcelos Corga ¹⁰⁰, J.B. De Vivie De Regie ¹³¹, C. Debenedetti ¹⁴⁵, D.V. Dedovich ⁷⁸, N. Dehghanian ³, A.M. Deiana ¹⁰⁴, M. Del Gaudio ^{41b,41a}, J. Del Peso ⁹⁷, Y. Delabat Diaz ⁴⁵, D. Delgove ¹³¹, F. Deliot ¹⁴⁴, C.M. Delitzsch ⁷, M. Della Pietra ^{68a,68b}, D. Della Volpe ⁵³, A. Dell'Acqua ³⁶, L. Dell'Asta ²⁵, M. Delmastro ⁵, C. Delporte ¹³¹, P.A. Delsart ⁵⁷, D.A. DeMarco ¹⁶⁶, S. Demers ¹⁸², M. Demichev ⁷⁸, S.P. Denisov ¹²², D. Denysiuk ¹¹⁹, L. D'Eramo ¹³⁵, D. Derendarz ⁸³, J.E. Derkaoui ^{35d}, F. Derue ¹³⁵, P. Dervan ⁸⁹, K. Desch ²⁴, C. Deterre ⁴⁵, K. Dette ¹⁶⁶, M.R. Devesa ³⁰, P.O. Deviveiros ³⁶, A. Dewhurst ¹⁴³, S. Dhaliwal ²⁶, F.A. Di Bello ⁵³, A. Di Ciaccio ^{72a,72b}, L. Di Ciaccio ⁵, W.K. Di Clemente ¹³⁶, C. Di Donato ^{68a,68b}, A. Di Girolamo ³⁶, G. Di Gregorio ^{70a,70b}, B. Di Micco ^{73a,73b}, R. Di Nardo ¹⁰¹, K.F. Di Petrillo ⁵⁸, R. Di Sipio ¹⁶⁶, D. Di Valentino ³⁴, C. Diaconu ¹⁰⁰, M. Diamond ¹⁶⁶, F.A. Dias ⁴⁰, T. Dias Do Vale ^{139a}, M.A. Diaz ^{146a}, J. Dickinson ¹⁸, E.B. Diehl ¹⁰⁴, J. Dietrich ¹⁹, S. Díez Cornell ⁴⁵, A. Dimitrievska ¹⁸, J. Dingfelder ²⁴, F. Dittus ³⁶, F. Djama ¹⁰⁰, T. Djobava ^{158b}, J.I. Djuvsland ^{60a}, M.A.B. Do Vale ^{79c}, M. Dobre ^{27b}, D. Dodsworth ²⁶, C. Doglioni ⁹⁵, J. Dolejsi ¹⁴², Z. Dolezal ¹⁴², M. Donadelli ^{79d}, J. Donini ³⁸, A. D'Onofrio ⁹¹, M. D'Onofrio ⁸⁹, J. Dopke ¹⁴³, A. Doria ^{68a}, M.T. Dova ⁸⁷, A.T. Doyle ⁵⁶, E. Drechsler ⁵², E. Dreyer ¹⁵¹, T. Dreyer ⁵², Y. Du ^{59b}, F. Dubinin ¹⁰⁹, M. Dubovsky ^{28a}, A. Dubreuil ⁵³, E. Duchovni ¹⁷⁹, G. Duckeck ¹¹³, A. Ducourthial ¹³⁵, O.A. Ducu ^{108,v}, D. Duda ¹¹⁴, A. Dudarev ³⁶, A.C. Dudder ⁹⁸, E.M. Duffield ¹⁸, L. Duflot ¹³¹, M. Dührssen ³⁶, C. Dülsen ¹⁸¹, M. Dumancic ¹⁷⁹, A.E. Dumitriu ^{27b,d}, A.K. Duncan ⁵⁶, M. Dunford ^{60a}, A. Duperrin ¹⁰⁰, H. Duran Yildiz ^{4a}, M. Düren ⁵⁵, A. Durglishvili ^{158b}, D. Duschinger ⁴⁷, B. Dutta ⁴⁵, D. Duvnjak ¹, M. Dyndal ⁴⁵, S. Dysch ⁹⁹, B.S. Dziedzic ⁸³, C. Eckardt ⁴⁵, K.M. Ecker ¹¹⁴, R.C. Edgar ¹⁰⁴, T. Eifert ³⁶, G. Eigen ¹⁷, K. Einsweiler ¹⁸, T. Ekelof ¹⁷¹, M. El Kacimi ^{35c}, R. El Kosseifi ¹⁰⁰, V. Ellajosyula ¹⁰⁰, M. Ellert ¹⁷¹, F. Ellinghaus ¹⁸¹, A.A. Elliot ⁹¹, N. Ellis ³⁶, J. Elmsheuser ²⁹, M. Elsing ³⁶, D. Emeliyanov ¹⁴³, A. Emerman ³⁹, Y. Enari ¹⁶², J.S. Ennis ¹⁷⁷, M.B. Epland ⁴⁸, J. Erdmann ⁴⁶, A. Ereditato ²⁰, S. Errede ¹⁷², M. Escalier ¹³¹, C. Escobar ¹⁷³, O. Estrada Pastor ¹⁷³, A.I. Etievre ¹⁴⁴, E. Etzion ¹⁶⁰, H. Evans ⁶⁴, A. Ezhilov ¹³⁷, M. Ezzi ^{35e}, F. Fabbri ⁵⁶, L. Fabbri ^{23b,23a}, V. Fabiani ¹¹⁸, G. Facini ⁹³, R.M. Faisca Rodrigues Pereira ^{139a}, R.M. Fakhruddinov ¹²², S. Falciano ^{71a}, P.J. Falke ⁵, S. Falke ⁵, J. Faltova ¹⁴², Y. Fang ^{15a}, M. Fanti ^{67a,67b}, A. Farbin ⁸, A. Farilla ^{73a}, E.M. Farina ^{69a,69b}, T. Farooque ¹⁰⁵, S. Farrell ¹⁸, S.M. Farrington ¹⁷⁷, P. Farthouat ³⁶, F. Fassi ^{35e}, P. Fassnacht ³⁶, D. Fassouliotis ⁹, M. Fauci Giannelli ⁴⁹, A. Favareto ^{54b,54a}, W.J. Fawcett ³², L. Fayard ¹³¹, O.L. Fedin ^{137,o}, W. Fedorko ¹⁷⁴, M. Feickert ⁴², S. Feigl ¹³³, L. Felgioni ¹⁰⁰, C. Feng ^{59b}, E.J. Feng ³⁶, M. Feng ⁴⁸, M.J. Fenton ⁵⁶, A.B. Fenyuk ¹²², L. Feremenga ⁸, J. Ferrando ⁴⁵, A. Ferrari ¹⁷¹, P. Ferrari ¹¹⁹, R. Ferrari ^{69a}, D.E. Ferreira de Lima ^{60b}, A. Ferrer ¹⁷³, D. Ferrere ⁵³, C. Ferretti ¹⁰⁴, F. Fiedler ⁹⁸, A. Filipčič ⁹⁰, F. Filthaut ¹¹⁸, K.D. Finelli ²⁵, M.C.N. Fiolhais ^{139a,139c,a}, L. Fiorini ¹⁷³, C. Fischer ¹⁴, W.C. Fisher ¹⁰⁵, N. Flaschel ⁴⁵, I. Fleck ¹⁵⁰, P. Fleischmann ¹⁰⁴, R.R.M. Fletcher ¹³⁶, T. Flick ¹⁸¹, B.M. Flierl ¹¹³, L.F. Flores ¹³⁶, L.R. Flores Castillo ^{62a}, F.M. Follega ^{74a,74b}, N. Fomin ¹⁷, G.T. Forcolin ^{74a,74b}, A. Formica ¹⁴⁴, F.A. Förster ¹⁴,

A.C. Forti⁹⁹, A.G. Foster²¹, D. Fournier¹³¹, H. Fox⁸⁸, S. Fracchia¹⁴⁸, P. Francavilla^{70a,70b},
 M. Franchini^{23b,23a}, S. Franchino^{60a}, D. Francis³⁶, L. Franconi¹⁴⁵, M. Franklin⁵⁸, M. Frate¹⁷⁰,
 M. Fraternali^{69a,69b}, A.N. Fray⁹¹, D. Freeborn⁹³, S.M. Fressard-Batraneanu³⁶, B. Freund¹⁰⁸,
 W.S. Freund^{79b}, E.M. Freundlich⁴⁶, D.C. Frizzell¹²⁷, D. Froidevaux³⁶, J.A. Frost¹³⁴, C. Fukunaga¹⁶³,
 E. Fullana Torregrosa¹⁷³, T. Fusayasu¹¹⁵, J. Fuster¹⁷³, O. Gabizon¹⁵⁹, A. Gabrielli^{23b,23a}, A. Gabrielli¹⁸,
 G.P. Gach^{82a}, S. Gadatsch⁵³, P. Gadow¹¹⁴, G. Gagliardi^{54b,54a}, L.G. Gagnon¹⁰⁸, C. Galea^{27b},
 B. Galhardo^{139a,139c}, E.J. Gallas¹³⁴, B.J. Gallop¹⁴³, P. Gallus¹⁴¹, G. Galster⁴⁰, R. Gamboa Goni⁹¹,
 K.K. Gan¹²⁵, S. Ganguly¹⁷⁹, J. Gao^{59a}, Y. Gao⁸⁹, Y.S. Gao^{31,l}, C. García¹⁷³, J.E. García Navarro¹⁷³,
 J.A. García Pascual^{15a}, M. Garcia-Sciveres¹⁸, R.W. Gardner³⁷, N. Garelli¹⁵², V. Garonne¹³³,
 K. Gasnikova⁴⁵, A. Gaudiello^{54b,54a}, G. Gaudio^{69a}, I.L. Gavrilenko¹⁰⁹, A. Gavrilyuk¹¹⁰, C. Gay¹⁷⁴,
 G. Gaycken²⁴, E.N. Gazis¹⁰, C.N.P. Gee¹⁴³, J. Geisen⁵², M. Geisen⁹⁸, M.P. Geisler^{60a}, K. Gellerstedt^{44a,44b},
 C. Gemme^{54b}, M.H. Genest⁵⁷, C. Geng¹⁰⁴, S. Gentile^{71a,71b}, S. George⁹², D. Gerbaudo¹⁴, G. Gessner⁴⁶,
 S. Ghasemi¹⁵⁰, M. Ghasemi Bostanabad¹⁷⁵, M. Ghneimat²⁴, B. Giacobbe^{23b}, S. Giagu^{71a,71b},
 N. Giangiacomi^{23b,23a}, P. Giannetti^{70a}, A. Giannini^{68a,68b}, S.M. Gibson⁹², M. Gignac¹⁴⁵, D. Gillberg³⁴,
 G. Gilles¹⁸¹, D.M. Gingrich^{3,aq}, M.P. Giordani^{65a,65c}, F.M. Giorgi^{23b}, P.F. Giraud¹⁴⁴, P. Giromini⁵⁸,
 G. Giugliarelli^{65a,65c}, D. Giugni^{67a}, F. Giuli¹³⁴, M. Giulini^{60b}, S. Gkaitatzis¹⁶¹, I. Gkialas^{9,h},
 E.L. Gkougkousis¹⁴, P. Gkoutoumis¹⁰, L.K. Gladilin¹¹², C. Glasman⁹⁷, J. Glatzer¹⁴, P.C.F. Glaysher⁴⁵,
 A. Glazov⁴⁵, M. Goblirsch-Kolb²⁶, J. Godlewski⁸³, S. Goldfarb¹⁰³, T. Golling⁵³, D. Golubkov¹²²,
 A. Gomes^{139a,139b}, R. Goncalves Gama^{79a}, R. Gonçalves^{139a}, G. Gonella⁵¹, L. Gonella²¹, A. Gongadze⁷⁸,
 F. Gonnella²¹, J.L. Gonski⁵⁸, S. González de la Hoz¹⁷³, S. Gonzalez-Sevilla⁵³, L. Goossens³⁶,
 P.A. Gorbounov¹¹⁰, H.A. Gordon²⁹, B. Gorini³⁶, E. Gorini^{66a,66b}, A. Gorišek⁹⁰, A.T. Goshaw⁴⁸,
 C. Gössling⁴⁶, M.I. Gostkin⁷⁸, C.A. Gottardo²⁴, C.R. Goudet¹³¹, D. Goujdami^{35c}, A.G. Goussiou¹⁴⁷,
 N. Govender^{33b,b}, C. Goy⁵, E. Gozani¹⁵⁹, I. Grabowska-Bold^{82a}, P.O.J. Gradin¹⁷¹, E.C. Graham⁸⁹,
 J. Gramling¹⁷⁰, E. Gramstad¹³³, S. Grancagnolo¹⁹, V. Gratchev¹³⁷, P.M. Gravila^{27f}, F.G. Gravili^{66a,66b},
 C. Gray⁵⁶, H.M. Gray¹⁸, Z.D. Greenwood⁹⁴, C. Greife²⁴, K. Gregersen⁹⁵, I.M. Gregor⁴⁵, P. Grenier¹⁵²,
 K. Grevtsov⁴⁵, N.A. Grieser¹²⁷, J. Griffiths⁸, A.A. Grillo¹⁴⁵, K. Grimm^{31,k}, S. Grinstein^{14,x}, Ph. Gris³⁸,
 J.-F. Grivaz¹³¹, S. Groh⁹⁸, E. Gross¹⁷⁹, J. Grosse-Knetter⁵², G.C. Grossi⁹⁴, Z.J. Grout⁹³, C. Grud¹⁰⁴,
 A. Grummer¹¹⁷, L. Guan¹⁰⁴, W. Guan¹⁸⁰, J. Guenther³⁶, A. Guerguichon¹³¹, F. Guescini^{167a},
 D. Guest¹⁷⁰, R. Gugel⁵¹, B. Gui¹²⁵, T. Guillemin⁵, S. Guindon³⁶, U. Gul⁵⁶, C. Gumpert³⁶, J. Guo^{59c},
 W. Guo¹⁰⁴, Y. Guo^{59a,q}, Z. Guo¹⁰⁰, R. Gupta⁴⁵, S. Gurbuz^{12c}, G. Gustavino¹²⁷, B.J. Gutelman¹⁵⁹,
 P. Gutierrez¹²⁷, C. Gutschow⁹³, C. Guyot¹⁴⁴, M.P. Guzik^{82a}, C. Gwenlan¹³⁴, C.B. Gwilliam⁸⁹, A. Haas¹²³,
 C. Haber¹⁸, H.K. Hadavand⁸, N. Haddad^{35e}, A. Hadeef^{59a}, S. Hageböck²⁴, M. Hagihara¹⁶⁸,
 H. Hakobyan^{183,*}, M. Haleem¹⁷⁶, J. Haley¹²⁸, G. Halladjian¹⁰⁵, G.D. Hallewell¹⁰⁰, K. Hamacher¹⁸¹,
 P. Hamal¹²⁹, K. Hamano¹⁷⁵, A. Hamilton^{33a}, G.N. Hamity¹⁴⁸, K. Han^{59a,ae}, L. Han^{59a}, S. Han^{15a,15d},
 K. Hanagaki^{80,t}, M. Hance¹⁴⁵, D.M. Handl¹¹³, B. Haney¹³⁶, R. Hankache¹³⁵, P. Hanke^{60a}, E. Hansen⁹⁵,
 J.B. Hansen⁴⁰, J.D. Hansen⁴⁰, M.C. Hansen²⁴, P.H. Hansen⁴⁰, E.C. Hanson⁹⁹, K. Hara¹⁶⁸, A.S. Hard¹⁸⁰,
 T. Harenberg¹⁸¹, S. Harkusha¹⁰⁶, P.F. Harrison¹⁷⁷, N.M. Hartmann¹¹³, Y. Hasegawa¹⁴⁹, A. Hasib⁴⁹,
 S. Hassani¹⁴⁴, S. Haug²⁰, R. Hauser¹⁰⁵, L. Hauswald⁴⁷, L.B. Havener³⁹, M. Havranek¹⁴¹, C.M. Hawkes²¹,
 R.J. Hawking³⁶, D. Hayden¹⁰⁵, C. Hayes¹⁵⁴, C.P. Hays¹³⁴, J.M. Hays⁹¹, H.S. Hayward⁸⁹, S.J. Haywood¹⁴³,
 M.P. Heath⁴⁹, V. Hedberg⁹⁵, L. Heelan⁸, S. Heer²⁴, K.K. Heidegger⁵¹, J. Heilman³⁴, S. Heim⁴⁵,
 T. Heim¹⁸, B. Heinemann^{45,al}, J.J. Heinrich¹¹³, L. Heinrich¹²³, C. Heinz⁵⁵, J. Hejbal¹⁴⁰, L. Helary³⁶,
 A. Held¹⁷⁴, S. Hellesund¹³³, S. Hellman^{44a,44b}, C. Helsens³⁶, R.C.W. Henderson⁸⁸, Y. Heng¹⁸⁰,
 S. Henkelmann¹⁷⁴, A.M. Henriques Correia³⁶, G.H. Herbert¹⁹, H. Herde²⁶, V. Herget¹⁷⁶,
 Y. Hernández Jiménez^{33c}, H. Herr⁹⁸, M.G. Herrmann¹¹³, T. Herrmann⁴⁷, G. Herten⁵¹,
 R. Hertenberger¹¹³, L. Hervas³⁶, T.C. Herwig¹³⁶, G.G. Hesketh⁹³, N.P. Hessey^{167a}, A. Higashida¹⁶²,
 S. Higashino⁸⁰, E. Higón-Rodríguez¹⁷³, K. Hildebrand³⁷, E. Hill¹⁷⁵, J.C. Hill³², K.K. Hill²⁹, K.H. Hiller⁴⁵,
 S.J. Hillier²¹, M. Hils⁴⁷, I. Hinchliffe¹⁸, M. Hirose¹³², D. Hirschbuehl¹⁸¹, B. Hiti⁹⁰, O. Hladik¹⁴⁰,
 D.R. Hlaluku^{33c}, X. Hoad⁴⁹, J. Hobbs¹⁵⁴, N. Hod^{167a}, M.C. Hodgkinson¹⁴⁸, A. Hoecker³⁶,
 M.R. Hoferkamp¹¹⁷, F. Hoenic¹¹³, D. Hohn²⁴, D. Hohov¹³¹, T.R. Holmes³⁷, M. Holzbock¹¹³,
 M. Homann⁴⁶, S. Honda¹⁶⁸, T. Honda⁸⁰, T.M. Hong¹³⁸, A. Hönle¹¹⁴, B.H. Hooberman¹⁷²,
 W.H. Hopkins¹³⁰, Y. Horii¹¹⁶, P. Horn⁴⁷, A.J. Horton¹⁵¹, L.A. Horyn³⁷, J.-Y. Hostachy⁵⁷, A. Hostiuc¹⁴⁷,
 S. Hou¹⁵⁷, A. Hoummada^{35a}, J. Howarth⁹⁹, J. Hoya⁸⁷, M. Hrabovsky¹²⁹, J. Hrdinka³⁶, I. Hristova¹⁹,

J. Hrivnac¹³¹, A. Hrynevich¹⁰⁷, T. Hryn'ova⁵, P.J. Hsu⁶³, S.-C. Hsu¹⁴⁷, Q. Hu²⁹, S. Hu^{59c}, Y. Huang^{15a}, Z. Hubacek¹⁴¹, F. Hubaut¹⁰⁰, M. Huebner²⁴, F. Huegging²⁴, T.B. Huffman¹³⁴, M. Huhtinen³⁶, R.F.H. Hunter³⁴, P. Huo¹⁵⁴, A.M. Hupe³⁴, N. Huseynov^{78.ac}, J. Huston¹⁰⁵, J. Huth⁵⁸, R. Hyneman¹⁰⁴, G. Iacobucci⁵³, G. Iakovidis²⁹, I. Ibragimov¹⁵⁰, L. Iconomidou-Fayard¹³¹, Z. Idrissi^{35e}, P.I. Iengo³⁶, R. Ignazzi⁴⁰, O. Igonkina^{119.y}, R. Iguchi¹⁶², T. Iizawa⁵³, Y. Ikegami⁸⁰, M. Ikeno⁸⁰, D. Iliadis¹⁶¹, N. Ilic¹¹⁸, F. Iltzsche⁴⁷, G. Introzzi^{69a,69b}, M. Iodice^{73a}, K. Iordanidou³⁹, V. Ippolito^{71a,71b}, M.F. Isacson¹⁷¹, N. Ishijima¹³², M. Ishino¹⁶², M. Ishitsuka¹⁶⁴, W. Islam¹²⁸, C. Issever¹³⁴, S. Istin¹⁵⁹, F. Ito¹⁶⁸, J.M. Iturbe Ponce^{62a}, R. Iuppa^{74a,74b}, A. Ivina¹⁷⁹, H. Iwasaki⁸⁰, J.M. Izen⁴³, V. Izzo^{68a}, P. Jacka¹⁴⁰, P. Jackson¹, R.M. Jacobs²⁴, V. Jain², G. Jäkel¹⁸¹, K.B. Jakobi⁹⁸, K. Jakobs⁵¹, S. Jakobsen⁷⁵, T. Jakoubek¹⁴⁰, D.O. Jamin¹²⁸, R. Jansky⁵³, J. Janssen²⁴, M. Janus⁵², P.A. Janus^{82a}, G. Jarlskog⁹⁵, N. Javadov^{78.ac}, T. Javůrek³⁶, M. Javurkova⁵¹, F. Jeanneau¹⁴⁴, L. Jeanty¹⁸, J. Jejelava^{158a.ad}, A. Jelinskas¹⁷⁷, P. Jenni^{51.c}, J. Jeong⁴⁵, N. Jeong⁴⁵, S. Jézéquel⁵, H. Ji¹⁸⁰, J. Jia¹⁵⁴, H. Jiang⁷⁷, Y. Jiang^{59a}, Z. Jiang¹⁵², S. Jiggins⁵¹, F.A. Jimenez Morales³⁸, J. Jimenez Pena¹⁷³, S. Jin^{15c}, A. Jinaru^{27b}, O. Jinnouchi¹⁶⁴, H. Jivan^{33c}, P. Johansson¹⁴⁸, K.A. Johns⁷, C.A. Johnson⁶⁴, W.J. Johnson¹⁴⁷, K. Jon-And^{44a,44b}, R.W.L. Jones⁸⁸, S.D. Jones¹⁵⁵, S. Jones⁷, T.J. Jones⁸⁹, J. Jongmanns^{60a}, P.M. Jorge^{139a,139b}, J. Jovicevic^{167a}, X. Ju¹⁸, J.J. Junggeburth¹¹⁴, A. Juste Rozas^{14.x}, A. Kaczmarska⁸³, M. Kado¹³¹, H. Kagan¹²⁵, M. Kagan¹⁵², T. Kaji¹⁷⁸, E. Kajomovitz¹⁵⁹, C.W. Kalderon⁹⁵, A. Kaluza⁹⁸, S. Kama⁴², A. Kamenshchikov¹²², L. Kanjir⁹⁰, Y. Kano¹⁶², V.A. Kantserov¹¹¹, J. Kanzaki⁸⁰, B. Kaplan¹²³, L.S. Kaplan¹⁸⁰, D. Kar^{33c}, M.J. Kareem^{167b}, E. Karentzos¹⁰, S.N. Karpov⁷⁸, Z.M. Karpova⁷⁸, V. Kartvelishvili⁸⁸, A.N. Karyukhin¹²², L. Kashif¹⁸⁰, R.D. Kass¹²⁵, A. Kastanas^{44a,44b}, Y. Kataoka¹⁶², C. Kato^{59d,59c}, J. Katzy⁴⁵, K. Kawade⁸¹, K. Kawagoe⁸⁶, T. Kawamoto¹⁶², G. Kawamura⁵², E.F. Kay⁸⁹, V.F. Kazanin^{121b,121a}, R. Keeler¹⁷⁵, R. Kehoe⁴², J.S. Keller³⁴, E. Kellermann⁹⁵, J.J. Kempster²¹, J. Kendrick²¹, O. Kepka¹⁴⁰, S. Kersten¹⁸¹, B.P. Kerševan⁹⁰, S. Ketabchi Haghighat¹⁶⁶, R.A. Keyes¹⁰², M. Khader¹⁷², F. Khalil-Zada¹³, A. Khanov¹²⁸, A.G. Kharlamov^{121b,121a}, T. Kharlamova^{121b,121a}, E.E. Khoda¹⁷⁴, A. Khodinov¹⁶⁵, T.J. Khoo⁵³, E. Khramov⁷⁸, J. Khubua^{158b}, S. Kido⁸¹, M. Kiehn⁵³, C.R. Kilby⁹², Y.K. Kim³⁷, N. Kimura^{65a,65c}, O.M. Kind¹⁹, B.T. King^{89,*}, D. Kirchmeier⁴⁷, J. Kirk¹⁴³, A.E. Kiryunin¹¹⁴, T. Kishimoto¹⁶², D. Kisielewska^{82a}, V. Kitali⁴⁵, O. Kivernyk⁵, E. Kladiva^{28b,*}, T. Klapdor-Kleingrothaus⁵¹, M.H. Klein¹⁰⁴, M. Klein⁸⁹, U. Klein⁸⁹, K. Kleinknecht⁹⁸, P. Klimek¹²⁰, A. Klimentov²⁹, T. Klingl²⁴, T. Klioutchnikova³⁶, F.F. Klitzner¹¹³, P. Kluit¹¹⁹, S. Kluth¹¹⁴, E. Kneringer⁷⁵, E.B.F.G. Knoops¹⁰⁰, A. Knue⁵¹, A. Kobayashi¹⁶², D. Kobayashi⁸⁶, T. Kobayashi¹⁶², M. Kobel⁴⁷, M. Kocian¹⁵², P. Kodys¹⁴², P.T. Koenig²⁴, T. Koffas³⁴, E. Koffeman¹¹⁹, N.M. Köhler¹¹⁴, T. Koi¹⁵², M. Kolb^{60b}, I. Koletsou⁵, T. Kondo⁸⁰, N. Kondrashova^{59c}, K. Köneke⁵¹, A.C. König¹¹⁸, T. Kono¹²⁴, R. Konoplich^{123,ah}, V. Konstantinides⁹³, N. Konstantinidis⁹³, B. Konya⁹⁵, R. Kopeliansky⁶⁴, S. Koperny^{82a}, K. Korcyl⁸³, K. Kordas¹⁶¹, G. Koren¹⁶⁰, A. Korn⁹³, I. Korolkov¹⁴, E.V. Korolkova¹⁴⁸, N. Korotkova¹¹², O. Kortner¹¹⁴, S. Kortner¹¹⁴, T. Kosek¹⁴², V.V. Kostyukhin²⁴, A. Kotwal⁴⁸, A. Koulouris¹⁰, A. Kourkoumeli-Charalampidi^{69a,69b}, C. Kourkoumelis⁹, E. Kourlitis¹⁴⁸, V. Kouskoura²⁹, A.B. Kowalewska⁸³, R. Kowalewski¹⁷⁵, T.Z. Kowalski^{82a}, C. Kozakai¹⁶², W. Kozanecki¹⁴⁴, A.S. Kozhin¹²², V.A. Kramarenko¹¹², G. Kramberger⁹⁰, D. Krasnopevtsev^{59a}, M.W. Krasny¹³⁵, A. Krasznahorkay³⁶, D. Krauss¹¹⁴, J.A. Kremer^{82a}, J. Kretschmar⁸⁹, P. Krieger¹⁶⁶, K. Krizka¹⁸, K. Kroeninger⁴⁶, H. Kroha¹¹⁴, J. Kroll¹⁴⁰, J. Kroll¹³⁶, J. Krstic¹⁶, U. Kruchonak⁷⁸, H. Krüger²⁴, N. Krumnack⁷⁷, M.C. Kruse⁴⁸, T. Kubota¹⁰³, S. Kuday^{4b}, J.T. Kuechler¹⁸¹, S. Kuehn³⁶, A. Kugel^{60a}, F. Kuger¹⁷⁶, T. Kuhl⁴⁵, V. Kukhtin⁷⁸, R. Kukla¹⁰⁰, Y. Kulchitsky¹⁰⁶, S. Kuleshov^{146b}, Y.P. Kulinich¹⁷², M. Kuna⁵⁷, T. Kunigo⁸⁴, A. Kupco¹⁴⁰, T. Kupfer⁴⁶, O. Kuprash¹⁶⁰, H. Kurashige⁸¹, L.L. Kurchaninov^{167a}, Y.A. Kurochkin¹⁰⁶, A. Kurova¹¹¹, M.G. Kurth^{15a,15d}, E.S. Kuwertz³⁶, M. Kuze¹⁶⁴, J. Kvita¹²⁹, T. Kwan¹⁰², A. La Rosa¹¹⁴, J.L. La Rosa Navarro^{79d}, L. La Rotonda^{41b,41a}, F. La Ruffa^{41b,41a}, C. Lacasta¹⁷³, F. Lacava^{71a,71b}, J. Lacey⁴⁵, D.P.J. Lack⁹⁹, H. Lacker¹⁹, D. Lacour¹³⁵, E. Ladygin⁷⁸, R. Lafaye⁵, B. Laforge¹³⁵, T. Lagouri^{33c}, S. Lai⁵², S. Lammers⁶⁴, W. Lampl⁷, E. Lançon²⁹, U. Landgraf⁵¹, M.P.J. Landon⁹¹, M.C. Lanfermann⁵³, V.S. Lang⁴⁵, J.C. Lange⁵², R.J. Langenberg³⁶, A.J. Lankford¹⁷⁰, F. Lanni²⁹, K. Lantzsch²⁴, A. Lanza^{69a}, A. Lapertosa^{54b,54a}, S. Laplace¹³⁵, J.F. Laporte¹⁴⁴, T. Lari^{67a}, F. Lasagni Manghi^{23b,23a}, M. Lassnig³⁶, T.S. Lau^{62a}, A. Laudrain¹³¹, M. Lavorgna^{68a,68b}, M. Lazzaroni^{67a,67b}, B. Le¹⁰³, O. Le Dortz¹³⁵, E. Le Guirriec¹⁰⁰, E.P. Le Quilleuc¹⁴⁴, M. LeBlanc⁷, T. LeCompte⁶, F. Ledroit-Guillon⁵⁷, C.A. Lee²⁹, G.R. Lee^{146a}, L. Lee⁵⁸, S.C. Lee¹⁵⁷, B. Lefebvre¹⁰², M. Lefebvre¹⁷⁵, F. Legger¹¹³, C. Leggett¹⁸, K. Lehmann¹⁵¹, N. Lehmann¹⁸¹, G. Lehmann Miotto³⁶,

W.A. Leight⁴⁵, A. Leisos^{161,u}, M.A.L. Leite^{79d}, R. Leitner¹⁴², D. Lellouch^{179,*}, K.J.C. Leney⁹³, T. Lenz²⁴, B. Lenzi³⁶, R. Leone⁷, S. Leone^{70a}, C. Leonidopoulos⁴⁹, G. Lerner¹⁵⁵, C. Leroy¹⁰⁸, R. Les¹⁶⁶, A.A.J. Lesage¹⁴⁴, C.G. Lester³², M. Levchenko¹³⁷, J. Levêque⁵, D. Levin¹⁰⁴, L.J. Levinson¹⁷⁹, D. Lewis⁹¹, B. Li^{15b}, B. Li¹⁰⁴, C.-Q. Li^{59a,ag}, H. Li^{59b}, L. Li^{59c}, M. Li^{15a}, Q. Li^{15a,15d}, Q.Y. Li^{59a}, S. Li^{59d,59c}, X. Li^{59c}, Y. Li¹⁵⁰, Z. Liang^{15a}, B. Liberti^{72a}, A. Liblong¹⁶⁶, K. Lie^{62c}, S. Liem¹¹⁹, A. Limosani¹⁵⁶, C.Y. Lin³², K. Lin¹⁰⁵, T.H. Lin⁹⁸, R.A. Linck⁶⁴, J.H. Lindon²¹, B.E. Lindquist¹⁵⁴, A.L. Lioni⁵³, E. Lipeles¹³⁶, A. Lipniacka¹⁷, M. Lisovsky^{60b}, T.M. Liss^{172,an}, A. Lister¹⁷⁴, A.M. Litke¹⁴⁵, J.D. Little⁸, B. Liu⁷⁷, B.L. Liu⁶, H.B. Liu²⁹, H. Liu¹⁰⁴, J.B. Liu^{59a}, J.K.K. Liu¹³⁴, K. Liu¹³⁵, M. Liu^{59a}, P. Liu¹⁸, Y. Liu^{15a,15d}, Y.L. Liu^{59a}, Y.W. Liu^{59a}, M. Livan^{69a,69b}, A. Lleres⁵⁷, J. Llorente Merino^{15a}, S.L. Lloyd⁹¹, C.Y. Lo^{62b}, F. Lo Sterzo⁴², E.M. Lobodzinska⁴⁵, P. Loch⁷, T. Lohse¹⁹, K. Lohwasser¹⁴⁸, M. Lokajicek¹⁴⁰, J.D. Long¹⁷², R.E. Long⁸⁸, L. Longo^{66a,66b}, K.A. Looper¹²⁵, J.A. Lopez^{146b}, I. Lopez Paz⁹⁹, A. Lopez Solis¹⁴⁸, J. Lorenz¹¹³, N. Lorenzo Martinez⁵, M. Losada²², P.J. Lösel¹¹³, A. Lösle⁵¹, X. Lou⁴⁵, X. Lou^{15a}, A. Lounis¹³¹, J. Love⁶, P.A. Love⁸⁸, J.J. Lozano Bahilo¹⁷³, H. Lu^{62a}, M. Lu^{59a}, N. Lu¹⁰⁴, Y.J. Lu⁶³, H.J. Lubatti¹⁴⁷, C. Luci^{71a,71b}, A. Lucotte⁵⁷, C. Luedtke⁵¹, F. Luehring⁶⁴, I. Luise¹³⁵, L. Luminari^{71a}, B. Lund-Jensen¹⁵³, M.S. Lutz¹⁰¹, P.M. Luzi¹³⁵, D. Lynn²⁹, R. Lysak¹⁴⁰, E. Lytken⁹⁵, F. Lyu^{15a}, V. Lyubushkin⁷⁸, T. Lyubushkina⁷⁸, H. Ma²⁹, L.L. Ma^{59b}, Y. Ma^{59b}, G. Maccarrone⁵⁰, A. Macchiolo¹¹⁴, C.M. Macdonald¹⁴⁸, J. Machado Miguens^{136,139b}, D. Madaffari¹⁷³, R. Madar³⁸, W.F. Mader⁴⁷, A. Madsen⁴⁵, N. Madysa⁴⁷, J. Maeda⁸¹, K. Maekawa¹⁶², S. Maeland¹⁷, T. Maeno²⁹, M. Maerker⁴⁷, A.S. Maevskiy¹¹², V. Magerl⁵¹, D.J. Mahon³⁹, C. Maidantchik^{79b}, T. Maier¹¹³, A. Maio^{139a,139b,139d}, O. Majersky^{28a}, S. Majewski¹³⁰, Y. Makida⁸⁰, N. Makovec¹³¹, B. Malaescu¹³⁵, Pa. Malecki⁸³, V.P. Maleev¹³⁷, F. Malek⁵⁷, U. Mallik⁷⁶, D. Malon⁶, C. Malone³², S. Maltezos¹⁰, S. Malyukov³⁶, J. Mamuzic¹⁷³, G. Mancini⁵⁰, I. Mandić⁹⁰, J. Maneira^{139a}, L. Manhaes de Andrade Filho^{79a}, J. Manjarres Ramos⁴⁷, K.H. Mankinen⁹⁵, A. Mann¹¹³, A. Manousos⁷⁵, B. Mansoulie¹⁴⁴, J.D. Mansour^{15a}, M. Mantoani⁵², S. Manzoni^{67a,67b}, A. Marantis¹⁶¹, G. Marceca³⁰, L. March⁵³, L. Marchese¹³⁴, G. Marchiori¹³⁵, M. Marcisovsky¹⁴⁰, C.A. Marin Tobon³⁶, M. Marjanovic³⁸, D.E. Marley¹⁰⁴, F. Marroquim^{79b}, Z. Marshall¹⁸, M.U.F. Martensson¹⁷¹, S. Marti-Garcia¹⁷³, C.B. Martin¹²⁵, T.A. Martin¹⁷⁷, V.J. Martin⁴⁹, B. Martin dit Latour¹⁷, M. Martinez^{14,x}, V.I. Martinez Outschoorn¹⁰¹, S. Martin-Haugh¹⁴³, V.S. Martouiu^{27b}, A.C. Martyniuk⁹³, A. Marzin³⁶, L. Masetti⁹⁸, T. Mashimo¹⁶², R. Mashinistov¹⁰⁹, J. Masik⁹⁹, A.L. Maslennikov^{121b,121a}, L.H. Mason¹⁰³, L. Massa^{72a,72b}, P. Massarotti^{68a,68b}, P. Mastrandrea⁵, A. Mastroberardino^{41b,41a}, T. Masubuchi¹⁶², P. Mättig¹⁸¹, J. Maurer^{27b}, B. Maček⁹⁰, S.J. Maxfield⁸⁹, D.A. Maximov^{121b,121a}, R. Mazini¹⁵⁷, I. Maznas¹⁶¹, S.M. Mazza¹⁴⁵, G. Mc Goldrick¹⁶⁶, S.P. Mc Kee¹⁰⁴, T.G. McCarthy¹¹⁴, L.I. McClymont⁹³, E.F. McDonald¹⁰³, J.A. MCFayden³⁶, M.A. McKay⁴², K.D. McLean¹⁷⁵, S.J. McMahon¹⁴³, P.C. McNamara¹⁰³, C.J. McNicol¹⁷⁷, R.A. McPherson^{175,aa}, J.E. Mdhluli^{33c}, Z.A. Meadows¹⁰¹, S. Meehan¹⁴⁷, T. Megy⁵¹, S. Mehlhase¹¹³, A. Mehta⁸⁹, T. Meideck⁵⁷, B. Meirose⁴³, D. Melini^{173,ar}, B.R. Mellado Garcia^{33c}, J.D. Mellenthin⁵², M. Melo^{28a}, F. Meloni⁴⁵, A. Melzer²⁴, S.B. Menary⁹⁹, E.D. Mendes Gouveia^{139a}, L. Meng⁸⁹, X.T. Meng¹⁰⁴, A. Mengarelli^{23b,23a}, S. Menke¹¹⁴, E. Meoni^{41b,41a}, S. Mergelmeyer¹⁹, S.A.M. Merkt¹³⁸, C. Merlassino²⁰, P. Mermod⁵³, L. Merola^{68a,68b}, C. Meroni^{67a}, F.S. Merritt³⁷, A. Messina^{71a,71b}, J. Metcalfe⁶, A.S. Mete¹⁷⁰, C. Meyer¹³⁶, J. Meyer¹⁵⁹, J.-P. Meyer¹⁴⁴, H. Meyer Zu Theenhausen^{60a}, F. Miano¹⁵⁵, R.P. Middleton¹⁴³, L. Mijović⁴⁹, G. Mikenberg¹⁷⁹, M. Mikesikova¹⁴⁰, M. Mikuz⁹⁰, M. Milesi¹⁰³, A. Milic¹⁶⁶, D.A. Millar⁹¹, D.W. Miller³⁷, A. Milov¹⁷⁹, D.A. Milstead^{44a,44b}, A.A. Minaenko¹²², M. Miñano Moya¹⁷³, I.A. Minashvili^{158b}, A.I. Mincer¹²³, B. Mindur^{82a}, M. Mineev⁷⁸, Y. Minegishi¹⁶², Y. Ming¹⁸⁰, L.M. Mir¹⁴, A. Mirto^{66a,66b}, K.P. Mistry¹³⁶, T. Mitani¹⁷⁸, J. Mitrevski¹¹³, V.A. Mitsou¹⁷³, M. Mittal^{59c}, A. Miucci²⁰, P.S. Miyagawa¹⁴⁸, A. Mizukami⁸⁰, J.U. Mjörnmark⁹⁵, T. Mkrtychyan¹⁸³, M. Mlynarikova¹⁴², T. Moa^{44a,44b}, K. Mochizuki¹⁰⁸, P. Mogg⁵¹, S. Mohapatra³⁹, S. Molander^{44a,44b}, R. Moles-Valls²⁴, M.C. Mondragon¹⁰⁵, K. Mönig⁴⁵, J. Monk⁴⁰, E. Monnier¹⁰⁰, A. Montalbano¹⁵¹, J. Montejo Berlingen³⁶, F. Monticelli⁸⁷, S. Monzani^{67a}, N. Morange¹³¹, D. Moreno²², M. Moreno Llacer³⁶, P. Morettini^{54b}, M. Morgenstern¹¹⁹, S. Morgenstern⁴⁷, D. Mori¹⁵¹, M. Morii⁵⁸, M. Morinaga¹⁷⁸, V. Morisbak¹³³, A.K. Morley³⁶, G. Mornacchi³⁶, A.P. Morris⁹³, J.D. Morris⁹¹, L. Morvaj¹⁵⁴, P. Moschovakos¹⁰, M. Mosidze^{158b}, H.J. Moss¹⁴⁸, J. Moss^{31,m}, K. Motohashi¹⁶⁴, R. Mount¹⁵², E. Mountricha³⁶, E.J.W. Moyses¹⁰¹, S. Muanza¹⁰⁰, F. Mueller¹¹⁴, J. Mueller¹³⁸, R.S.P. Mueller¹¹³, D. Muenstermann⁸⁸, G.A. Mullier⁹⁵, F.J. Munoz Sanchez⁹⁹, P. Murin^{28b}, W.J. Murray^{177,143}, A. Murrone^{67a,67b}, M. Muškinja⁹⁰, C. Mwewa^{33a},

A.G. Myagkov^{122,ai}, J. Myers¹³⁰, M. Myska¹⁴¹, B.P. Nachman¹⁸, O. Nackenhorst⁴⁶, K. Nagai¹³⁴,
 K. Nagano⁸⁰, Y. Nagasaka⁶¹, M. Nagel⁵¹, E. Nagy¹⁰⁰, A.M. Nairz³⁶, Y. Nakahama¹¹⁶, K. Nakamura⁸⁰,
 T. Nakamura¹⁶², I. Nakano¹²⁶, H. Nanjo¹³², F. Napolitano^{60a}, R.F. Naranjo Garcia⁴⁵, R. Narayan¹¹,
 D.I. Narrias Villar^{60a}, I. Naryshkin¹³⁷, T. Naumann⁴⁵, G. Navarro²², R. Nayyar⁷, H.A. Neal^{104,*},
 P.Y. Nechaeva¹⁰⁹, T.J. Neep¹⁴⁴, A. Negri^{69a,69b}, M. Negrini^{23b}, S. Nektarijevic¹¹⁸, C. Nellist⁵²,
 M.E. Nelson¹³⁴, S. Nemecek¹⁴⁰, P. Nemethy¹²³, M. Nessi^{36,e}, M.S. Neubauer¹⁷², M. Neumann¹⁸¹,
 P.R. Newman²¹, T.Y. Ng^{62c}, Y.S. Ng¹⁹, H.D.N. Nguyen¹⁰⁰, T. Nguyen Manh¹⁰⁸, E. Nibigira³⁸,
 R.B. Nickerson¹³⁴, R. Nicolaidou¹⁴⁴, D.S. Nielsen⁴⁰, J. Nielsen¹⁴⁵, N. Nikiforou¹¹, V. Nikolaenko^{122,ai},
 I. Nikolic-Audit¹³⁵, K. Nikolopoulos²¹, P. Nilsson²⁹, Y. Ninomiya⁸⁰, A. Nisati^{71a}, N. Nishu^{59c},
 R. Nisius¹¹⁴, I. Nitsche⁴⁶, T. Nitta¹⁷⁸, T. Nobe¹⁶², Y. Noguchi⁸⁴, M. Nomachi¹³², I. Nomidis¹³⁵,
 M.A. Nomura²⁹, T. Nooney⁹¹, M. Nordberg³⁶, N. Norjoharuddeen¹³⁴, T. Novak⁹⁰, O. Novgorodova⁴⁷,
 R. Novotny¹⁴¹, L. Nozka¹²⁹, K. Ntekas¹⁷⁰, E. Nurse⁹³, F. Nuti¹⁰³, F.G. Oakham^{34,aa}, H. Oberlack¹¹⁴,
 J. Ocariz¹³⁵, A. Ochi⁸¹, I. Ochoa³⁹, J.P. Ochoa-Ricoux^{146a}, K. O'Connor²⁶, S. Oda⁸⁶, S. Odaka⁸⁰,
 S. Oerdek⁵², A. Oh⁹⁹, S.H. Oh⁴⁸, C.C. Ohm¹⁵³, H. Oide^{54b,54a}, M.L. Ojeda¹⁶⁶, H. Okawa¹⁶⁸, Y. Okazaki⁸⁴,
 Y. Okumura¹⁶², T. Okuyama⁸⁰, A. Olariu^{27b}, L.F. Oleiro Seabra^{139a}, S.A. Olivares Pino^{146a},
 D. Oliveira Damazio²⁹, J.L. Oliver¹, M.J.R. Olsson³⁷, A. Olszewski⁸³, J. Olszowska⁸³, D.C. O'Neil¹⁵¹,
 A. Onofre^{139a,139e}, K. Onogi¹¹⁶, P.U.E. Onyisi¹¹, H. Oppen¹³³, M.J. Oreglia³⁷, G.E. Orellana⁸⁷, Y. Oren¹⁶⁰,
 D. Orestano^{73a,73b}, N. Orlando^{62b}, A.A. O'Rourke⁴⁵, R.S. Orr¹⁶⁶, B. Osculati^{54b,54a,*}, V. O'Shea⁵⁶,
 R. Ospanov^{59a}, G. Otero y Garzon³⁰, H. Otono⁸⁶, M. Ouchrif^{35d}, F. Ould-Saada¹³³, A. Ouraou¹⁴⁴,
 Q. Ouyang^{15a}, M. Owen⁵⁶, R.E. Owen²¹, V.E. Ozcan^{12c}, N. Ozturk⁸, J. Pacalt¹²⁹, H.A. Pacey³²,
 K. Pachal¹⁵¹, A. Pacheco Pages¹⁴, L. Pacheco Rodriguez¹⁴⁴, C. Padilla Aranda¹⁴, S. Pagan Griso¹⁸,
 M. Paganini¹⁸², G. Palacino⁶⁴, S. Palazzo⁴⁹, S. Palestini³⁶, M. Palka^{82b}, D. Pallin³⁸, I. Panagoulas¹⁰,
 C.E. Pandini³⁶, J.G. Panduro Vazquez⁹², P. Pani³⁶, G. Panizzo^{65a,65c}, L. Paolozzi⁵³, T.D. Papadopoulou¹⁰,
 K. Papageorgiou^{9,h}, A. Paramonov⁶, D. Paredes Hernandez^{62b}, S.R. Paredes Saenz¹³⁴, B. Parida¹⁶⁵,
 T.H. Park³⁴, A.J. Parker⁸⁸, K.A. Parker⁴⁵, M.A. Parker³², F. Parodi^{54b,54a}, J.A. Parsons³⁹, U. Parzefall⁵¹,
 V.R. Pascuzzi¹⁶⁶, J.M.P. Pasner¹⁴⁵, E. Pasqualucci^{71a}, S. Passaggio^{54b}, F. Pastore⁹², P. Pasuwan^{44a,44b},
 S. Pataria⁹⁸, J.R. Pater⁹⁹, A. Pathak¹⁸⁰, T. Pauly³⁶, B. Pearson¹¹⁴, M. Pedersen¹³³, L. Pedraza Diaz¹¹⁸,
 R. Pedro^{139a,139b}, S.V. Peleganchuk^{121b,121a}, O. Penc¹⁴⁰, C. Peng^{15a}, H. Peng^{59a}, B.S. Peralva^{79a},
 M.M. Perego¹³¹, A.P. Pereira Peixoto^{139a}, D.V. Perepelitsa²⁹, F. Peri¹⁹, L. Perini^{67a,67b}, H. Pernegger³⁶,
 S. Perrella^{68a,68b}, V.D. Peshekhonov^{78,*}, K. Peters⁴⁵, R.F.Y. Peters⁹⁹, B.A. Petersen³⁶, T.C. Petersen⁴⁰,
 E. Petit⁵⁷, A. Petridis¹, C. Petridou¹⁶¹, P. Petroff¹³¹, M. Petrov¹³⁴, F. Petrucci^{73a,73b}, M. Pettee¹⁸²,
 N.E. Pettersson¹⁰¹, A. Peyaud¹⁴⁴, R. Pezoa^{146b}, T. Pham¹⁰³, F.H. Phillips¹⁰⁵, P.W. Phillips¹⁴³,
 M.W. Phipps¹⁷², G. Piacquadio¹⁵⁴, E. Pianori¹⁸, A. Picazio¹⁰¹, M.A. Pickering¹³⁴, R.H. Pickles⁹⁹,
 R. Piegaia³⁰, J.E. Pilcher³⁷, A.D. Pilkington⁹⁹, M. Pinamonti^{72a,72b}, J.L. Pinfold³, M. Pitt¹⁷⁹,
 L. Pizzimento^{72a,72b}, M.-A. Pleier²⁹, V. Pleskot¹⁴², E. Plotnikova⁷⁸, D. Pluth⁷⁷, P. Podberezko^{121b,121a},
 R. Poettgen⁹⁵, R. Poggi⁵³, L. Poggioli¹³¹, I. Pogrebnyak¹⁰⁵, D. Pohl²⁴, I. Pokharel⁵², G. Polesello^{69a},
 A. Poley¹⁸, A. Policicchio^{71a,71b}, R. Polifka³⁶, A. Polini^{23b}, C.S. Pollard⁴⁵, V. Polychronakos²⁹,
 D. Ponomarenko¹¹¹, L. Pontecorvo³⁶, G.A. Popeneciu^{27d}, L. Portales⁵, D.M. Portillo Quintero¹³⁵,
 S. Pospisil¹⁴¹, K. Potamianos⁴⁵, I.N. Potrap⁷⁸, C.J. Potter³², H. Potti¹¹, T. Poulsen⁹⁵, J. Poveda³⁶,
 T.D. Powell¹⁴⁸, M.E. Pozo Astigarraga³⁶, P. Pralavorio¹⁰⁰, S. Prell⁷⁷, D. Price⁹⁹, M. Primavera^{66a},
 S. Prince¹⁰², N. Proklova¹¹¹, K. Prokofiev^{62c}, F. Prokoshin^{146b}, S. Protopopescu²⁹, J. Proudfoot⁶,
 M. Przybycien^{82a}, A. Puri¹⁷², P. Puzo¹³¹, J. Qian¹⁰⁴, Y. Qin⁹⁹, A. Quadt⁵², M. Queitsch-Maitland⁴⁵,
 A. Qureshi¹, P. Rados¹⁰³, F. Ragusa^{67a,67b}, G. Rahal⁹⁶, J.A. Raine⁵³, S. Rajagopalan²⁹,
 A. Ramirez Morales⁹¹, T. Rashid¹³¹, S. Raspopov⁵, M.G. Ratti^{67a,67b}, D.M. Rauch⁴⁵, F. Rauscher¹¹³,
 S. Rave⁹⁸, B. Ravina¹⁴⁸, I. Ravinovich¹⁷⁹, J.H. Rawling⁹⁹, M. Raymond³⁶, A.L. Read¹³³, N.P. Readioff⁵⁷,
 M. Reale^{66a,66b}, D.M. Rebuzzi^{69a,69b}, A. Redelbach¹⁷⁶, G. Redlinger²⁹, R. Reece¹⁴⁵, R.G. Reed^{33c},
 K. Reeves⁴³, L. Rehnisch¹⁹, J. Reichert¹³⁶, D. Reikher¹⁶⁰, A. Reiss⁹⁸, C. Rembser³⁶, H. Ren^{15a},
 M. Rescigno^{71a}, S. Resconi^{67a}, E.D. Resseguie¹³⁶, S. Rettie¹⁷⁴, E. Reynolds²¹, O.L. Rezanova^{121b,121a},
 P. Reznicek¹⁴², E. Ricci^{74a,74b}, R. Richter¹¹⁴, S. Richter⁴⁵, E. Richter-Was^{82b}, O. Ricken²⁴, M. Ridel¹³⁵,
 P. Rieck¹¹⁴, C.J. Riegel¹⁸¹, O. Rifki⁴⁵, M. Rijssenbeek¹⁵⁴, A. Rimoldi^{69a,69b}, M. Rimoldi²⁰, L. Rinaldi^{23b},
 G. Ripellino¹⁵³, B. Ristić⁸⁸, E. Ritsch³⁶, I. Riu¹⁴, J.C. Rivera Vergara^{146a}, F. Rizatdinova¹²⁸, E. Rizvi⁹¹,
 C. Rizzi¹⁴, R.T. Roberts⁹⁹, S.H. Robertson^{102,aa}, D. Robinson³², J.E.M. Robinson⁴⁵, A. Robson⁵⁶,

E. Rocco⁹⁸, C. Roda^{70a,70b}, Y. Rodina¹⁰⁰, S. Rodriguez Bosca¹⁷³, A. Rodriguez Perez¹⁴,
 D. Rodriguez Rodriguez¹⁷³, A.M. Rodríguez Vera^{167b}, S. Roe³⁶, C.S. Rogan⁵⁸, O. Røhne¹³³, R. Röhrig¹¹⁴,
 C.P.A. Roland⁶⁴, J. Roloff⁵⁸, A. Romaniouk¹¹¹, M. Romano^{23b,23a}, N. Rompotis⁸⁹, M. Ronzani¹²³,
 L. Roos¹³⁵, S. Rosati^{71a}, K. Rosbach⁵¹, N.-A. Rosien⁵², B.J. Rosser¹³⁶, E. Rossi⁴⁵, E. Rossi^{73a,73b},
 E. Rossi^{68a,68b}, L.P. Rossi^{54b}, L. Rossini^{67a,67b}, J.H.N. Rosten³², R. Rosten¹⁴, M. Rotaru^{27b}, J. Rothberg¹⁴⁷,
 D. Rousseau¹³¹, D. Roy^{33c}, A. Rozanov¹⁰⁰, Y. Rozen¹⁵⁹, X. Ruan^{33c}, F. Rubbo¹⁵², F. Rühr⁵¹,
 A. Ruiz-Martinez¹⁷³, Z. Rurikova⁵¹, N.A. Rusakovich⁷⁸, H.L. Russell¹⁰², J.P. Rutherford⁷,
 E.M. Rüttinger^{45,j}, Y.F. Ryabov¹³⁷, M. Rybar¹⁷², G. Rybkin¹³¹, S. Ryu⁶, A. Ryzhov¹²², G.F. Rzehorz⁵²,
 P. Sabatini⁵², G. Sabato¹¹⁹, S. Sacerdoti¹³¹, H.F.-W. Sadrozinski¹⁴⁵, R. Sadykov⁷⁸, F. Safai Tehrani^{71a},
 P. Saha¹²⁰, M. Sahinsoy^{60a}, A. Sahu¹⁸¹, M. Saimpert⁴⁵, M. Saito¹⁶², T. Saito¹⁶², H. Sakamoto¹⁶²,
 A. Sakharov^{123,ah}, D. Salamani⁵³, G. Salamanna^{73a,73b}, J.E. Salazar Loyola^{146b}, P.H. Sales De Bruin¹⁷¹,
 D. Salihgic^{114,*}, A. Salnikov¹⁵², J. Salt¹⁷³, D. Salvatore^{41b,41a}, F. Salvatore¹⁵⁵, A. Salvucci^{62a,62b,62c},
 A. Salzburger³⁶, J. Samarati³⁶, D. Sammel⁵¹, D. Sampsonidis¹⁶¹, D. Sampsonidou¹⁶¹, J. Sánchez¹⁷³,
 A. Sanchez Pineda^{65a,65c}, H. Sandaker¹³³, C.O. Sander⁴⁵, M. Sandhoff¹⁸¹, C. Sandoval²²,
 D.P.C. Sankey¹⁴³, M. Sannino^{54b,54a}, Y. Sano¹¹⁶, A. Sansoni⁵⁰, C. Santoni³⁸, H. Santos^{139a},
 I. Santoyo Castillo¹⁵⁵, A. Santra¹⁷³, A. Saponov⁷⁸, J.G. Saraiva^{139a,139d}, O. Sasaki⁸⁰, K. Sato¹⁶⁸,
 E. Sauvan⁵, P. Savard^{166,aq}, N. Savic¹¹⁴, R. Sawada¹⁶², C. Sawyer¹⁴³, L. Sawyer^{94,af}, C. Sbarra^{23b},
 A. Sbrizzi^{23a}, T. Scanlon⁹³, J. Schaarschmidt¹⁴⁷, P. Schacht¹¹⁴, B.M. Schachtner¹¹³, D. Schaefer³⁷,
 L. Schaefer¹³⁶, J. Schaeffer⁹⁸, S. Schaepe³⁶, U. Schäfer⁹⁸, A.C. Schaffer¹³¹, D. Schaile¹¹³,
 R.D. Schamberger¹⁵⁴, N. Scharmberg⁹⁹, V.A. Schegelsky¹³⁷, D. Scheirich¹⁴², F. Schenck¹⁹,
 M. Schernau¹⁷⁰, C. Schiavi^{54b,54a}, S. Schier¹⁴⁵, L.K. Schildgen²⁴, Z.M. Schillaci²⁶, E.J. Schioppa³⁶,
 M. Schioppa^{41b,41a}, K.E. Schleicher⁵¹, S. Schlenker³⁶, K.R. Schmidt-Sommerfeld¹¹⁴, K. Schmieden³⁶,
 C. Schmitt⁹⁸, S. Schmitt⁴⁵, S. Schmitz⁹⁸, J.C. Schmoeckel⁴⁵, U. Schnoor⁵¹, L. Schoeffel¹⁴⁴,
 A. Schoening^{60b}, E. Schopf¹³⁴, M. Schott⁹⁸, J.F.P. Schouwenberg¹¹⁸, J. Schovancova³⁶, S. Schramm⁵³,
 A. Schulte⁹⁸, H.-C. Schultz-Coulon^{60a}, M. Schumacher⁵¹, B.A. Schumm¹⁴⁵, Ph. Schune¹⁴⁴,
 A. Schwartzman¹⁵², T.A. Schwarz¹⁰⁴, Ph. Schwemling¹⁴⁴, R. Schwienhorst¹⁰⁵, A. Sciandra²⁴,
 G. Sciolla²⁶, M. Scornajenghi^{41b,41a}, F. Scuri^{70a}, F. Scutti¹⁰³, L.M. Scyboz¹¹⁴, C.D. Sebastiani^{71a,71b},
 P. Seema¹⁹, S.C. Seidel¹¹⁷, A. Seiden¹⁴⁵, T. Seiss³⁷, J.M. Seixas^{79b}, G. Sekhniaidze^{68a}, K. Sekhon¹⁰⁴,
 S.J. Sekula⁴², N. Semprini-Cesari^{23b,23a}, S. Sen⁴⁸, S. Senkin³⁸, C. Serfon¹³³, L. Serin¹³¹, L. Serkin^{65a,65b},
 M. Sessa^{59a}, H. Severini¹²⁷, F. Sforza¹⁶⁹, A. Sfyrta⁵³, E. Shabalina⁵², J.D. Shahinian¹⁴⁵,
 N.W. Shaikh^{44a,44b}, L.Y. Shan^{15a}, R. Shang¹⁷², J.T. Shank²⁵, M. Shapiro¹⁸, A.S. Sharma¹, A. Sharma¹³⁴,
 P.B. Shatalov¹¹⁰, K. Shaw¹⁵⁵, S.M. Shaw⁹⁹, A. Shcherbakova¹³⁷, Y. Shen¹²⁷, N. Sherafati³⁴,
 A.D. Sherman²⁵, P. Sherwood⁹³, L. Shi^{157,am}, S. Shimizu⁸⁰, C.O. Shimmin¹⁸², Y. Shimogama¹⁷⁸,
 M. Shimojima¹¹⁵, I.P.J. Shipsey¹³⁴, S. Shirabe⁸⁶, M. Shiyakova⁷⁸, J. Shlomi¹⁷⁹, A. Shmeleva¹⁰⁹,
 D. Shoaleh Saadi¹⁰⁸, M.J. Shochet³⁷, S. Shojaii¹⁰³, D.R. Shope¹²⁷, S. Shrestha¹²⁵, E. Shulga¹¹¹,
 P. Sicho¹⁴⁰, A.M. Sickles¹⁷², P.E. Sidebo¹⁵³, E. Sideras Haddad^{33c}, O. Sidiropoulou³⁶, A. Sidoti^{23b,23a},
 F. Siegert⁴⁷, Dj. Sijacki¹⁶, J. Silva^{139a}, M. Silva Jr.¹⁸⁰, M.V. Silva Oliveira^{79a}, S.B. Silverstein^{44a},
 S. Simion¹³¹, E. Simioni⁹⁸, M. Simon⁹⁸, R. Simoniello⁹⁸, P. Sinervo¹⁶⁶, N.B. Sinev¹³⁰, M. Sioli^{23b,23a},
 G. Siragusa¹⁷⁶, I. Siral¹⁰⁴, S.Yu. Sivoklov¹¹², J. Sjölin^{44a,44b}, P. Skubic¹²⁷, M. Slater²¹, T. Slavicek¹⁴¹,
 M. Slawinska⁸³, K. Sliwa¹⁶⁹, R. Slovak¹⁴², V. Smakhtin¹⁷⁹, B.H. Smart⁵, J. Smiesko^{28a}, N. Smirnov¹¹¹,
 S.Yu. Smirnov¹¹¹, Y. Smirnov¹¹¹, L.N. Smirnova^{112,r}, O. Smirnova⁹⁵, J.W. Smith⁵², M. Smizanska⁸⁸,
 K. Smolek¹⁴¹, A. Smykiewicz⁸³, A.A. Snesarev¹⁰⁹, I.M. Snyder¹³⁰, S. Snyder²⁹, R. Sobie^{175,aa},
 A.M. Soffa¹⁷⁰, A. Soffer¹⁶⁰, A. Sogaard⁴⁹, D.A. Soh¹⁵⁷, G. Sokhrannyi⁹⁰, C.A. Solans Sanchez³⁶,
 M. Solar¹⁴¹, E.Yu. Soldatov¹¹¹, U. Soldevila¹⁷³, A.A. Solodkov¹²², A. Soloshenko⁷⁸, O.V. Solovyanov¹²²,
 V. Solovyev¹³⁷, P. Sommer¹⁴⁸, H. Son¹⁶⁹, W. Song¹⁴³, W.Y. Song^{167b}, A. Sopczak¹⁴¹, F. Sopkova^{28b},
 C.L. Sotiropoulou^{70a,70b}, S. Sottocornola^{69a,69b}, R. Soualah^{65a,65c,g}, A.M. Soukharev^{121b,121a}, D. South⁴⁵,
 B.C. Sowden⁹², S. Spagnolo^{66a,66b}, M. Spalla¹¹⁴, M. Spangenberg¹⁷⁷, F. Spanò⁹², D. Sperlich¹⁹,
 T.M. Spieker^{60a}, R. Spighi^{23b}, G. Spigo³⁶, L.A. Spiller¹⁰³, D.P. Spiteri⁵⁶, M. Spousta¹⁴², A. Stabile^{67a,67b},
 R. Stamen^{60a}, S. Stamm¹⁹, E. Stanecka⁸³, R.W. Stanek⁶, C. Stanescu^{73a}, B. Stanislaus¹³⁴,
 M.M. Stanitzki⁴⁵, B. Stapf¹¹⁹, S. Stapnes¹³³, E.A. Starchenko¹²², G.H. Stark³⁷, J. Stark⁵⁷, S.H. Stark⁴⁰,
 P. Staroba¹⁴⁰, P. Starovoitov^{60a}, S. Stärz³⁶, R. Staszewski⁸³, M. Stegler⁴⁵, P. Steinberg²⁹, B. Stelzer¹⁵¹,
 H.J. Stelzer³⁶, O. Stelzer-Chilton^{167a}, H. Stenzel⁵⁵, T.J. Stevenson¹⁵⁵, G.A. Stewart³⁶, M.C. Stockton³⁶,

G. Stoicea^{27b}, P. Stolte⁵², S. Stonjek¹¹⁴, A. Straessner⁴⁷, J. Strandberg¹⁵³, S. Strandberg^{44a,44b}, M. Strauss¹²⁷, P. Strizeneč^{28b}, R. Ströhmer¹⁷⁶, D.M. Strom¹³⁰, R. Stroynowski⁴², A. Strubig⁴⁹, S.A. Stucci²⁹, B. Stugu¹⁷, J. Stupak¹²⁷, N.A. Styles⁴⁵, D. Su¹⁵², J. Su¹³⁸, S. Suchek^{60a}, Y. Sugaya¹³², M. Suk¹⁴¹, V.V. Sulin¹⁰⁹, M.J. Sullivan⁸⁹, D.M.S. Sultan⁵³, S. Sultansoy^{4c}, T. Sumida⁸⁴, S. Sun¹⁰⁴, X. Sun³, K. Suruliz¹⁵⁵, C.J.E. Suster¹⁵⁶, M.R. Sutton¹⁵⁵, S. Suzuki⁸⁰, M. Svatos¹⁴⁰, M. Swiatlowski³⁷, S.P. Swift², A. Sydorenko⁹⁸, I. Sykora^{28a}, T. Sykora¹⁴², D. Ta⁹⁸, K. Tackmann⁴⁵, J. Taenzer¹⁶⁰, A. Taffard¹⁷⁰, R. Tafirout^{167a}, E. Tahirovic⁹¹, N. Taiblum¹⁶⁰, H. Takai²⁹, R. Takashima⁸⁵, E.H. Takasugi¹¹⁴, K. Takeda⁸¹, T. Takeshita¹⁴⁹, Y. Takubo⁸⁰, M. Talby¹⁰⁰, A.A. Talyshv^{121b,121a}, J. Tanaka¹⁶², M. Tanaka¹⁶⁴, R. Tanaka¹³¹, B.B. Tannenwald¹²⁵, S. Tapia Araya^{146b}, S. Tapprogge⁹⁸, A. Tarek Abouelfadl Mohamed¹³⁵, S. Tarem¹⁵⁹, G. Tarna^{27b,d}, G.F. Tartarelli^{67a}, P. Tas¹⁴², M. Tasevsky¹⁴⁰, T. Tashiro⁸⁴, E. Tassi^{41b,41a}, A. Tavares Delgado^{139a,139b}, Y. Tayalati^{35e}, A.C. Taylor¹¹⁷, A.J. Taylor⁴⁹, G.N. Taylor¹⁰³, P.T.E. Taylor¹⁰³, W. Taylor^{167b}, A.S. Tee⁸⁸, P. Teixeira-Dias⁹², H. Ten Kate³⁶, J.J. Teoh¹¹⁹, S. Terada⁸⁰, K. Terashi¹⁶², J. Terron⁹⁷, S. Terzo¹⁴, M. Testa⁵⁰, R.J. Teuscher^{166,aa}, S.J. Thais¹⁸², T. Theveneaux-Pelzer⁴⁵, F. Thiele⁴⁰, D.W. Thomas⁹², J.P. Thomas²¹, A.S. Thompson⁵⁶, P.D. Thompson²¹, L.A. Thomsen¹⁸², E. Thomson¹³⁶, Y. Tian³⁹, R.E. Ticse Torres⁵², V.O. Tikhomirov^{109,aj}, Yu.A. Tikhonov^{121b,121a}, S. Timoshenko¹¹¹, P. Tipton¹⁸², S. Tisserant¹⁰⁰, K. Todome¹⁶⁴, S. Todorova-Nova⁵, S. Todt⁴⁷, J. Tojo⁸⁶, S. Tokár^{28a}, K. Tokushuku⁸⁰, E. Tolley¹²⁵, K.G. Tomiwa^{33c}, M. Tomoto¹¹⁶, L. Tompkins¹⁵², K. Toms¹¹⁷, B. Tong⁵⁸, P. Tornambe⁵¹, E. Torrence¹³⁰, H. Torres⁴⁷, E. Torró Pastor¹⁴⁷, C. Toscirì¹³⁴, J. Toth^{100,z}, F. Touchard¹⁰⁰, D.R. Tovey¹⁴⁸, C.J. Treado¹²³, T. Trefzger¹⁷⁶, F. Tresoldi¹⁵⁵, A. Tricoli²⁹, I.M. Trigger^{167a}, S. Trincaz-Duvoid¹³⁵, M.F. Tripiana¹⁴, W. Trischuk¹⁶⁶, B. Trocmé⁵⁷, A. Trofymov¹³¹, C. Troncon^{67a}, M. Trovatelli¹⁷⁵, F. Trovato¹⁵⁵, L. Truong^{33b}, M. Trzebinski⁸³, A. Trzupek⁸³, F. Tsai⁴⁵, J.C.-L. Tseng¹³⁴, P.V. Tsiarshka¹⁰⁶, A. Tsirigotis¹⁶¹, N. Tsirintanis⁹, V. Tsiskaridze¹⁵⁴, E.G. Tskhadadze^{158a}, I.I. Tsukerman¹¹⁰, V. Tsulaia¹⁸, S. Tsuno⁸⁰, D. Tsybychev¹⁵⁴, Y. Tu^{62b}, A. Tudorache^{27b}, V. Tudorache^{27b}, T.T. Tulbure^{27a}, A.N. Tuna⁵⁸, S. Turchikhin⁷⁸, D. Turgeman¹⁷⁹, I. Turk Cakir^{4b,s}, R.T. Turra^{67a}, P.M. Tuts³⁹, E. Tzovara⁹⁸, G. Uccielli^{23b,23a}, I. Ueda⁸⁰, M. Ughetto^{44a,44b}, F. Ukegawa¹⁶⁸, G. Unal³⁶, A. Undrus²⁹, G. Unel¹⁷⁰, F.C. Ungaro¹⁰³, Y. Unno⁸⁰, K. Uno¹⁶², J. Urban^{28b}, P. Urquijo¹⁰³, P. Urrejola⁹⁸, G. Usai⁸, J. Usui⁸⁰, L. Vacavant¹⁰⁰, V. Vacek¹⁴¹, B. Vachon¹⁰², K.O.H. Vadla¹³³, A. Vaidya⁹³, C. Valderanis¹¹³, E. Valdes Santurio^{44a,44b}, M. Valente⁵³, S. Valentinetti^{23b,23a}, A. Valero¹⁷³, L. Valéry⁴⁵, R.A. Vallance²¹, A. Vallier⁵, J.A. Valls Ferrer¹⁷³, T.R. Van Daalen¹⁴, H. Van der Graaf¹¹⁹, P. Van Gemmeren⁶, J. Van Nieuwkoop¹⁵¹, I. Van Vulpen¹¹⁹, M. Vanadia^{72a,72b}, W. Vandelli³⁶, A. Vaniachine¹⁶⁵, P. Vankov¹¹⁹, R. Vari^{71a}, E.W. Varnes⁷, C. Varni^{54b,54a}, T. Varol⁴², D. Varouchas¹³¹, K.E. Varvell¹⁵⁶, G.A. Vasquez^{146b}, J.G. Vasquez¹⁸², F. Vazeille³⁸, D. Vazquez Furelos¹⁴, T. Vazquez Schroeder³⁶, J. Veatch⁵², V. Vecchio^{73a,73b}, L.M. Veloce¹⁶⁶, F. Veloso^{139a,139c}, S. Veneziano^{71a}, A. Ventura^{66a,66b}, M. Venturi¹⁷⁵, N. Venturi³⁶, V. Vercesi^{69a}, M. Verducci^{73a,73b}, C.M. Vergel Infante⁷⁷, C. Vergis²⁴, W. Verkerke¹¹⁹, A.T. Vermeulen¹¹⁹, J.C. Vermeulen¹¹⁹, M.C. Vetterli^{151,aq}, N. Viaux Maira^{146b}, M. Vicente Barreto Pinto⁵³, I. Vichou^{172,*}, T. Vickey¹⁴⁸, O.E. Vickey Boeriu¹⁴⁸, G.H.A. Viehhauser¹³⁴, S. Viel¹⁸, L. Vigani¹³⁴, M. Villa^{23b,23a}, M. Villaplana Perez^{67a,67b}, E. Vilucchi⁵⁰, M.G. Vincter³⁴, V.B. Vinogradov⁷⁸, A. Vishwakarma⁴⁵, C. Vittori^{23b,23a}, I. Vivarelli¹⁵⁵, S. Vlachos¹⁰, M. Vogel¹⁸¹, P. Vokac¹⁴¹, G. Volpi¹⁴, S.E. von Buddenbrock^{33c}, E. Von Toerne²⁴, V. Vorobel¹⁴², K. Vorobev¹¹¹, M. Vos¹⁷³, J.H. Vosseveld⁸⁹, N. Vranjes¹⁶, M. Vranjes Milosavljevic¹⁶, V. Vrba¹⁴¹, M. Vreeswijk¹¹⁹, T. Šfiligoj⁹⁰, R. Vuillermet³⁶, I. Vukotic³⁷, T. Ženiš^{28a}, L. Živković¹⁶, P. Wagner²⁴, W. Wagner¹⁸¹, J. Wagner-Kuhr¹¹³, H. Wahlberg⁸⁷, S. Wahrenmund⁴⁷, K. Wakamiya⁸¹, V.M. Walbrecht¹¹⁴, J. Walder⁸⁸, R. Walker¹¹³, S.D. Walker⁹², W. Walkowiak¹⁵⁰, V. Wallangen^{44a,44b}, A.M. Wang⁵⁸, C. Wang^{59b,d}, F. Wang¹⁸⁰, H. Wang¹⁸, H. Wang³, J. Wang¹⁵⁶, J. Wang^{60b}, P. Wang⁴², Q. Wang¹²⁷, R.-J. Wang¹³⁵, R. Wang^{59a}, R. Wang⁶, S.M. Wang¹⁵⁷, W.T. Wang^{59a}, W. Wang^{15c,ab}, W.X. Wang^{59a,ab}, Y. Wang^{59a,ag}, Z. Wang^{59c}, C. Wanotayaroj⁴⁵, A. Warburton¹⁰², C.P. Ward³², D.R. Wardrope⁹³, A. Washbrook⁴⁹, P.M. Watkins²¹, A.T. Watson²¹, M.F. Watson²¹, G. Watts¹⁴⁷, S. Watts⁹⁹, B.M. Waugh⁹³, A.F. Webb¹¹, S. Webb⁹⁸, C. Weber¹⁸², M.S. Weber²⁰, S.A. Weber³⁴, S.M. Weber^{60a}, A.R. Weidberg¹³⁴, B. Weinert⁶⁴, J. Weingarten⁴⁶, M. Weirich⁹⁸, C. Weiser⁵¹, P.S. Wells³⁶, T. Wenaus²⁹, T. Wengler³⁶, S. Wenig³⁶, N. Wermes²⁴, M.D. Werner⁷⁷, P. Werner³⁶, M. Wessels^{60a}, T.D. Weston²⁰, K. Whalen¹³⁰, N.L. Whallon¹⁴⁷, A.M. Wharton⁸⁸, A.S. White¹⁰⁴, A. White⁸, M.J. White¹, R. White^{146b}, D. Whiteson¹⁷⁰,

B.W. Whitmore⁸⁸, F.J. Wickens¹⁴³, W. Wiedenmann¹⁸⁰, M. Wielers¹⁴³, C. Wiglesworth⁴⁰, L.A.M. Wiik-Fuchs⁵¹, F. Wilk⁹⁹, H.G. Wilkens³⁶, L.J. Wilkins⁹², H.H. Williams¹³⁶, S. Williams³², C. Willis¹⁰⁵, S. Willocq¹⁰¹, J.A. Wilson²¹, I. Wingerter-Seez⁵, E. Winkels¹⁵⁵, F. Winklmeier¹³⁰, O.J. Winston¹⁵⁵, B.T. Winter⁵¹, M. Wittgen¹⁵², M. Wobisch⁹⁴, A. Wolf⁹⁸, T.M.H. Wolf¹¹⁹, R. Wolff¹⁰⁰, M.W. Wolter⁸³, H. Wolters^{139a,139c}, V.W.S. Wong¹⁷⁴, N.L. Woods¹⁴⁵, S.D. Worm²¹, B.K. Wosiek⁸³, K.W. Woźniak⁸³, K. Wraight⁵⁶, M. Wu³⁷, S.L. Wu¹⁸⁰, X. Wu⁵³, Y. Wu^{59a}, T.R. Wyatt⁹⁹, B.M. Wynne⁴⁹, S. Xella⁴⁰, Z. Xi¹⁰⁴, L. Xia¹⁷⁷, D. Xu^{15a}, H. Xu^{59a,d}, L. Xu²⁹, T. Xu¹⁴⁴, W. Xu¹⁰⁴, B. Yabsley¹⁵⁶, S. Yacoob^{33a}, K. Yajima¹³², D.P. Yallup⁹³, D. Yamaguchi¹⁶⁴, Y. Yamaguchi¹⁶⁴, A. Yamamoto⁸⁰, T. Yamanaka¹⁶², F. Yamane⁸¹, M. Yamatani¹⁶², T. Yamazaki¹⁶², Y. Yamazaki⁸¹, Z. Yan²⁵, H.J. Yang^{59c,59d}, H.T. Yang¹⁸, S. Yang⁷⁶, Y. Yang¹⁶², Z. Yang¹⁷, W.-M. Yao¹⁸, Y.C. Yap⁴⁵, Y. Yasu⁸⁰, E. Yatsenko^{59c,59d}, J. Ye⁴², S. Ye²⁹, I. Yeletsikh⁷⁸, E. Yigitbasi²⁵, E. Yildirim⁹⁸, K. Yorita¹⁷⁸, K. Yoshihara¹³⁶, C.J.S. Young³⁶, C. Young¹⁵², J. Yu⁸, J. Yu⁷⁷, X. Yue^{60a}, S.P.Y. Yuen²⁴, B. Zabinski⁸³, G. Zacharis¹⁰, E. Zaffaroni⁵³, R. Zaidan¹⁴, A.M. Zaitsev^{122,ai}, T. Zakareishvili^{158b}, N. Zakharchuk³⁴, J. Zalieckas¹⁷, S. Zambito⁵⁸, D. Zanzi³⁶, D.R. Zaripovas⁵⁶, S.V. Zeiřner⁴⁶, C. Zeitnitz¹⁸¹, G. Zemaityte¹³⁴, J.C. Zeng¹⁷², Q. Zeng¹⁵², O. Zenin¹²², D. Zerwas¹³¹, M. Zgubić¹³⁴, D.F. Zhang^{59b}, D. Zhang¹⁰⁴, F. Zhang¹⁸⁰, G. Zhang^{59a}, G. Zhang^{15b}, H. Zhang^{15c}, J. Zhang⁶, L. Zhang^{15c}, L. Zhang^{59a}, M. Zhang¹⁷², P. Zhang^{15c}, R. Zhang^{59a}, R. Zhang²⁴, X. Zhang^{59b}, Y. Zhang^{15a,15d}, Z. Zhang¹³¹, P. Zhao⁴⁸, Y. Zhao^{59b,131,ae}, Z. Zhao^{59a}, A. Zhemchugov⁷⁸, Z. Zheng¹⁰⁴, D. Zhong¹⁷², B. Zhou¹⁰⁴, C. Zhou¹⁸⁰, L. Zhou⁴², M.S. Zhou^{15a,15d}, M. Zhou¹⁵⁴, N. Zhou^{59c}, Y. Zhou⁷, C.G. Zhu^{59b}, H.L. Zhu^{59a}, H. Zhu^{15a}, J. Zhu¹⁰⁴, Y. Zhu^{59a}, X. Zhuang^{15a}, K. Zhukov¹⁰⁹, V. Zhulanov^{121b,121a}, A. Zibell¹⁷⁶, D. Zieminska⁶⁴, N.I. Zimine⁷⁸, S. Zimmermann⁵¹, Z. Zinonos¹¹⁴, M. Zinser⁹⁸, M. Ziolkowski¹⁵⁰, G. Zobernig¹⁸⁰, A. Zoccoli^{23b,23a}, K. Zoch⁵², T.G. Zorbas¹⁴⁸, R. Zou³⁷, M. Zur Nedden¹⁹, L. Zwalinski³⁶

¹ Department of Physics, University of Adelaide, Adelaide, Australia

² Physics Department, SUNY Albany, Albany, NY, United States of America

³ Department of Physics, University of Alberta, Edmonton, AB, Canada

⁴ (a) Department of Physics, Ankara University, Ankara; (b) Istanbul Aydin University, Istanbul; (c) Division of Physics, TOBB University of Economics and Technology, Ankara, Turkey

⁵ LAPP, Université Grenoble Alpes, Université Savoie Mont Blanc, CNRS/IN2P3, Annecy, France

⁶ High Energy Physics Division, Argonne National Laboratory, Argonne, IL, United States of America

⁷ Department of Physics, University of Arizona, Tucson, AZ, United States of America

⁸ Department of Physics, University of Texas at Arlington, Arlington, TX, United States of America

⁹ Physics Department, National and Kapodistrian University of Athens, Athens, Greece

¹⁰ Physics Department, National Technical University of Athens, Zografou, Greece

¹¹ Department of Physics, University of Texas at Austin, Austin, TX, United States of America

¹² (a) Bahcesehir University, Faculty of Engineering and Natural Sciences, Istanbul; (b) Istanbul Bilgi University, Faculty of Engineering and Natural Sciences, Istanbul; (c) Department of Physics, Bogazici University, Istanbul; (d) Department of Physics Engineering, Gaziantep University, Gaziantep, Turkey

¹³ Institute of Physics, Azerbaijan Academy of Sciences, Baku, Azerbaijan

¹⁴ Institut de Física d'Altes Energies (IFAE), Barcelona Institute of Science and Technology, Barcelona, Spain

¹⁵ (a) Institute of High Energy Physics, Chinese Academy of Sciences, Beijing; (b) Physics Department, Tsinghua University, Beijing; (c) Department of Physics, Nanjing University, Nanjing;

(d) University of Chinese Academy of Science (UCAS), Beijing, China

¹⁶ Institute of Physics, University of Belgrade, Belgrade, Serbia

¹⁷ Department for Physics and Technology, University of Bergen, Bergen, Norway

¹⁸ Physics Division, Lawrence Berkeley National Laboratory and University of California, Berkeley, CA, United States of America

¹⁹ Institut für Physik, Humboldt Universität zu Berlin, Berlin, Germany

²⁰ Albert Einstein Center for Fundamental Physics and Laboratory for High Energy Physics, University of Bern, Bern, Switzerland

²¹ School of Physics and Astronomy, University of Birmingham, Birmingham, United Kingdom

²² Facultad de Ciencias y Centro de Investigaciones, Universidad Antonio Nariño, Bogotá, Colombia

²³ (a) INFN Bologna and Università di Bologna, Dipartimento di Fisica; (b) INFN Sezione di Bologna, Italy

²⁴ Physikalisches Institut, Universität Bonn, Bonn, Germany

²⁵ Department of Physics, Boston University, Boston, MA, United States of America

²⁶ Department of Physics, Brandeis University, Waltham, MA, United States of America

²⁷ (a) Transilvania University of Brasov, Brasov; (b) Horia Hulubei National Institute of Physics and Nuclear Engineering, Bucharest; (c) Department of Physics, Alexandru Ioan Cuza University of Iasi, Iasi; (d) National Institute for Research and Development of Isotopic and Molecular Technologies, Physics Department, Cluj-Napoca; (e) University Politehnica Bucharest, Bucharest; (f) West University in Timisoara, Timisoara, Romania

²⁸ (a) Faculty of Mathematics, Physics and Informatics, Comenius University, Bratislava; (b) Department of Subnuclear Physics, Institute of Experimental Physics of the Slovak Academy of Sciences, Kosice, Slovak Republic

²⁹ Physics Department, Brookhaven National Laboratory, Upton, NY, United States of America

³⁰ Departamento de Física, Universidad de Buenos Aires, Buenos Aires, Argentina

³¹ California State University, CA, United States of America

³² Cavendish Laboratory, University of Cambridge, Cambridge, United Kingdom

³³ (a) Department of Physics, University of Cape Town, Cape Town; (b) Department of Mechanical Engineering Science, University of Johannesburg, Johannesburg; (c) School of Physics, University of the Witwatersrand, Johannesburg, South Africa

³⁴ Department of Physics, Carleton University, Ottawa, ON, Canada

³⁵ (a) Faculté des Sciences Ain Chock, Réseau Universitaire de Physique des Hautes Energies – Université Hassan II, Casablanca; (b) Faculté des Sciences, Université Ibn-Tofail, Kénitra;

(c) Faculté des Sciences Semlalia, Université Cadi Ayyad, LPHEA, Marrakech; (d) Faculté des Sciences, Université Mohamed Premier and LPTPM, Oujda; (e) Faculté des sciences, Université Mohammed V, Rabat, Morocco

³⁶ CERN, Geneva, Switzerland

³⁷ Enrico Fermi Institute, University of Chicago, Chicago, IL, United States of America

- ³⁸ LPC, Université Clermont Auvergne, CNRS/IN2P3, Clermont-Ferrand, France
- ³⁹ Nevis Laboratory, Columbia University, Irvington, NY, United States of America
- ⁴⁰ Niels Bohr Institute, University of Copenhagen, Copenhagen, Denmark
- ⁴¹ (a) Dipartimento di Fisica, Università della Calabria, Rende; (b) INFN Gruppo Collegato di Cosenza, Laboratori Nazionali di Frascati, Italy
- ⁴² Physics Department, Southern Methodist University, Dallas, TX, United States of America
- ⁴³ Physics Department, University of Texas at Dallas, Richardson, TX, United States of America
- ⁴⁴ (a) Department of Physics, Stockholm University; (b) Oskar Klein Centre, Stockholm, Sweden
- ⁴⁵ Deutsches Elektronen-Synchrotron DESY, Hamburg and Zeuthen, Germany
- ⁴⁶ Lehrstuhl für Experimentelle Physik IV, Technische Universität Dortmund, Dortmund, Germany
- ⁴⁷ Institut für Kern- und Teilchenphysik, Technische Universität Dresden, Dresden, Germany
- ⁴⁸ Department of Physics, Duke University, Durham, NC, United States of America
- ⁴⁹ SUPA – School of Physics and Astronomy, University of Edinburgh, Edinburgh, United Kingdom
- ⁵⁰ INFN e Laboratori Nazionali di Frascati, Frascati, Italy
- ⁵¹ Physikalisches Institut, Albert-Ludwigs-Universität Freiburg, Freiburg, Germany
- ⁵² II. Physikalisches Institut, Georg-August-Universität Göttingen, Göttingen, Germany
- ⁵³ Département de Physique Nucléaire et Corpusculaire, Université de Genève, Genève, Switzerland
- ⁵⁴ (a) Dipartimento di Fisica, Università di Genova, Genova; (b) INFN Sezione di Genova, Italy
- ⁵⁵ II. Physikalisches Institut, Justus-Liebig-Universität Giessen, Giessen, Germany
- ⁵⁶ SUPA – School of Physics and Astronomy, University of Glasgow, Glasgow, United Kingdom
- ⁵⁷ LPSC, Université Grenoble Alpes, CNRS/IN2P3, Grenoble INP, Grenoble, France
- ⁵⁸ Laboratory for Particle Physics and Cosmology, Harvard University, Cambridge, MA, United States of America
- ⁵⁹ (a) Department of Modern Physics and State Key Laboratory of Particle Detection and Electronics, University of Science and Technology of China, Hefei; (b) Institute of Frontier and Interdisciplinary Science and Key Laboratory of Particle Physics and Particle Irradiation (MOE), Shandong University, Qingdao; (c) School of Physics and Astronomy, Shanghai Jiao Tong University, KLPPAC-MoE, SKLPPC, Shanghai; (d) Tsung-Dao Lee Institute, Shanghai, China
- ⁶⁰ (a) Kirchhoff-Institut für Physik, Ruprecht-Karls-Universität Heidelberg, Heidelberg; (b) Physikalisches Institut, Ruprecht-Karls-Universität Heidelberg, Heidelberg, Germany
- ⁶¹ Faculty of Applied Information Science, Hiroshima Institute of Technology, Hiroshima, Japan
- ⁶² (a) Department of Physics, Chinese University of Hong Kong, Shatin, N.T., Hong Kong; (b) Department of Physics, University of Hong Kong, Hong Kong; (c) Department of Physics and Institute for Advanced Study, Hong Kong University of Science and Technology, Clear Water Bay, Kowloon, Hong Kong, China
- ⁶³ Department of Physics, National Tsing Hua University, Hsinchu, Taiwan
- ⁶⁴ Department of Physics, Indiana University, Bloomington, IN, United States of America
- ⁶⁵ (a) INFN Gruppo Collegato di Udine, Sezione di Trieste, Udine; (b) ICTP, Trieste; (c) Dipartimento Politecnico di Ingegneria e Architettura, Università di Udine, Udine, Italy
- ⁶⁶ (a) INFN Sezione di Lecce; (b) Dipartimento di Matematica e Fisica, Università del Salento, Lecce, Italy
- ⁶⁷ (a) INFN Sezione di Milano; (b) Dipartimento di Fisica, Università di Milano, Milano, Italy
- ⁶⁸ (a) INFN Sezione di Napoli; (b) Dipartimento di Fisica, Università di Napoli, Napoli, Italy
- ⁶⁹ (a) INFN Sezione di Pavia; (b) Dipartimento di Fisica, Università di Pavia, Pavia, Italy
- ⁷⁰ (a) INFN Sezione di Pisa; (b) Dipartimento di Fisica E. Fermi, Università di Pisa, Pisa, Italy
- ⁷¹ (a) INFN Sezione di Roma; (b) Dipartimento di Fisica, Sapienza Università di Roma, Roma, Italy
- ⁷² (a) INFN Sezione di Roma Tor Vergata; (b) Dipartimento di Fisica, Università di Roma Tor Vergata, Roma, Italy
- ⁷³ (a) INFN Sezione di Roma Tre; (b) Dipartimento di Matematica e Fisica, Università Roma Tre, Roma, Italy
- ⁷⁴ (a) INFN-TIFPA; (b) Università degli Studi di Trento, Trento, Italy
- ⁷⁵ Institut für Astro- und Teilchenphysik, Leopold-Franzens-Universität, Innsbruck, Austria
- ⁷⁶ University of Iowa, Iowa City, IA, United States of America
- ⁷⁷ Department of Physics and Astronomy, Iowa State University, Ames, IA, United States of America
- ⁷⁸ Joint Institute for Nuclear Research, Dubna, Russia
- ⁷⁹ (a) Departamento de Engenharia Elétrica, Universidade Federal de Juiz de Fora (UFJF), Juiz de Fora; (b) Universidade Federal do Rio De Janeiro COPPE/EE/IF, Rio de Janeiro; (c) Universidade Federal de São João del Rei (UFSJ), São João del Rei; (d) Instituto de Física, Universidade de São Paulo, São Paulo, Brazil
- ⁸⁰ KEK, High Energy Accelerator Research Organization, Tsukuba, Japan
- ⁸¹ Graduate School of Science, Kobe University, Kobe, Japan
- ⁸² (a) AGH University of Science and Technology, Faculty of Physics and Applied Computer Science, Krakow; (b) Marian Smoluchowski Institute of Physics, Jagiellonian University, Krakow, Poland
- ⁸³ Institute of Nuclear Physics Polish Academy of Sciences, Krakow, Poland
- ⁸⁴ Faculty of Science, Kyoto University, Kyoto, Japan
- ⁸⁵ Kyoto University of Education, Kyoto, Japan
- ⁸⁶ Research Center for Advanced Particle Physics and Department of Physics, Kyushu University, Fukuoka, Japan
- ⁸⁷ Instituto de Física La Plata, Universidad Nacional de La Plata and CONICET, La Plata, Argentina
- ⁸⁸ Physics Department, Lancaster University, Lancaster, United Kingdom
- ⁸⁹ Oliver Lodge Laboratory, University of Liverpool, Liverpool, United Kingdom
- ⁹⁰ Department of Experimental Particle Physics, Jožef Stefan Institute and Department of Physics, University of Ljubljana, Ljubljana, Slovenia
- ⁹¹ School of Physics and Astronomy, Queen Mary University of London, London, United Kingdom
- ⁹² Department of Physics, Royal Holloway University of London, Egham, United Kingdom
- ⁹³ Department of Physics and Astronomy, University College London, London, United Kingdom
- ⁹⁴ Louisiana Tech University, Ruston, LA, United States of America
- ⁹⁵ Fysiska institutionen, Lunds universitet, Lund, Sweden
- ⁹⁶ Centre de Calcul de l'Institut National de Physique Nucléaire et de Physique des Particules (IN2P3), Villeurbanne, France
- ⁹⁷ Departamento de Física Teórica C-15 and CIAFF, Universidad Autónoma de Madrid, Madrid, Spain
- ⁹⁸ Institut für Physik, Universität Mainz, Mainz, Germany
- ⁹⁹ School of Physics and Astronomy, University of Manchester, Manchester, United Kingdom
- ¹⁰⁰ CPPM, Aix-Marseille Université, CNRS/IN2P3, Marseille, France
- ¹⁰¹ Department of Physics, University of Massachusetts, Amherst, MA, United States of America
- ¹⁰² Department of Physics, McGill University, Montreal, QC, Canada
- ¹⁰³ School of Physics, University of Melbourne, Victoria, Australia
- ¹⁰⁴ Department of Physics, University of Michigan, Ann Arbor, MI, United States of America
- ¹⁰⁵ Department of Physics and Astronomy, Michigan State University, East Lansing, MI, United States of America
- ¹⁰⁶ B.I. Stepanov Institute of Physics, National Academy of Sciences of Belarus, Minsk, Belarus
- ¹⁰⁷ Research Institute for Nuclear Problems of Byelorussian State University, Minsk, Belarus
- ¹⁰⁸ Group of Particle Physics, University of Montreal, Montreal, QC, Canada
- ¹⁰⁹ P.N. Lebedev Physical Institute of the Russian Academy of Sciences, Moscow, Russia
- ¹¹⁰ Institute for Theoretical and Experimental Physics of the National Research Centre Kurchatov Institute, Moscow, Russia
- ¹¹¹ National Research Nuclear University MEPhI, Moscow, Russia

- 112 D.V. Skobeltsyn Institute of Nuclear Physics, M.V. Lomonosov Moscow State University, Moscow, Russia
- 113 Fakultät für Physik, Ludwig-Maximilians-Universität München, München, Germany
- 114 Max-Planck-Institut für Physik (Werner-Heisenberg-Institut), München, Germany
- 115 Nagasaki Institute of Applied Science, Nagasaki, Japan
- 116 Graduate School of Science and Kobayashi–Maskawa Institute, Nagoya University, Nagoya, Japan
- 117 Department of Physics and Astronomy, University of New Mexico, Albuquerque, NM, United States of America
- 118 Institute for Mathematics, Astrophysics and Particle Physics, Radboud University Nijmegen/Nikhef, Nijmegen, Netherlands
- 119 Nikhef National Institute for Subatomic Physics and University of Amsterdam, Amsterdam, Netherlands
- 120 Department of Physics, Northern Illinois University, DeKalb, IL, United States of America
- 121 ^(a) Budker Institute of Nuclear Physics and NSU, SB RAS, Novosibirsk; ^(b) Novosibirsk State University, Novosibirsk, Russia
- 122 Institute for High Energy Physics of the National Research Centre Kurchatov Institute, Protvino, Russia
- 123 Department of Physics, New York University, New York, NY, United States of America
- 124 Ochanomizu University, Otsuka, Bunkyo-ku, Tokyo, Japan
- 125 Ohio State University, Columbus, OH, United States of America
- 126 Faculty of Science, Okayama University, Okayama, Japan
- 127 Homer L. Dodge Department of Physics and Astronomy, University of Oklahoma, Norman, OK, United States of America
- 128 Department of Physics, Oklahoma State University, Stillwater, OK, United States of America
- 129 Palacký University, RCPTM, Joint Laboratory of Optics, Olomouc, Czech Republic
- 130 Center for High Energy Physics, University of Oregon, Eugene, OR, United States of America
- 131 LAL, Université Paris-Sud, CNRS/IN2P3, Université Paris-Saclay, Orsay, France
- 132 Graduate School of Science, Osaka University, Osaka, Japan
- 133 Department of Physics, University of Oslo, Oslo, Norway
- 134 Department of Physics, Oxford University, Oxford, United Kingdom
- 135 LPNHE, Sorbonne Université, Paris Diderot Sorbonne Paris Cité, CNRS/IN2P3, Paris, France
- 136 Department of Physics, University of Pennsylvania, Philadelphia, PA, United States of America
- 137 Konstantinov Nuclear Physics Institute of National Research Centre “Kurchatov Institute”, PNPI, St. Petersburg, Russia
- 138 Department of Physics and Astronomy, University of Pittsburgh, Pittsburgh, PA, United States of America
- 139 ^(a) Laboratório de Instrumentação e Física Experimental de Partículas – LIP; ^(b) Departamento de Física, Faculdade de Ciências, Universidade de Lisboa, Lisboa; ^(c) Departamento de Física, Universidade de Coimbra, Coimbra; ^(d) Centro de Física Nuclear da Universidade de Lisboa, Lisboa; ^(e) Departamento de Física, Universidade do Minho, Braga; ^(f) Universidad de Granada, Granada (Spain); ^(g) Dep Física and CEFITEC de Faculdade de Ciências e Tecnologia, Universidade Nova de Lisboa, Caparica, Portugal
- 140 Institute of Physics of the Czech Academy of Sciences, Prague, Czech Republic
- 141 Czech Technical University in Prague, Prague, Czech Republic
- 142 Charles University, Faculty of Mathematics and Physics, Prague, Czech Republic
- 143 Particle Physics Department, Rutherford Appleton Laboratory, Didcot, United Kingdom
- 144 IRFU, CEA, Université Paris-Saclay, Gif-sur-Yvette, France
- 145 Santa Cruz Institute for Particle Physics, University of California Santa Cruz, Santa Cruz, CA, United States of America
- 146 ^(a) Departamento de Física, Pontificia Universidad Católica de Chile, Santiago; ^(b) Departamento de Física, Universidad Técnica Federico Santa María, Valparaíso, Chile
- 147 Department of Physics, University of Washington, Seattle, WA, United States of America
- 148 Department of Physics and Astronomy, University of Sheffield, Sheffield, United Kingdom
- 149 Department of Physics, Shinshu University, Nagano, Japan
- 150 Department Physik, Universität Siegen, Siegen, Germany
- 151 Department of Physics, Simon Fraser University, Burnaby, BC, Canada
- 152 SLAC National Accelerator Laboratory, Stanford, CA, United States of America
- 153 Physics Department, Royal Institute of Technology, Stockholm, Sweden
- 154 Departments of Physics and Astronomy, Stony Brook University, Stony Brook, NY, United States of America
- 155 Department of Physics and Astronomy, University of Sussex, Brighton, United Kingdom
- 156 School of Physics, University of Sydney, Sydney, Australia
- 157 Institute of Physics, Academia Sinica, Taipei, Taiwan
- 158 ^(a) E. Andronikashvili Institute of Physics, Iv. Javakishvili Tbilisi State University, Tbilisi; ^(b) High Energy Physics Institute, Tbilisi State University, Tbilisi, Georgia
- 159 Department of Physics, Technion, Israel Institute of Technology, Haifa, Israel
- 160 Raymond and Beverly Sackler School of Physics and Astronomy, Tel Aviv University, Tel Aviv, Israel
- 161 Department of Physics, Aristotle University of Thessaloniki, Thessaloniki, Greece
- 162 International Center for Elementary Particle Physics and Department of Physics, University of Tokyo, Tokyo, Japan
- 163 Graduate School of Science and Technology, Tokyo Metropolitan University, Tokyo, Japan
- 164 Department of Physics, Tokyo Institute of Technology, Tokyo, Japan
- 165 Tomsk State University, Tomsk, Russia
- 166 Department of Physics, University of Toronto, Toronto, ON, Canada
- 167 ^(a) TRIUMF, Vancouver, BC; ^(b) Department of Physics and Astronomy, York University, Toronto, ON, Canada
- 168 Division of Physics and Tomonaga Center for the History of the Universe, Faculty of Pure and Applied Sciences, University of Tsukuba, Tsukuba, Japan
- 169 Department of Physics and Astronomy, Tufts University, Medford, MA, United States of America
- 170 Department of Physics and Astronomy, University of California Irvine, Irvine, CA, United States of America
- 171 Department of Physics and Astronomy, University of Uppsala, Uppsala, Sweden
- 172 Department of Physics, University of Illinois, Urbana, IL, United States of America
- 173 Instituto de Física Corpuscular (IFIC), Centro Mixto Universidad de Valencia – CSIC, Valencia, Spain
- 174 Department of Physics, University of British Columbia, Vancouver, BC, Canada
- 175 Department of Physics and Astronomy, University of Victoria, Victoria, BC, Canada
- 176 Fakultät für Physik und Astronomie, Julius-Maximilians-Universität Würzburg, Würzburg, Germany
- 177 Department of Physics, University of Warwick, Coventry, United Kingdom
- 178 Waseda University, Tokyo, Japan
- 179 Department of Particle Physics, Weizmann Institute of Science, Rehovot, Israel
- 180 Department of Physics, University of Wisconsin, Madison, WI, United States of America
- 181 Fakultät für Mathematik und Naturwissenschaften, Fachgruppe Physik, Bergische Universität Wuppertal, Wuppertal, Germany
- 182 Department of Physics, Yale University, New Haven, CT, United States of America
- 183 Yerevan Physics Institute, Yerevan, Armenia

^a Also at Borough of Manhattan Community College, City University of New York, New York NY; United States of America.

^b Also at Centre for High Performance Computing, CSIR Campus, Rosebank, Cape Town; South Africa.

^c Also at CERN, Geneva; Switzerland.

- ^d Also at CPPM, Aix-Marseille Université, CNRS/IN2P3, Marseille; France.
- ^e Also at Département de Physique Nucléaire et Corpusculaire, Université de Genève, Genève; Switzerland.
- ^f Also at Departament de Física de la Universitat Autònoma de Barcelona, Barcelona; Spain.
- ^g Also at Department of Applied Physics and Astronomy, University of Sharjah, Sharjah; United Arab Emirates.
- ^h Also at Department of Financial and Management Engineering, University of the Aegean, Chios; Greece.
- ⁱ Also at Department of Physics and Astronomy, University of Louisville, Louisville, KY; United States of America.
- ^j Also at Department of Physics and Astronomy, University of Sheffield, Sheffield; United Kingdom.
- ^k Also at Department of Physics, California State University, East Bay; United States of America.
- ^l Also at Department of Physics, California State University, Fresno; United States of America.
- ^m Also at Department of Physics, California State University, Sacramento; United States of America.
- ⁿ Also at Department of Physics, King's College London, London; United Kingdom.
- ^o Also at Department of Physics, St. Petersburg State Polytechnical University, St. Petersburg; Russia.
- ^p Also at Department of Physics, University of Fribourg, Fribourg; Switzerland.
- ^q Also at Department of Physics, University of Michigan, Ann Arbor MI; United States of America.
- ^r Also at Faculty of Physics, M.V. Lomonosov Moscow State University, Moscow; Russia.
- ^s Also at Giresun University, Faculty of Engineering, Giresun; Turkey.
- ^t Also at Graduate School of Science, Osaka University, Osaka; Japan.
- ^u Also at Hellenic Open University, Patras; Greece.
- ^v Also at Horia Hulubei National Institute of Physics and Nuclear Engineering, Bucharest; Romania.
- ^w Also at II. Physikalisches Institut, Georg-August-Universität Göttingen, Göttingen; Germany.
- ^x Also at Institutio Catalana de Recerca i Estudis Avancats, ICREA, Barcelona; Spain.
- ^y Also at Institute for Mathematics, Astrophysics and Particle Physics, Radboud University Nijmegen/Nikhef, Nijmegen; Netherlands.
- ^z Also at Institute for Particle and Nuclear Physics, Wigner Research Centre for Physics, Budapest; Hungary.
- ^{aa} Also at Institute of Particle Physics (IPP); Canada.
- ^{ab} Also at Institute of Physics, Academia Sinica, Taipei; Taiwan.
- ^{ac} Also at Institute of Physics, Azerbaijan Academy of Sciences, Baku; Azerbaijan.
- ^{ad} Also at Institute of Theoretical Physics, Ilia State University, Tbilisi; Georgia.
- ^{ae} Also at LAL, Université Paris-Sud, CNRS/IN2P3, Université Paris-Saclay, Orsay; France.
- ^{af} Also at Louisiana Tech University, Ruston LA; United States of America.
- ^{ag} Also at LPNHE, Sorbonne Université, Paris Diderot Sorbonne Paris Cité, CNRS/IN2P3, Paris; France.
- ^{ah} Also at Manhattan College, New York NY; United States of America.
- ^{ai} Also at Moscow Institute of Physics and Technology State University, Dolgoprudny; Russia.
- ^{aj} Also at National Research Nuclear University MEPhI, Moscow; Russia.
- ^{ak} Also at Physics Department, An-Najah National University, Nablus; Palestine.
- ^{al} Also at Physikalisches Institut, Albert-Ludwigs-Universität Freiburg, Freiburg; Germany.
- ^{am} Also at School of Physics, Sun Yat-sen University, Guangzhou; China.
- ^{an} Also at The City College of New York, New York NY; United States of America.
- ^{ao} Also at The Collaborative Innovation Center of Quantum Matter (CICQM), Beijing; China.
- ^{ap} Also at Tomsk State University, Tomsk, and Moscow Institute of Physics and Technology State University, Dolgoprudny; Russia.
- ^{aq} Also at TRIUMF, Vancouver BC; Canada.
- ^{ar} Also at Universidad de Granada, Granada (Spain); Spain.
- ^{as} Also at Università di Napoli Parthenope, Napoli; Italy.
- * Deceased.